Universidad de Valladolid


**PROGRAMA DE DOCTORADO EN MATEMÁTICAS**

TESIS DOCTORAL:

# SOME INVERSE PROBLEMS ON FINITE NETWORKS

Presentada por Álvaro Samperio Valdivieso para optar al grado de
Doctor/a por la Universidad de Valladolid

Dirigida por:
Dr. Antonio Campillo López
Dr. Andrés Marcos Encinas Bachiller

# Funding


- Supported by a FPI grant of the Research Project PGC2018-096446-BC21 (with the help of the FEDER Program).
- Partially supported by the project PID2022-138906NB-C21 funded by MICIU/AEI/ 10.13039/501100011033 and by ERDF/EU.
- Partially supported by the Spanish Research Council (Ministerio de Ciencia e Innovación) under project PID2021-122501NB-I00.

# Acknowledgments

May the reader forgive me for writing the acknowledgments partially in Spanish.

A mis directores de tesis, Antonio Campillo y Andrés Marcos Encinas, cuyo apoyo ha sido esencial para el desarrollo de esta tesis. Ha sido una experiencia profundamente enriquecedora trabajar con dos matemáticos tan excelentes. Estoy muy agradecido a Antonio por confiar en mí para desarrollar esta tesis y por lo mucho que he aprendido de él durante tantos años. También estoy muy agradecido a Andrés por su enorme dedicación, y por su apuesta por este trabajo, que ha sido decisiva para que saliera adelante.

A Félix Delgado, que ha sido como un tercer director de esta tesis. Además de su gran ayuda con los contenidos de la tesis, y haber aprendido mucho de él compartiendo docencia, ha sido la persona que más me ha influido estos años, un verdadero ejemplo a seguir que me ha hecho mejor matemático y mejor persona.

I would like to thank the members of the jury for reading this work, and I would also like to thank the referees for their helpful comments and suggestions on a first version of this thesis.

A mis compañeros del Departamento de Álgebra, Geometría, Topología y Análisis matemático de la Universidad de Valladolid, a mis compañeros de doctorado y a los miembros del grupo de investigación SINGACOM. Ha sido un honor trabajar en la Universidad de Valladolid, y el ambiente de trabajo ha sido inmejorable. Me gustaría agradecer especialmente su gran apoyo a mis compañeros de doctorado con los que he tenido la suerte de coincidir más tiempo: Şeyma Bodur, Daniel Camazón, Ignacio de Miguel y María Martín, que han sido como hermanos para mí. Los comienzos en investigación son difíciles y ha sido fundamental compartir el viaje desde el principio con este grupo, que ha sido como mi familia académica.

A los miembros del Departamento de Matemáticas y del grupo de investigación MAPTHE de la Universidad Politécnica de Cataluña por ser mi segunda casa en este doctorado, incluyendo a Enric Monsó, Margarida Mitjana y Leonardo Acho. Entre ellos, me gustaría dedicar un agradecimiento especial a mis coautores Ángeles Carmona, María José Jiménez, y al propio Andrés, cuya influencia y ayuda en esta tesis me cuesta describir con palabras. Es un placer cuando se encuentra un grupo con el que uno está tan cómodo dentro y fuera del trabajo, especialmente siendo un grupo del que he aprendido tanto. Cada visita a Barcelona, por pequeña que sea, hace una gran diferencia.

Al coordinador del programa de doctorado, Alfonso Gordaliza, por su cercanía; por estar siempre preocupado y disponible para ayudar en todo lo posible en el desarrollo de la tesis

y por su gran esfuerzo en el proceso burocrático.

A todas las personas que me han invitado a dar conferencias a su universidad y también a todos los compañeros que he conocido en congresos, por lo mucho que he aprendido de ellos en tantas ponencias y también en conversaciones más informales. En especial me querría acordar de la Red ALAMA, a la que considero una de las comunidades científicas más activas y acogedoras de este país, y particularmente me querría acordar de sus miembros Carlos Marijuan, Miriam Pisonero, José Más, Alicia Roca, Julio Moro, Silvia Marcaida y Gorka Armentia.

Thank you to the Algebraic Combinatorics group of the Eindhoven University of Technology and in particular to Aida Abiad, for inviting me for a research stay. During the time that I was there, I learned a lot from her and the experience was amazing both at a professional and a personal level. I am also grateful to the entire group for being so welcoming, especially my friend Ignacio Echave.

A mis coautores Alberto González, Gilles Mordant y Bodhivastava Sen, con quienes estoy encantado de estar trabajando en una colaboración muy estimulante. De los mejores momentos del doctorado han sido las visitas a Valladolid de Alberto, que es siempre una referencia para mí, tanto como matemático como eligiendo vino entre ratos de trabajo.

Me gustaría agradecer a CARTIF su apuesta decidida por la investigación en matemáticas, acordarme de mis compañeros de la División de Energía de la que estoy encantado de formar parte, y especialmente dar las gracias a Ali Vasallo, Fernando Frechoso y Sergio Saludes por su confianza y flexibilidad que han sido muy importantes para poder hacer el doctorado.

A mis profesores de la Universidad de Valladolid por brindarme una formación excelente y a tantos compañeros de la carrera por compartir años muy felices. Mención especial merecen mis compañeros del Grado en Matemáticas, Álvaro Vielba, Diego Martín, Alonso Sánchez, Juan Manuel Velasco, Alicia Nieto, Laura Carreras, Laura Esteban, Elena Sobrini y Elena de la Vega, junto a los que empezó esta pasión por las matemáticas entre San Bourbakis y tangos de la muerte.

A mis amigos de siempre por su apoyo. Es muy importante para mí saber que siempre van a estar ahí en los momentos difíciles aunque no nos podamos ver tan a menudo como me gustaría. Querría destacar sobre todo a Álvaro Delgado y a mis amigos de Valdunquillo Mario Valdivieso, David Fernández, Luis Pascual, Musáfira Tami y Jorge Blanco.

Me gustaría finalizar con lo más importante, agradeciendo su apoyo incondicional a toda mi familia en los buenos y malos momentos. A mi hermana, mis tíos y mis primos por estar siempre para lo que haga falta. A mi madre María José Valdivieso por enseñarme desde pequeño la importancia de estudiar y por su calidez y cariño. A mi padre José Antonio Samperio también por enseñarme la importancia de estudiar y trabajar duro para conseguir lo que me propongo. Espero que este año veamos por fin al Racing volver a Primera. A mis abuelos Eloisa Rodríguez, Mariano Valdivieso y Amelia López, y a la memoria de mi abuelo José Samperio, por haber sido parte fundamental de mi vida. No hay cariño tan desinteresado y puro como el que he tenido la suerte de recibir de mis abuelos.

# Contents

# Introduction

Inverse problems are a class of mathematical problems where the objective is to determine unknown causes from their known effects. Many inverse problems have garnered attention because their resolution allows to infer information that in some cases is not directly observable, and in other cases is directly observable, but observing it is more expensive and/or destructive than inferring it from its known effects.

Inverse problems have applications in many different fields. For instance, they are common in deblurring images, signal recovery, and other areas of digital processing. Moreover, techniques like magnetic resonance imaging (MRI) and computed tomography (CT) scans rely on solving inverse problems to create images of the interior of the body. Inverse problems also help in interpreting seismic data for oil exploration or in analyzing astronomical data.

Most inverse problems are ill-posed, meaning they do not meet for every data set the criteria of existence, uniqueness and stability of the solution. In an unstable problem, even if there is a unique solution for a data set, small changes in the data can lead to much greater changes in the solution. Regularization techniques are often used to handle this, [4, 21]. Regularization is a method to stabilize inverse problems by introducing additional information or constraints. Techniques like Tikhonov regularization or L1-regularization help in dealing with ill-posedness and improving the robustness of solutions, [1, 4, 89, 104].

In this work we focus on the study of inverse problems on finite electrical networks. We will consider Direct Current (DC) networks and balanced Alternating Current (AC) electrical networks in which all lines are inductive and "short", (*i.e.*, their length is shorter than 80km). An electrical network, (see Definition 1.3.1), is a pair $\Gamma = (V, a)$ where $V$ is a finite nonempty set called *vertex set*, and $a$ is a complex symmetric function on $V \times V$ with nonnegative real part and nonpositive imaginary part such that $a(x, x) = 0$ for any $x \in V$, called *admittance*. In the case of DC networks, $a$ is a real function and it is called conductance. A network has an associated graph called its "*network topology*", whose vertex set is $V$ and whose edges are the pairs $\{x, y\}$ of distinct vertices such that $a(x, y) \neq 0$. The value $a(x, y) \neq 0$ is called the value of the admittance at the edge $\{x, y\}$.

At a given time, there exist physical quantities, such as potential, current injected or power injected, which are defined at the vertices of the network. The value of each of these quantities at a set $F \subseteq V$ can be represented by a complex function on $F$ for AC networks and by a real function on $F$ for DC networks. There are relations between these functions, which can be expressed in terms of difference operators that depend on the electrical network. Inverse problems on networks usually consist in determining information about the network

such as its topology and/or the values of the admittance at its edges from certain measured functions of potential, current and/or power, and sometimes alongside additional known information.

The objective of Chapter 1 is to establish a version of discrete vector calculus on networks, which gives us the framework to formulate the inverse problems that we study in this text, and also to introduce concepts and results that we use to solve those problems. Over time, many authors have proposed different approaches to define a discrete vector calculus on networks according to their needs and aims. On the one hand, in the area of numerical methods for solving boundary problems, the so-called *Mimetic Methods* describe how finite difference schemes on logically rectangular grids can be related to an operational calculus that follows the lines of differential operators, see for example [68, 69, 90]. In the field of finite or infinite networks or graphs, the vector calculus follows the guidelines of Algebraic Topology, see for instance [59, 74], especially when the graphs are part of simplicial complexes. The consideration of some boundary value problems on graphs and networks, and their variational treatment also led to the consideration of some operators as derivative, normal derivative, Laplacian, Green operator and Green functions, see for instance [44, 46, 67]. In the last decade, the need to deal with irregular graphs and abstract data with irregular interrelationships has revived the interest in vector calculus on graphs and networks, see [74, 84]. A good description of the interest of these methodologies can be found on the website [100], especially devoted to its use in image modeling.

It is interesting to note that most of the above mentioned papers ignore developments made by other groups. For example, the theoretical description made on the web [100] is very similar to the one proposed in [47], although this paper is absent from the references. Furthermore, all the authors seem to be unaware of the systematic work that Japanese geometers and analysts have developed since the the last decades of the past century, see as example [70]. Another common feature of most vector calculus developed on graphs and networks is that the vector fields are identified with functions on the edge set and therefore limited to flows. This allows the formulation of Green's identities, but not the Divergence Theorem, and also limits the study to the so-called purely resistive networks.

In [18, 20, 35, 36], the authors introduced a discrete vector calculus for DC networks following the guidelines of differential geometry, whose central concept is the introduction of the tangent space at each vertex of the network. With this concept, the authors obtain discrete versions of several differential operators, vector fields, and boundary value problems that mimic the properties of its continuum analogues. The version proposed here extends that work to the case of AC networks, with some modifications.

In Section 1.1 we start by introducing the general properties of the vector spaces and operators that we use throughout the document. Then, in Section 1.2 we study several topological and geometrical concepts associated to a graph without considering any weighting on the edge set. Those concepts include the *tangent space* at a vertex, difference operators such as the *derivative* and *divergence*, that are analogous in the discrete setting to the differential operators with the same name of the continuous calculus, and the boundary of a set of vertices.

In Section 1.3 we set the fundamentals for the discrete calculus on networks. We consider the concepts introduced in the previous section, which only depend on the network topology,

and we introduce other difference operators depending on the topology and admittance which are analogous to the *gradient*, to the *normal derivative*, and to the *Laplace-Beltrami operator*. With those operators we can explain the physical laws relating the potential, current and power injected at the whole network, (see Remark 1.3.8). We prove that the operators introduced satisfy discrete versions of the Green Identities and Gauss' Theorem.

Then, in Section 1.4 we study the Dirichlet and Poisson problems on a subset $F \subseteq V$ of the vertices of a network $\Gamma$, and their associated Green and Poisson operators. We extend the formulation of [35] to consider Dirichlet and Poisson problems on a subset that is not necessarily connected. The study of those problems allow us to introduce in Section 1.5 the Dirichlet-to-Neumann map of $\Gamma$ and $F$. Under the condition that there is zero injected current at the vertices of $F$ for any potential, this operator gives us the linear relationship between the potential and the respective injected current at $F^c = V \setminus F$, *i.e.*, at the complementary set of $F$. We extend the definition of [35] to consider also networks with edges between vertices of $F^c$.

Section 1.6 is dedicated to survey previous results from [9] and [35] of monotonicity of real functions on DC networks in order to prove additional properties of the Dirichlet-to-Neumann map of a DC network. In particular, we have that any Dirichlet-to-Neumann map is the Laplacian (the discrete analogous to the Laplace-Beltrami operator) of another network, the *Kron reduction of* $\Gamma$ *with respect to* $F$. We show that for AC networks, the previous result is not always true, but it is true when $F^c = \{x, y\} \subset V$. In Section 1.7 we introduce the effective admittance between two vertices $x$ and $y$ from the Dirichlet-to-Neumann map of $\Gamma$ and $F = V \setminus \{x, y\}$, and therefore, by the previous result, we can relate it to a Kron reduction of $\Gamma$.

Chapter 2 is dedicated to study the inverse conductance problem on a DC network, which is the discrete version of the continuous Calderón problem. In 1980, A.P. Calderón published the seminal paper "On an inverse boundary value problem" ([34]), which has motivated numerous developments in inverse problems. Calderón's problem establishes whether the electrical conductivity of a medium can be determined by making voltage and current measurements at the boundary.

The problem at hand involves an unknown conductivity that needs to be determined and possibly reconstructed using boundary measurements of current and voltage. This intriguing challenge has garnered significant attention due to its wide range of applications in diverse fields, including noninvasive medical imaging, which stands as one of the most complex and compelling areas of interest (see [4, 42, 82, 91]).

Calderón's problem is severely ill-posed, and significant efforts are being made to develop algorithms that can accurately solve it. This includes optimization algorithms, heuristic methods, and machine learning techniques, (see [24, 41]).

The discrete inverse conductance problem consists in determining the conductance of a DC network from its Dirichlet-to-Neumann map. We study the problem for well-connected spider networks, which are a subfamily of critical circular planar networks and were first introduced in [54] because of their remarkable properties. In [51, 52, 53, 54, 55] it was established that for critical planar networks the problem has a unique solution. They also introduced an explicit method to solve the problem for well-connected spider networks from

a finite number of elementary algebraic operations, and the method was generalized in [10].

Well-connected spider networks are among the most used networks to study the inverse conductance problem. Moreover, the resolution of the inverse problem in those networks has been also studied as part of a process to get a numerical solution of Calderón's problem, that is, to recover the conductivity of continuous media, from a finite number of (voltage and current) measurements, (see [8, 26, 55]).

Nevertheless, as its continuous counterpart, the discrete problem is severely ill-posed even for relatively small-sized networks. This poor performance explains why the use of these networks in medical applications is restricted to networks with fewer than 16 nodes on the boundary (see [91, 104]).

In Chapter 2, we review and extend the results from [38] and [37], in which the authors proposed a stable reformulation of the inverse conductance problem and studied the process to solve it. First, in Section 2.1, we expose in detail the background of both the discrete inverse problem and the continuous one, in order to explain the relevance of the original contributions of [38] and [37].

Then, in Section 2.2 we show an example to demonstrate that, in practice, the use of the explicit method from [10] yields a big numerical error in the recovered conductance due to the ill-posedness of the problem. Because of that, in [38] it was proposed to reformulate the problem, (see Problem 2.3.1). In Section 2.3 we review this reformulation, which is a polynomial optimization problem incorporating a regularization term that penalizes the deviation with respect to the conductance being piecewise constant on a partition of the edge set known *a priori*.

When the conductance of a network is piecewise constant on a partition whose number of subsets is small compared to the total number of edges, we say that the *piecewise constant conductance hypothesis* holds. In Section 2.4 we show several examples from [38] in which we solve Problem 2.3.1 with a partition in the regularization term such that the conductance of the real network is piecewise constant on that partition. We show that if the number of subsets is small, that is, if the piecewise constant conductance hypothesis holds, in all the examples we recover the conductance of all the networks with stability. In particular, we have been able to recover the conductances on spider networks with up to 47 boundary nodes, improving the known methods that show instabilities when the number of boundary nodes is greater than 16, see for instance [1, 27, 38, 89, 104].

In Section 2.5 and Section 2.6 we review the results from [38]. These results examine the application of Problem 2.3.1 when we penalize deviations with respect to a constant piecewise conductance hypothesis in a given partition of the edge set that may not be satisfied by the actual conductance. Even so, in the studied cases, the obtained solutions are good approximations to the real conductances.

In Section 2.5 we provide an example of the variation of the error in the recovered conductance with respect to the penalty parameter $\mu \geq 0$. The case when $\mu = 0$ corresponds to the unstable recovery without regularization, and the case when $\mu \to \infty$ corresponds to imposing the piecewise constant conductance hypothesis exactly. We show an example in which we solve Problem 2.3.1 using a partition with few subsets such that the real conductance is not piecewise constant on the partition but is not far from a piecewise constant conductance

on this partition. Recovering a conductance for several values of $\mu$, we obtain the one that is closest to the real one when we use an intermediate value of the parameter $\mu \in (0, \infty)$, that is, when we allow deviations with respect to the hypothesis but we also avoid the instability of the problem without regularization. This example supports the penalty formulation of Problem 2.3.1.

Finally, in Section 2.6, we study the application of techniques of Sum of Squares (SOS) decompositions of polynomials in order to seek a guarantee that a minimum of Problem 2.3.1 obtained with a numerical method is a global minimum, and thus a solution of the problem.

In Chapter 3 we study the inverse problem of simultaneously recovering the admittance and topology of an AC or DC network from a set of measurements of voltage and its corresponding power injected at all vertices. The chapter is an extension and review of the results from [88], in which the problem is reformulated to the recovery of a sparse network.

Nowadays, electrical systems are expanding and increasing in complexity really fast due to the deregulation and proliferation of distributed energy resources. Because of this expansion, sometimes the system operators do not have precise and updated information about the admittance or the topology of the network. Also, the dependence of the admittance on temperature can cause the information about them to be incorrect [2]. The lack of topology information is especially frequent in the secondary distribution network [72], in which the lines are short [29]. Moreover, recently, the availability and accuracy of measured data in the electrical system has increased significantly. At the nodes, power injection and voltage magnitude can be measured using smart meters and the phase angle information can be obtained by micro phasor measurement units [72]. In that scenario, the simultaneous recovery of the topology and admittance of a network from voltage and power data is of great interest from an applied point of view. We start the chapter comparing the formulation of our inverse problem with other inverse problems on networks which involve the recovery of the topology.

In an example in Section 3.1 we show that the general problem of admittance and topology recovery is ill-posed, in some cases even having multiple solutions. As a result, if we have a set of edges $E$ that are candidate to belong to the network, we usually obtain a solution in which the value of the admittance at all edges in $E$ is distinct from zero, and thus the set of edges of the solution is the whole $E$. When $E$ is large, the recovered network is not efficient for applications. Therefore, in Section 3.2 we reformulate that inverse problem to obtain Problem 3.2.1, which consists in recovering a sparse network such that the fitting error to the data is below a fixed tolerance. Such a network would allow the efficient and accurate resolution of usual problems in electrical networks which require the admittance and topology. Those applications include failure identification, power flow optimization or generation scheduling [57].

In Section 3.3 we review the notion of spectral sparsification of a network introduced in [95] by Spielman and Teng. In [16] the authors proposed Algorithm 1 in order to construct a sparse approximation of a network with less edges than the original. The results in Section 1.7 allow us to give a novel physical interpretation to the product of the conductance of an edge by its effective resistance and, as a consequence, to Algorithm 1.

In Section 3.4, we present original theoretical results (see Theorems 3.4.1 and 3.4.4)

that give an upper bound on the increase of the fitting error of a network in the process of removing edges of a network using the techniques of spectral sparsification of networks of the previous section. These results are the basis for the Algorithm 2 that we propose in Section 3.5 to obtain a solution to Problem 3.2.1. It consists in an iterative procedure of recovering a network and sparsifying it, with an automatic exploration to find the levels of closeness of sparsification that allow us to remove edges without increasing the error in the data above the fixed tolerance.

Finally, in Section 3.6 we show several experimental results of the application of Algorithm 2. We see that, in some cases, we are able to recover the exact network (with the actual topology and low error in the admittance). We show other cases in which we recover an electrical network which is electrically equivalent to the original one under conditions satisfied by the data set (such as the power injected at some node being always zero). Moreover, we show that, in some cases, the algorithm has the advantage of providing a sparse approximation of the real electrical network, in which computation is faster than in the real network.

# Chapter 1

# Discrete vector calculus on networks

In this chapter we introduce a version of vector calculus in networks, establishing the fundamental concepts, results and notation that we will use throughout the text. We use the notation $\mathbb{N}, \mathbb{Z}, \mathbb{Q}, \mathbb{R}$ and $\mathbb{C}$ for the sets of natural, integer, rational, real and complex numbers, respectively. In addition, $\mathbb{N}^* = \mathbb{N} \setminus \{0\}$ and the same applies to the other number sets. Given $z \in \mathbb{C}$, $\Re(z)$ and $\Im(z)$ denote the real and imaginary part of $z$, $\bar{z}$ denotes its conjugate and $|z|$ denotes its modulus. We always identify $\mathbb{R}$ with the set of complex numbers with null imaginary part.

The set of nonnegative real numbers is denoted by $[0, \infty)$. Moreover we add the symbol $\infty$ to $[0, \infty)$ and use the usual order and arithmetic in the interval $[0, \infty]$:

(i) $a < \infty$ for any $a \in [0, \infty)$.

(ii) $a + \infty = \infty$ for any $a \in [0, \infty]$.

(iii) $a\infty = \infty$ for any $a \in (0, \infty]$ and $0\infty = 0$.

(iv) $\dfrac{1}{0} = \infty$ and $\dfrac{1}{\infty} = 0$.

## 1.1 Function spaces

In all the document $V$ indicates a finite set, with cardinality $|V|$, whose elements are generically denoted by $x, y, z \in V$; and $F$ indicates a subset of $V$. For any $F \subseteq V$, $F^c = V \setminus F$ stands for the complementary set of $F$ in $V$.

The spaces of real and complex functions on $V$ are denoted as $\mathscr{C}(V) = \{u \colon V \longrightarrow \mathbb{R}\}$ and $\mathscr{C}(V, \mathbb{C}) = \{u \colon V \longrightarrow \mathbb{C}\}$, respectively. Given $u \in \mathscr{C}(V, \mathbb{C})$, $\Re(u)$ and $\Im(u)$ are called the *real and imaginary parts of* $u$, and we have $u = \Re(u) + i\Im(u)$. The notation $\bar{u}$ for $u \in \mathscr{C}(V, \mathbb{C})$ corresponds to the function defined by $\bar{u}(x) = \overline{u(x)}$, for each $x \in V$. Clearly, $\mathscr{C}(V)$ is identified with the subset of $\mathscr{C}(V, \mathbb{C})$ of functions having null real part and hence, we have $u = \bar{u}$ iff $u \in \mathscr{C}(V)$. The notation $|u|$ for $u \in \mathscr{C}(V, \mathbb{C})$ corresponds to the function of $\mathscr{C}(V)$ defined by $|u|(x) = |u(x)|$, for each $x \in V$.

The space $\mathscr{C}(V)$, respectively $\mathscr{C}(V,\mathbb{C})$, is a real, respectively complex, vector space of dimension $\dim_{\mathbb{R}}(\mathscr{C}(V)) = \dim_{\mathbb{C}}(\mathscr{C}(V,\mathbb{C})) = |V|$. Furthermore, $u \geq 0$ denotes a nonnegative function of $\mathscr{C}(V)$, that is, a function such that $u(x) \geq 0$ for each $x \in V$, and the space of nonnegative functions is denoted by $\mathscr{C}^+(V)$.

The *support* of $u \in \mathscr{C}(V,\mathbb{C})$ is the set $\mathsf{supp}(u) = \{x \in V : u(x) \neq 0\}$. Given $F \subseteq V$, $\mathscr{C}(F,\mathbb{C}) = \{u \in \mathscr{C}(V,\mathbb{C}) : u = 0 \text{ in } F^c\} = \{u \in \mathscr{C}(V,\mathbb{C}) : \mathsf{supp}(u) \subseteq F\}$ and moreover, $\mathscr{C}(F) = \mathscr{C}(V) \cap \mathscr{C}(F,\mathbb{C})$.

The *characteristic function of* $F$, $\chi_{_F} \in \mathscr{C}(V)$, is defined as $\chi_{_F}(x) = 1$ when $x \in F$ and $\chi_{_F}(x) = 0$ otherwise. In particular, if $F = \{x\}$, its characteristic function is denoted by $\varepsilon_x$.

Given $F \subseteq V$, for each $u \in \mathscr{C}(V,\mathbb{C})$ we define

$$\int_F u dx = \sum_{x\in F} u(x) = \sum_{x\in F} \Re(u)(x) + i \sum_{x\in F} \Im(u)(x) = \int_F \Re(u) dx + i \int_F \Im(u) dx.$$

Of course, $\displaystyle\int_F u dx \in \mathbb{R}$ when $u \in \mathscr{C}(V)$.

We consider the following inner product on $\mathscr{C}(V,\mathbb{C})$

$$\langle u, v\rangle = \int_V u\bar{v} dx,$$

whose associated norm is denoted by $||\cdot|| = ||\cdot||_2$. It is clear that the above inner product induces an inner product on $\mathscr{C}(V)$. Given a subset $S \in \mathscr{C}(V,\mathbb{C})$, its *orthogonal complement* is the subspace $S^\perp = \{u \in \mathscr{C}(V,\mathbb{C}) \text{ such that } \langle u, v\rangle = 0 \text{ for all } v \in S\}$. When $S \in \mathscr{C}(V)$ we denote by $S^\perp_{_{\mathbb{R}}}$ its orthogonal complement in $\mathscr{C}(V)$ with the induced inner product; that is, $S^\perp_{_{\mathbb{R}}} = S^\perp \cap \mathscr{C}(V)$. We drop the subindex $\mathbb{R}$ when it does not lead to confusion.

We also consider in $\mathscr{C}(V,\mathbb{C})$ the norm $||\cdot||_\infty$, which is defined for each $u \in \mathscr{C}(V,\mathbb{C})$ as $||u||_\infty = \max\limits_{x\in V}\{|u(x)|\}$.

Given $m \in \mathbb{N}^*$, $m \geq 2$, we generalize the above spaces to the spaces of vector functions $\mathscr{C}(V,\mathbb{R}^m)$ and $\mathscr{C}(V,\mathbb{C}^m)$. Clearly, we can consider $\mathscr{C}(V,\mathbb{R}^m) \subset \mathscr{C}(V,\mathbb{C}^m)$. Moreover, each function $\boldsymbol{u} \in \mathscr{C}(V,\mathbb{C}^m)$ has $m$ *component functions* $u_1,\ldots,u_m$ that are elements of $\mathscr{C}(V,\mathbb{C})$ and hence,

$$\mathscr{C}(V,\mathbb{C}^m) = \big\{\boldsymbol{u} = (u_1,...,u_m) \text{ such that } u_j \in \mathscr{C}(V,\mathbb{C}) \text{ for all } j = 1,...,m\big\}.$$

Again, functions in $\mathscr{C}(V,\mathbb{R}^m)$ are identified with those functions in $\mathscr{C}(V,\mathbb{C}^m)$ whose components belong all to $\mathscr{C}(V,\mathbb{R})$.

On $\mathscr{C}(V,\mathbb{C}^m)$ we consider the inner product

$$\langle \boldsymbol{u}, \boldsymbol{v}\rangle = \sum_{j=1}^m \langle u_j, v_j\rangle = \sum_{j=1}^m \int_V u_j \bar{v}_j dx, \quad \text{where } \boldsymbol{u} = (u_1,\ldots,u_m) \text{ and } \boldsymbol{v} = (v_1,\ldots,v_m)$$

whose associated norm is denoted by $||\cdot||$. Again, this inner product induces an inner product on $\mathscr{C}(V,\mathbb{R}^m)$.

As in the case $m = 1$, we also consider in $\mathscr{C}(V, \mathbb{C}^m)$ the norm $||\cdot||_\infty$, which is defined for each $\boldsymbol{u} = (u_1, ..., u_m) \in \mathscr{C}(V, \mathbb{C}^m)$ as $||\boldsymbol{u}||_\infty = \max\limits_{j=1,..,m} \{||u_j||_\infty\}$.

Of course, $\mathscr{C}(V, \mathbb{C}^m)$ can be identified with $\mathscr{C}(V, \mathbb{R}^{2m})$ and in particular $\mathscr{C}(V, \mathbb{C})$ is identified with $\mathscr{C}(V, \mathbb{R}^2)$.

The elements of $\mathscr{C}(V \times V) = \{K \colon V \times V \longrightarrow \mathbb{R}\}$ and $\mathscr{C}(V \times V, \mathbb{C}) = \{K \colon V \times V \longrightarrow \mathbb{C}\}$ are called real and complex *kernels*, respectively. The space of real nonnegative kernels is denoted by $\mathscr{C}^+(V \times V)$. We also define the space $\mathscr{C}^+_\infty(V \times V) = \{u \colon V \times V \longrightarrow [0, \infty]\}$. The support of $K \in \mathscr{C}(V \times V, \mathbb{C})$ is the set $\mathsf{supp}(K) = \{(x, y) \in V \times V : K(x, y) \neq 0\}$. Again, we always assume that $\mathscr{C}(V \times V) \subset \mathscr{C}(V \times V, \mathbb{C})$.

For every kernel $K \in \mathscr{C}(V \times V, \mathbb{C}) \supset \mathscr{C}(V \times V)$, its *transpose kernel* $K^\top$ is defined by $K^\top(x, y) = K(y, x)$, for each $x, y \in V$. Its *adjoint kernel* $K^*$ is defined by $K^*(x, y) = \overline{K(y, x)}$, for each $x, y \in V$. We have that $K$ is real, *i.e.*, $K \in \mathscr{C}(V \times V)$, iff $K^* \in \mathscr{C}(V \times V)$ or equivalently, iff $K^\top = K^*$. A kernel $K$ is called *symmetric* when $K = K^\top$; and it is called *self-adjoint* when $K = K^*$. Of course, being symmetric and self-adjoint is equivalent iff $K \in \mathscr{C}(V \times V)$. For every $K \in \mathscr{C}(V \times V, \mathbb{C})$ there exist $\Re(K), \Im(K) \in \mathscr{C}(V \times V)$ such that $K(x, y) = \Re(K)(x, y) + i\Im(K)(x, y)$ for each $x, y \in V$. These kernels are called the *real and imaginary parts of* $K$, respectively.

Given $K \in \mathscr{C}(V \times V, \mathbb{C})$, its *symmetric and antisymmetric parts* $K^s, K^a \in \mathscr{C}(V \times V, \mathbb{C})$ are respectively defined by $K^s(x, y) = \frac{1}{2}\big(K(x, y) + K(y, x)\big)$ and $K^a(x, y) = \frac{1}{2}\big(K(x, y) - K(y, x)\big)$ for each $x, y \in V$. Note that, if $K \in \mathscr{C}(V \times V)$, then $K^s, K^a \in \mathscr{C}(V \times V)$.

If $K \in \mathscr{C}(V \times V, \mathbb{C})$, its *trace* is $\mathrm{tr}(K) = \sum\limits_{x \in V} K(x, x) = \int_V K(x, x)dx$. Of course, if $K \in \mathscr{C}(V \times V)$, then $\mathrm{tr}(K) \in \mathbb{R}$. It is clear that $\mathrm{tr}(K) = \mathrm{tr}(K^s)$.

If $F_1$ and $F_2$ are nonempty subsets of $V$, then $\mathscr{C}(F_1 \times F_2)$, respectively $\mathscr{C}(F_1 \times F_2, \mathbb{C})$, denotes the set of kernels $K \in \mathscr{C}(V \times V)$, respectively $K \in \mathscr{C}(V \times V, \mathbb{C})$, such that $\mathsf{supp}(K) \subseteq F_1 \times F_2$. If $F$ is a nonempty subset of $V$, any function $K \in \mathscr{C}(F \times F)$, respectively $K \in \mathscr{C}(F \times F, \mathbb{C})$, will be called a real, respectively complex, *kernel on* $F$. Of course, if $F_1 \subset F_2$, then each kernel on $F_2$ is also a kernel on $F_1$.

If $K$ is a kernel on $F$, for each $x, y \in F$ we denote by $K^x$ and $K_y$ the functions of $\mathscr{C}(F, \mathbb{C})$ defined by $K^x(y) = K_y(x) = K(x, y)$. Note that $\overline{(K^*)^x} = K_x$ for each $x \in V$.

Given $F_1, F_2 \subseteq V$, for each $K \in \mathscr{C}(V \times V, \mathbb{C})$ we define

$$\int_{F_1 \times F_2} K dxdy = \sum_{x \in F_1} \sum_{y \in F_2} K(x, y) = \int_{F_1} \left( \int_{F_2} K^x dy \right) dx = \int_{F_2} \left( \int_{F_1} K_y dx \right) dy.$$

We can consider a labeling, or enumeration, on $V$, identifying it with the set $\{x_1, ..., x_n\}$, with $n = |V|$. After a labeling, $\mathscr{C}(V)$, respectively $\mathscr{C}(V, \mathbb{C})$, can be identified with $\mathbb{R}^{|V|}$, respectively with $\mathbb{C}^{|V|}$. Moreover, $\mathscr{C}(V \times V)$ and $\mathscr{C}(V \times V, \mathbb{C})$ can be identified with the spaces of square matrices $\mathscr{M}_{|V| \times |V|}(\mathbb{R})$ and $\mathscr{M}_{|V| \times |V|}(\mathbb{C})$, respectively. If a kernel $K$ is identified with a matrix $\mathsf{K}$, then $K^\top$ is identified with its *transpose matrix* $\mathsf{K}^\top$, and $K^*$ is identified with its *conjugate transpose matrix* $\mathsf{K}^*$. Observe that the determinant of a matrix can only be

defined after a labeling of $V$, but it is clearly independent of it. Moreover, the trace is also clearly independent of any labeling on $V$.

Given $x, y \in V$, we denote as $\mathsf{K}(x,y)$ the entry of the matrix $\mathsf{K}$ corresponding to vertices $x$ and $y$, that is, the entry $K(x,y)$ of the kernel $K$. More generally, given a pair of subsets $F_1, F_2 \subseteq V$, we define the submatrix of $\mathsf{K}$: $\mathsf{K}(F_1; F_2) = \big(\mathsf{K}(x,y)\big)_{(x,y)\in F_1\times F_2}$.

We call *operator* to any linear application $\mathscr{K}\colon P \longrightarrow Q$ between two finite dimensional complex or real vector spaces with inner product $P$ and $Q$. Its *null space* is the subspace of $P$ defined as $\ker(\mathscr{K}) = \{u \in P \text{ such that } \mathscr{K}(u) = 0\}$. Its *image* is the subspace of $Q$ defined as $\mathrm{Img}(\mathscr{K}) = \{\mathscr{K}(u) \text{ such that } u \in P\}$. When $P = Q$, we say that $\mathscr{K}\colon P \longrightarrow P$ is an *operator on* $P$. The following results are extensions of results of operators from [17] to include the complex case.

Given an operator $\mathscr{K}\colon P \longrightarrow Q$, we denote by $\mathscr{K}^*\colon Q \longrightarrow P$ its *adjoint*, which is the operator uniquely determined by the relation

$$\langle \mathscr{K}(u), v\rangle = \langle u, \mathscr{K}^*(v)\rangle,$$

for all $u \in P$ and $v \in Q$.

The following result is a consequence that follows almost immediately from the previous relation.

**Lemma 1.1.1** (Fredholm alternative)**.** *If $\mathscr{K}$ is an operator on $P$, then we have that*

$$\mathrm{Img}(\mathscr{K}) = \big[\ker(\mathscr{K}^*)\big]^{\perp}.$$

Given an operator $\mathscr{K}$ on $P$, we say that $u \in P$ is an eigenvector of $\mathscr{K}$ if $u \neq 0$ and there exists $\lambda \in \mathbb{C}$ such that $\mathscr{K}(u) = \lambda u$. In that case, $\lambda$ is called the eigenvalue of $\mathscr{K}$ associated to the eigenvector $u$. The number of eigenvalues of $\mathscr{K}$ is at most $\dim(P)$.

We say that an operator $\mathscr{K}$ on $P$ is *self-adjoint* if $\mathscr{K}^* = \mathscr{K}$. If $\mathscr{K}$ is self-adjoint, then $\langle \mathscr{K}(u), u\rangle \in \mathbb{R}$ for every $u \in P$. Moreover, each eigenvalue of $\mathscr{K}$ is real, and there is a basis $\big\{u_1, ..., u_{\dim(P)}\big\}$ of $P$ such that each $u_j$ is an eigenvector of $\mathscr{K}$, and $u_j \perp u_k$ whenever $j \neq k$.

We say that $\mathscr{K}$ is *positive semidefinite*, respectively *negative semidefinite*, if $\langle \mathscr{K}(u), u\rangle \geq 0$, respectively $\langle \mathscr{K}(u), u\rangle \leq 0$, for every $u \in \mathscr{C}(V, \mathbb{C})$. If $\mathscr{K}$ is positive semidefinite, respectively negative semidefinite, then each eigenvalue of $\mathscr{K}$ is nonnegative, respectively nonpositive.

Let $\mathscr{K}\colon P \longrightarrow Q$ be an operator, and let $m = \min\{\dim(P), \dim(Q)\}$. Then $\mathscr{K}^* \circ \mathscr{K}$ is a self-adjoint and positive semidefinite operator on $P$. We denote its eigenvalues by $\lambda_1 \geq ... \geq \lambda_{\dim(P)} \geq 0$. The *singular values* of $\mathscr{K}$ are the nonnegative numbers $\sigma_j = \sqrt{\lambda_j}$ for each $j = 1, ..., m$. Then, we define the condition number of $\mathscr{K}$ as $\kappa(\mathscr{K}) = \sigma_1/\sigma_m$. We have that $\kappa(\mathscr{K}) = \infty$ iff $\mathscr{K}$ is singular, *i.e.*, iff $\ker(\mathscr{K}) \neq \{0\}$. We also define the *spectral norm* of $\mathscr{K}$ as its largest singular value, $\|\mathscr{K}\|_2 = \sigma_1$.

Let $\mathscr{K}$ be a self-adjoint operator on $\mathscr{C}(V)$, respectively on $\mathscr{C}(V, \mathbb{R}^m)$. Then, by the Courant-Fisher theorem [94], we have that the maximum of the eigenvalues of $\mathscr{K}$ is equal to

$\max_{\|u\|=1}\{\langle\mathscr{K}(u),u\rangle\}$. Also, for any $u\in\mathscr{C}(V)$, respectively $u\in\mathscr{C}(V,\mathbb{R}^m)$, we have that $\|\mathscr{K}(u)\|\leq\|\mathscr{K}\|_2\|u\|$.

We denote by $\mathcal{C}\colon\mathscr{C}(V,\mathbb{C})\longrightarrow\mathscr{C}(V,\mathbb{C})$ the conjugation application, that is defined by $\mathcal{C}(u)=\bar{u}$ for each $u\in\mathscr{C}(V,\mathbb{C})$. We say that $\mathscr{K}\colon\mathscr{C}(V,\mathbb{C})\longrightarrow\mathscr{C}(V,\mathbb{C})$ is a *symmetric operator* if $\mathscr{K}^*=\mathcal{C}\circ\mathscr{K}\circ\mathcal{C}$ [83], or equivalently iff $\mathscr{K}=\mathcal{C}\circ\mathscr{K}^*\circ\mathcal{C}$. If we restrict the definition to operators in $\mathscr{C}(V)$, $\mathcal{C}$ is the identity, so being symmetric and self-adjoint is equivalent.

Given an operator $\mathscr{K}$ on $\mathscr{C}(V)$ or on $\mathscr{C}(V,\mathbb{C})$, we define its real and complex parts as $\Re(\mathscr{K})=\frac{1}{2}(\mathscr{K}+\mathscr{K}^*)$ and $\Im(\mathscr{K})=\frac{1}{2i}(\mathscr{K}-\mathscr{K}^*)$, respectively. It is clear that they are self-adjoint operators and $\mathscr{K}=\Re(\mathscr{K})+i\Im(\mathscr{K})$, (see [49]).

**Lemma 1.1.2.** *If $\mathscr{K}$ is a symmetric operator on $\mathscr{C}(V)$ or on $\mathscr{C}(V,\mathbb{C})$, then $\Re(\mathscr{K})|_{\mathscr{C}(V)}$ and $\Im(\mathscr{K})|_{\mathscr{C}(V)}$ are operators on $\mathscr{C}(V)$.*

*Proof.* Let $\mathscr{K}$ be a symmetric operator and $u\in\mathscr{C}(V)$. Then, $\mathscr{K}^*=\mathcal{C}\circ\mathscr{K}\circ\mathcal{C}$ and $\overline{u}=u$, so on one hand

$$\begin{aligned}\overline{\Re(\mathscr{K})(u)}&=\mathcal{C}\circ\Re(\mathscr{K})\big(\mathcal{C}(u)\big)=\tfrac{1}{2}\big(\mathcal{C}\circ(\mathscr{K}+\mathscr{K}^*)\circ\mathcal{C}\big)(u)\\&=\tfrac{1}{2}\big(\mathcal{C}\circ\mathscr{K}\circ\mathcal{C}+\mathcal{C}\circ\mathscr{K}^*\circ\mathcal{C}\big)(u)=\tfrac{1}{2}(\mathscr{K}^*+\mathscr{K})(u)=\Re(\mathscr{K})(u),\end{aligned}$$

and on the other hand

$$\begin{aligned}\overline{\Im(\mathscr{K})(u)}&=\mathcal{C}\circ\Im(\mathscr{K})\big(\mathcal{C}(u)\big)=\tfrac{-1}{2i}\big(\mathcal{C}\circ(\mathscr{K}-\mathscr{K}^*)\circ\mathcal{C}\big)(u)\\&=\tfrac{1}{2i}\big(\mathcal{C}\circ\mathscr{K}^*\circ\mathcal{C}-\mathcal{C}\circ\mathscr{K}\circ\mathcal{C}\big)(u)=\tfrac{1}{2i}(\mathscr{K}-\mathscr{K}^*)(u)=\Im(\mathscr{K})(u).\end{aligned}$$

□

If $K$ is a real, respectively complex, kernel on $F$, we define *the integral operator associated with $K$* as the endomorphism $\mathscr{K}\colon\mathscr{C}(F)\longrightarrow\mathscr{C}(F)$, respectively as the endomorphism $\mathscr{K}\colon\mathscr{C}(F,\mathbb{C})\longrightarrow\mathscr{C}(F,\mathbb{C})$, that assigns to each $u\in\mathscr{C}(F)$, respectively $u\in\mathscr{C}(F,\mathbb{C})$, the function $\mathscr{K}(u)(x)=\displaystyle\int_F K(x,y)\,u(y)\,dy$ for all $x\in V$.

The relationship between kernels, integral operators and endomorphisms of $\mathscr{C}(F)$ is given by the following result. Its first part can be seen as a discrete version of the *Schwartz's Kernel Theorem*, because of the natural identification between $\mathscr{C}(F)$ and its dual space.

**Proposition 1.1.3** (Kernel Theorem [19, Prop. 5.1])**.** *Each endomorphism $\mathscr{K}$ of $\mathscr{C}(F)$, respectively $\mathscr{C}(F,\mathbb{C})$, is an integral operator associated with a real, respectively complex, kernel $K$ on $F$ which is uniquely determined by the relation $K(x,y)=\mathscr{K}(\varepsilon_y)(x)$ for each $(x,y)\in F\times F$.*

*Moreover, if $\mathscr{K}$ is the integral operator on $F$ associated to the kernel $K$ and $A$ is a non empty subset of $F$, then the following statements hold:*

(i) *The adjoint of $\mathscr{K}$, $\mathscr{K}^*$, is the operator associated with the kernel $K^*$. Therefore, $\mathscr{K}$ is self-adjoint iff $K$ is self-adjoint.*

(ii) *The operator* $\mathcal{C} \circ \mathscr{K}^* \circ \mathcal{C}$ *is associated with the kernel* $K^\top$*. Therefore,* $\mathscr{K}$ *is symmetric iff* $K$ *is symmetric.*

(iii) $\mathsf{Img}\,\mathscr{K} \subseteq \mathscr{C}(A)$ *iff* $K \in \mathscr{C}(A \times F)$.

(iv) $\mathscr{C}(F \setminus A) \subseteq \ker \mathscr{K}$ *iff* $K \in \mathscr{C}(F \times A)$.

In particular, each endomorphism of $\mathscr{C}(V)$, respectively $\mathscr{C}(V, \mathbb{C})$, is the integral operator associated to some kernel. Given $\mathscr{K}$, $\mathscr{J}$ endomorphisms of $\mathscr{C}(V)$, respectively of $\mathscr{C}(V, \mathbb{C})$, whose kernels are respectively $K$ and $J$, then the kernel of $\mathscr{K} \circ \mathscr{J}$ is $K \circ J$, defined for each $x, y \in V$ as

$$(K \circ J)(x, y) = \sum_{z \in V} K(x, z)J(z, y) = \int_V K^x(z)J_y(z)dz = \langle J_y, \overline{K^x} \rangle.$$

In addition, we can define the *trace* on the space of endomorphisms of $\mathscr{C}(V)$ or $\mathscr{C}(V, \mathbb{C})$ as $\mathrm{tr}(\mathscr{K}) = \mathrm{tr}(K)$, where $K$ is the kernel of $\mathscr{K}$. From this definition, we can endow the space of endomorphisms of $\mathscr{C}(V)$ or of $\mathscr{C}(V, \mathbb{C})$, and as a consequence the space of kernels $\mathscr{C}(V \times V)$ or $\mathscr{C}(V \times V, \mathbb{C})$, with a natural inner product: if $K$ and $J$ are the kernels associated to the operators $\mathscr{K}$ and $\mathscr{J}$ respectively, then

$$\langle \mathscr{K}, \mathscr{J} \rangle = \mathrm{tr}(\mathscr{K} \circ \mathscr{J}^*) = \int_V \langle J_x, K_x \rangle dx = \mathrm{tr}(K^* \circ J).$$

In particular, $\langle \mathscr{K}, \mathscr{J} \rangle = \langle \mathscr{K}^*, \mathscr{J}^* \rangle$. The associated norm on the space of endomorphisms, or on the space of kernels, is named *Frobenius norm* and denoted as $||\cdot||_{\mathrm{Fr}}$. Therefore, $||\mathscr{K}||_{\mathrm{Fr}} = ||K||_{\mathrm{Fr}} = \mathrm{tr}(\mathscr{K}^* \circ \mathscr{K})^{\frac{1}{2}}$.

## 1.2 Topology and geometry of a graph

In this section we will present several topological and geometrical concepts associated to a graph. We start with the basic definitions, (see [19, 35] for a detailed discussion). Although almost all concepts we next introduce can be defined in infinite and locally finite graphs, every graph throughout this work will be finite, undirected and simple.

A graph is a pair $G = (V, E)$ where $V$ is a finite nonempty set called *vertex set*, and $E \subseteq \big\{\{x, y\}$ such that $x, y \in V$ and $x \neq y\big\}$ is called *edge set*.

A vertex is any $x \in V$. We say that $x, y \in V$ are *adjacent* iff $\{x, y\} \in E$ and usually we denote it as $x \sim y$. We will denote $\{x, y\} \in E$ also by $e_{xy}$ and so, $e_{xy} = e_{yx}$. In Figure 1.1, we show the representation of some examples of graphs.

We define the subspaces of kernels $\mathscr{C}(G) = \{f \in \mathscr{C}(V \times V) \,|\, f(x, y) = 0 \text{ if } e_{xy} \notin E\}$, $\mathscr{C}(G, \mathbb{C}) = \{f \in \mathscr{C}(V \times V, \mathbb{C}) \,|\, f(x, y) = 0 \text{ if } e_{xy} \notin E\}$ and $\mathscr{C}^+(G) = \{f \in \mathscr{C}^+(V \times V) \,|\, f(x, y) = 0 \text{ if } e_{xy} \notin E\}$. The subspaces of symmetric kernels of $\mathscr{C}(G)$, $\mathscr{C}(G, \mathbb{C})$ and $\mathscr{C}^+(G)$ can be identified with the function spaces on the edge set $\mathscr{C}(E)$, $\mathscr{C}(E, \mathbb{C})$ and $\mathscr{C}^+(E)$, respectively.

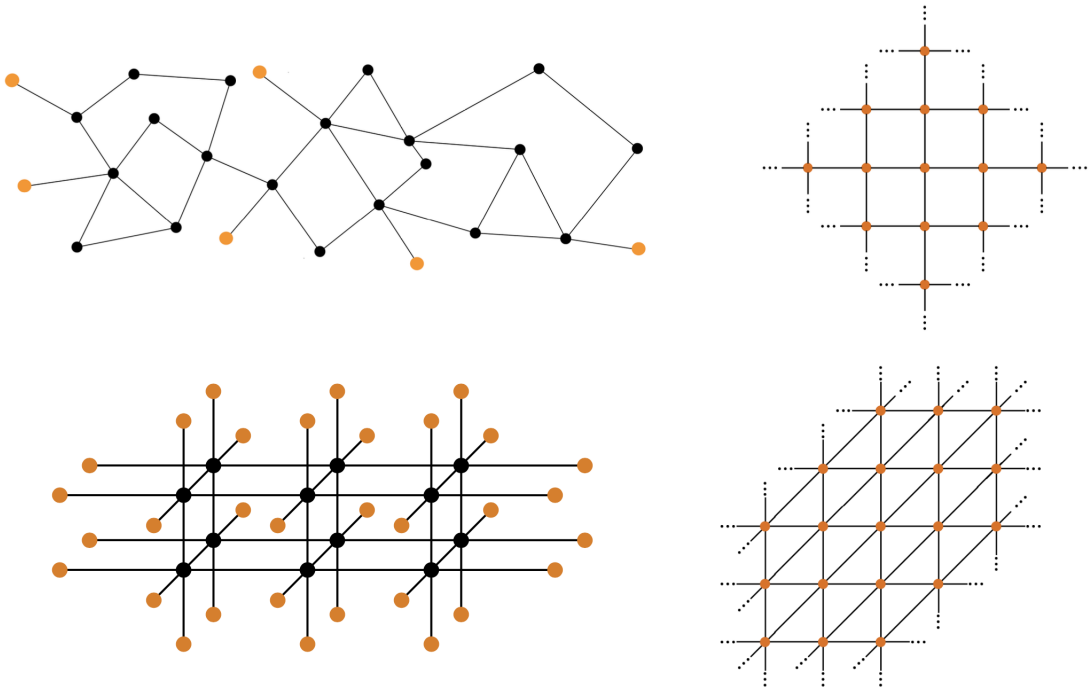

Figure 1.1: Examples of (locally finite) graphs

We say that a subset $F \subseteq V$ is connected if for any $x, y \in F$ there exists a path contained in $F$ from $x$ to $y$, that is, a (finite) sequence of vertices $x_0, \ldots, x_k \in F$ such that $x_0 = x$, $x_k = y$ and $e_{x_{j-1},x_j} \in E$ for all $j = 1, \ldots, k$. We say that a graph is connected if $V$ is connected. We say that two distinct vertices $x, y \in V$ are *connected through* $F$ if there exists a path from $x$ to $y$ such that every vertex of the path distinct from $x$ or $y$ belongs to $F$.

Given a graph $G = (V, E)$, and a subset $F \subseteq V$, we denote by $G^F$ the induced subgraph $G^F = (F, E^F)$ with vertex set $F$, and only the set of edges of $G$ which are adjacent to two vertices of $F$, *i.e.*, $E^F = \{e_{xy} \in E \text{ such that } x, y \in F\}$.

There is a unique partition of $V = V_1 \sqcup ... \sqcup V_s$, with $s \geq 1$, such that $E = E^{V_1} \sqcup ... \sqcup E^{V_s}$ and $G^{V_i}$ is connected for $i = 1, ..., s$. We call each $G^{V_i}$, or $V_i$, a *connected component* of $G$ and write $G = G^{V_1} \sqcup ... \sqcup G^{V_s}$.

Given $x, y \in V$, we denote by $d(x, y)$ the *geodesic distance* in the graph, that is defined as the minimum length of all paths from $x$ to $y$ if $x$ and $y$ belong to the same connected component of $G$ and as $d(x, y) = \infty$ otherwise. It is clear that $d$ gives a structure of metric space to the set of vertices of each connected component of the graph and that $d(x, y) = 1$ iff $x \sim y$.

Given $x \in V$, its *combinatorial degree* $k(x)$ is the number of vertices adjacent to $x$, that is $k(x) = |\{y \in V : y \sim x\}|$.

### 1.2.1 Tangent bundle of a graph

We follow the approach of [35, 36], in which the topological and geometrical concepts in a graph are based on the definition of a tangent space at each point of a graph. The main difference of our approach is that we consider the tangent space as a complex vector space with the standard inner product, instead of a real vector space.

We define the *tangent space* $T_x(G)$ of a vertex $x$ as the complex vector space of formal linear combinations of the set of edges $\{e_{xy} \in E : y \sim x\}$. The dimension of $T_x(G)$ is $k(x)$, and the set of those edges is a basis of $T_x(G)$, that we call its *coordinate basis*. In Figure 1.2 we show the coordinate basis at a vertex.

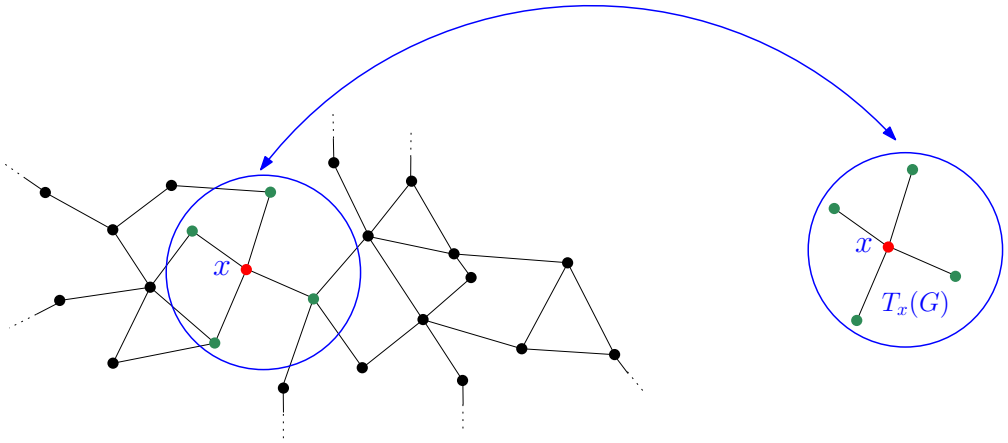


Figure 1.2: Graph and tangent space at vertex $x$.

A *vector field* on the graph is any function $\mathsf{f}\colon V \longrightarrow \bigcup_{x\in V} T_x(G)$ with the property that for every $x \in V$, $\mathsf{f}(x) \in T_x(G)$. We denote the space of vector fields by $\mathcal{X}(G)$. The *support of* $\mathsf{f}$ is defined as $\mathsf{supp}(\mathsf{f}) = \{x \in V : \mathsf{f}(x) \neq \mathsf{0}\}$.

A vector field $\mathsf{f} \in \mathcal{X}(G)$ is uniquely determined by its components in the coordinate basis, so we can define a kernel $f \in \mathscr{C}(G, \mathbb{C})$, which is called the *component function of* $\mathsf{f}$, such that for any $x \in V$, $\mathsf{f}(x) = \sum_{y\sim x} f(x,y)e_{xy}$. This association between $\mathsf{f}$ and $f$ defines an isomorphism between $\mathcal{X}(G)$ and $\mathscr{C}(G, \mathbb{C})$. Therefore, we can define the symmetric and antisymmetric components of $\mathsf{f} \in \mathcal{X}(G)$, $\mathsf{f}^s$ and $\mathsf{f}^a$, as the vector fields associated with $f^s$ and $f^a$, respectively. Note that $\mathsf{f} = \mathsf{f}^s + \mathsf{f}^a$. We say that $\mathsf{f}$ is symmetric if $\mathsf{f} = \mathsf{f}^s$ and that $\mathsf{f}$ is antisymmetric, or a *flow*, if $\mathsf{f} = \mathsf{f}^a$.

Given $u \in \mathscr{C}(V, \mathbb{C})$ and $\mathsf{f} \in \mathcal{X}(G)$ with component function $f$, we denote by $u\mathsf{f} \in \mathcal{X}(G)$ the vector field whose component function is $uf \in \mathscr{C}(G, \mathbb{C})$.

We define the inner product of $\mathsf{f}, \mathsf{g} \in \mathcal{X}(G)$ as

$$\langle \mathsf{f}, \mathsf{g} \rangle = \frac{1}{2} \int_V [\mathsf{f}(x), \mathsf{g}(x)]\, dx,$$

where for any $x \in V$ we denote by $[\mathsf{f}(x), \mathsf{g}(x)]$ the inner product on $T_x(G)$ determined by

the orthonormality of its coordinate basis, *i.e.*, for any $y, z$ such that $y \sim x$ and $z \sim x$, then $[e_{xy}, e_{xz}] = \varepsilon_y(z)$. As a consequence, if $f$ and $g$ are the respective component functions of $\mathsf{f}$ and $\mathsf{g}$, then

$$[\mathsf{f}(x), \mathsf{g}(x)] = \sum_{y \sim x} f(x,y)\overline{g(x,y)} = \sum_{y \in V} f(x,y)\overline{g(x,y)}.$$

We have included the factor $\frac{1}{2}$ in the definition of the inner product of $\mathcal{X}(G)$ because each edge is considered twice. In particular, including that factor we will avoid getting a factor 2 multiplying the sum in the result of Lemma 1.2.2.

**Lemma 1.2.1.** *If $\mathsf{f} \in \mathcal{X}(G)$ is symmetric and $\mathsf{g} \in \mathcal{X}(G)$ is a flow, then $\langle \mathsf{f}, \mathsf{g} \rangle = 0$. As a consequence, given any $\mathsf{f}, \mathsf{g} \in \mathcal{X}(G)$, we have that $\langle \mathsf{f}, \mathsf{g} \rangle = \langle \mathsf{f}^s, \mathsf{g}^s \rangle + \langle \mathsf{f}^a, \mathsf{g}^a \rangle$.*

*Proof.* Let $\mathsf{f} \in \mathcal{X}(G)$ be symmetric and $\mathsf{g} \in \mathcal{X}(G)$ be a flow. Then, we have

$$\langle \mathsf{f}, \mathsf{g} \rangle = \frac{1}{2} \int_{V \times V} f(x,y)\overline{g(x,y)} dy dx = -\frac{1}{2} \int_{V \times V} f(y,x)\overline{g(y,x)} dx dy = -\langle \mathsf{f}, \mathsf{g} \rangle.$$

The second statement follows trivially from the properties of any inner product. □

The following result is straightforward.

**Lemma 1.2.2.** *Let both $\mathsf{f}, \mathsf{g} \in \mathcal{X}(G)$ be either symmetric vector fields or flows, with component functions $f$ and $g$. Then:*

$$\langle \mathsf{f}, \mathsf{g} \rangle = \sum_{e_{xy} \in E} f(x,y)\overline{g(x,y)}.$$

Note that the sum in Lemma 1.2.2 is well defined because if both $\mathsf{f}$ and $\mathsf{g}$ are symmetric or are flows, then $f(x,y)\overline{g(x,y)} = f(y,x)\overline{g(y,x)}$ for every $x, y \in V$.

**Remark 1.2.3.** Due to the isomorphism between $\mathscr{C}(G, \mathbb{C})$ and $\mathcal{X}(G)$, the inner product on $\mathcal{X}(G)$ determines an inner product on $\mathscr{C}(G, \mathbb{C})$ defined for each $f, g \in \mathscr{C}(G, \mathbb{C})$ as $\langle \mathsf{f}, \mathsf{g} \rangle$, where $\mathsf{f}, \mathsf{g} \in \mathcal{X}(G)$ are the vector fields whose component functions are $f$ and $g$, respectively. The norm associated with this inner product is $||f|| = \langle \mathsf{f}, \mathsf{f} \rangle^{\frac{1}{2}}$. This inner product is different than the restriction to $\mathscr{C}(G, \mathbb{C})$ of the one in the space of kernels $\mathscr{C}(V \times V, \mathbb{C})$ defined at the end of Section 1.1 from the inner product on the space of endomorphisms, whose associated norm is $||f||_{\text{Fr}}$. Throughout the whole text, whenever we consider the norm of a kernel $f \in \mathscr{C}(G, \mathbb{C})$ for a graph $G$, we will use that first norm $||f||$ rather than the Frobenius one. If $f$ is symmetric, by Lemma 1.2.2 we have that $||f||^2 = \sum_{e_{xy} \in E} |f(x,y)|^2$.

## 1.2.2 Difference operators on a graph

Now, we will define the *derivative* and *divergence* as discrete *difference operators* on a graph. They are analogous to the differential operators with the same name in the continuous vector calculus.

We define the *derivative* [35] as the linear map $\mathsf{d}\colon \mathscr{C}(V,\mathbb{C}) \longrightarrow \mathcal{X}(G)$, which assigns to each $u \in \mathscr{C}(V,\mathbb{C})$ the flow $\mathsf{d}u$, such that for each $x \in V$, $\mathsf{d}u(x) = \sum_{y\sim x} (u(y) - u(x))e_{xy}$.

Analogously to the continuous case, $\mathsf{d}u = 0$ iff $u \in \mathscr{C}(V,\mathbb{C})$ is constant within each connected component of $G$.

We define the *divergence* as the linear map $\mathsf{div} = -\mathsf{d}^*\colon \mathcal{X}(G) \longrightarrow \mathscr{C}(V,\mathbb{C})$. Namely, for any $\mathsf{f} \in \mathcal{X}(G)$, $\mathsf{div}(\mathsf{f}) \in \mathscr{C}(V,\mathbb{C})$ is the function determined by:

$$\langle \mathsf{div}(\mathsf{f}), u\rangle = \int_V \mathsf{div}(\mathsf{f})\,\overline{u}\,dx = -\frac{1}{2}\int_V [\mathsf{f}(x), \mathsf{d}u(x)]\,dx = -\langle \mathsf{f}, \mathsf{d}u\rangle \tag{1.1}$$

Let $G = G^{V_1} \sqcup \ldots \sqcup G^{V_s}$ be the decomposition of $G$ in its connected components. For any $i = 1, ..., s$, substituting $u = \chi_{V_i}$ in the previous expression, we have $\int_{V_i} \mathsf{div}(\mathsf{f})\,dx = 0$ for any $\mathsf{f} \in \mathcal{X}(G)$. In particular, $\int_V \mathsf{div}(\mathsf{f})\,dx = 0$ for any $\mathsf{f} \in \mathcal{X}(G)$.

In [36], for any weighting $\omega \in \mathscr{C}^+(V)$ on the set of vertices, the authors define an inner product on $\mathscr{C}(V)$ associated to $\omega$. Then, they define the divergence as $\mathsf{div} = -\mathsf{d}^*$ with respect to that inner product. We do not consider any weighting on the vertices, although when we restrict the divergence to real vector fields, our definition of divergence agrees with the one in [36] when the weighting $\omega$ is equal to one. In [35], the divergence is introduced in a different manner because the authors consider an inner product on the tangent space at a vertex which is dependent on the electrical conductance on the edges. Nevertheless, that definition of divergence turns out to be independent of the conductance and it is also equivalent to our definition when we restrict it to real vector fields. As a consequence, our definition satisfies the following proposition from [35].

**Proposition 1.2.4.** *If $\mathsf{f} \in \mathcal{X}(G)$ and $f \in \mathscr{C}(G,\mathbb{C})$ is its component function, then for any $x \in V$:*

$$\mathsf{div}(\mathsf{f})(x) = \sum_{y\sim x} f^a(x,y) = \sum_{y\in V} f^a(x,y).$$

*Proof.* If for any $x \in V$ we substitute $u = \varepsilon_x$ in (1.1), then we get

$$\mathsf{div}(\mathsf{f})(x) = \langle \mathsf{div}(\mathsf{f}), \varepsilon_x\rangle = \langle \mathsf{f}, -\mathsf{d}\varepsilon_x\rangle = \langle \mathsf{f}^a, -\mathsf{d}\varepsilon_x\rangle,$$

where the last equality follows from Lemma 1.2.1. By definition, for any $z \in V$, $-\mathsf{d}\varepsilon_x(z) = \sum_{y\sim z} (\varepsilon_x(z) - \varepsilon_x(y))e_{zy}$. The component function of the flow $-\mathsf{d}\varepsilon_x$ is $-d\varepsilon_x(z,y) = \varepsilon_x(z) - \varepsilon_x(y)$, which is nonzero only if $y \sim z$ and $z$ or $y$ are equal to $x$. Moreover, $-d\varepsilon_x(x,y) = 1$, so, by Lemma 1.2.2:

$$\mathsf{div}(\mathsf{f})(x) = -\sum_{e_{xy}\in E} f^a(x,y)\overline{d\varepsilon_x(x,y)} = \sum_{y\sim x} f^a(x,y).$$

□

### 1.2.3 Boundary of a set

A subset of vertices $F \subseteq V$ of a graph can be seen as the discrete analogue to a compact manifold. In [35, 36] there are discrete concepts analogous to topological concepts involving a compact manifold such as its interior, boundary, closure, exterior normal vector field and the Divergence Theorem, which we review below.

The *interior* of $F$ is $\overset{\circ}{F}= \{x \in F : y \in F \text{ when } y \sim x\} = \big\{x \in F : \{y : d(x,y) \leq 1\} \subset F\big\}$.

The *boundary* of $F$ is $\delta(F) = \{x \in F^c |\ \exists y \in F \text{ such that } y \sim x\} = \{x \in V : d(x,F) = 1\}$.

The *interior boundary* of $F$ is $\delta(F^c) = F \setminus \overset{\circ}{F}= \{x \in V : d(x,F^c) = 1\}$.

The *closure* of $F$ is $\bar{F} = F \cup \delta(F) = \{x \in V : d(x,F) \leq 1\}$.

The *Exterior* of $F$ is $\mathrm{Ext}(F) = V \setminus \bar{F} = \{x \in V : d(x,F) > 1\}$.

The Figure 1.3 shows a vertex set $F$ in light brown color and its boundary in ochre color. Vertices in $\overset{\circ}{F}$, $\delta(F)$, $\delta(F^c)$ or $\mathrm{Ext}(F)$ are depicted in different color.

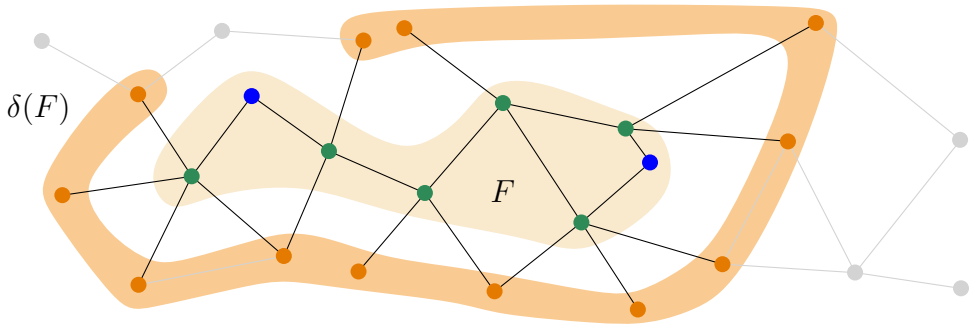


Figure 1.3: $\overset{\circ}{F}$ (blue), $\delta(F)$ (orange), $\delta(F^c)$ (green) and $\mathrm{Ext}(F)$ (light grey).

Observe that to define the above geometric notions, the (possible) edges between boundary vertices play no role. For this reason this kind of edges are depicted in light grey in Figure 1.3

The *normal vector field* to F is the flow $\mathsf{n}_{_F} = -\mathsf{d}\chi_{_F}$. Hence, its component function in $\mathscr{C}(G,\mathbb{C})$ is given by

$$n_{_F}(x,y) = \begin{cases} 1, & y \sim x \text{ and } (x,y) \in \delta(F^c) \times \delta(F) \\ -1, & y \sim x \text{ and } (x,y) \in \delta(F) \times \delta(F^c), \\ 0, & \text{otherwise} \end{cases}$$

As a consequence, $\mathsf{n}_{_{F^c}} = -\mathsf{n}_{_F}$ and $\mathsf{supp}(\mathsf{n}_{_F}) = \delta(F^c) \cup \delta(F)$. Therefore, given $x \in F$, $\mathsf{n}_{_F}(x)$ only takes into account the edges $e_{xy}$ such that $y \in F$ and hence $\mathsf{n}_{_F}$ has the meaning of exterior normal field.

The concept of the normal field to a set $F$ appears for the first time in the literature in [20], although it had already been used previously by the authors. Without the vector

field formalism considered here, the notion of normal derivative was already present in many works related to Graph Analysis, see for example [22, 44, 47, 67] where the authors introduce the notions more or less independently of each other. In fact, these authors ignore the work of M. Yamasaki and collaborators, who introduced several years earlier a similar concept related to the interior normal derivative, see [70] and references therein.

In Figure 1.4 we consider the same set $F$ as in Figure 1.3 and show that different vertices on the boundary could have different number of edges joining them with vertices in $F$.

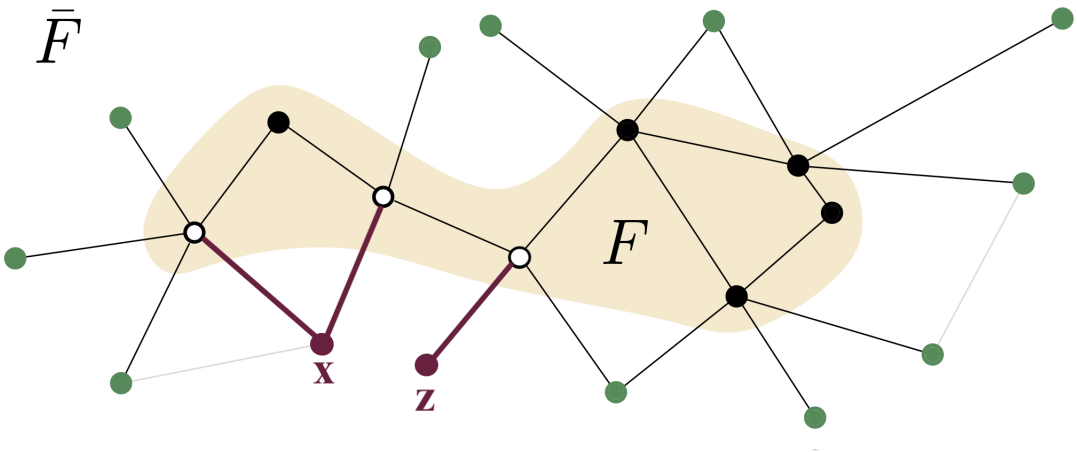


Figure 1.4: $x$ has two edges and $z$ has one edge joining them with vertices in $F$.

The motivation to introduce the normal field was to express the normal derivative of a function as the inner product of its derivative with a field representing the exterior normal, thus mimicking differential calculus with the aim of proving the divergence theorem and Green's identities. All the mentioned authors have their version for the Green Identities, see the next section, but none of them present something similar to the Divergence Theorem, due to the absence of the notion of normal field. As the proof of this result included in [20] is given in a more general setting that that considered in this work, we include here its proof.

**Proposition 1.2.5.** (Divergence Theorem) *For any* $\mathsf{f} \in \mathcal{X}(G)$*, it is verified that*

$$\int_F \mathsf{div}(\mathsf{f})\, dx = \int_{\delta(F)} [\mathsf{f}^a(x), \mathsf{n}_{_F}(x)]\, dx.$$

*Proof.* By the definition of divergence and normal vector field, and by Lemma 1.2.1, we have

$$\int_F \mathsf{div}(\mathsf{f})\, dx = \langle \mathsf{div}(\mathsf{f}), \chi_{_F} \rangle = -\langle \mathsf{f}, \mathsf{d}\chi_{_F} \rangle = -\langle \mathsf{f}^a, \mathsf{d}\chi_{_F} \rangle = \langle \mathsf{f}^a, \mathsf{n}_{_F} \rangle.$$

Denoting by $f$ the component function of $\mathsf{f}$, from Lemma 1.2.2 we get

$$\langle \mathsf{f}^a, \mathsf{n}_{_F} \rangle = \sum_{(x,y)\in\delta(F^c)\times\delta(F)} f^a(x,y) = \int_{\delta(F)} [\mathsf{f}^a(x), \mathsf{n}_{_F}(x)]\, dx.$$

□

**Definition 1.2.6.** We say that a graph $G = (V, E)$ is a *graph with boundary* if there is a proper subset $F \subset V$ such that $V = \bar{F}$ and the boundary $\delta(F)$ is totally disconnected, *i.e.*, $G^{\delta(F)} = (\delta(F), \emptyset)$.

### Well-connected spider graphs

Now we will introduce different subsets of graphs with boundary, in order to illustrate the previous concepts and, in particular, to define the *well-connected spider graphs*. Such graphs were initially introduced in [54] due to their exceptional characteristics and will be the type of graphs with boundary on which we will formulate the inverse problem in Chapter 2.

A circular planar graph [51] is a graph with boundary $G = (\bar{F}, E)$ which can be planarly embedded (*i.e.*, without crossing edges) in a disk $D \subset \mathbb{R}^2$, with the vertices within set $F$ located in the interior of $D$ ($\overset{\circ}{D}$) and the boundary vertices of $\delta(F)$ located in the circumference of $D$ ($\partial D$).

Now, let $G = (\bar{F}, E)$ be a circular planar graph and we fix an embedding of it with the characteristics of the last paragraph. A circular pair is a pair $(\Xi; \Sigma) = (\xi_1, ..., \xi_s; \sigma_1, ..., \sigma_s)$ of disjoint subsets of $\delta(F)$ such that the sequence $(\xi_1, ..., \xi_s, \sigma_1, ..., \sigma_s)$ is in clockwise order. A circular pair $(\Xi; \Sigma)$ is connected through $F$ if there are $s$ disjoint paths $\varrho_1, ..., \varrho_s$ such that each $\varrho_j$ starts at $\xi_j$, ends at $\sigma_j$ and, apart from these two, passes only through vertices of $F$ [51].

We consider the process of contracting an edge $e_{xy} \in E$, with $x \in F$, from a network with boundary $G = (\bar{F}, E)$, which consists in creating the graph $G' = (\overline{F'}, E')$ such that $F' = F \setminus \{x\}$ and $E' = \left(E \setminus \left\{e_{xz} \text{ such that } z \in \overline{F}\right\}\right) \cup \{e_{yz} \text{ such that } e_{xz} \in E \text{ and } z \neq y\}$. Note that $\delta(F') = \delta(F)$. We also consider the process of removing the edge $e_{xy} \in E$ from $G = (\bar{F}, E)$, which consists in creating the graph $G' = (\overline{F'}, E')$, with $F' = F$ and $E' = E \setminus \{e_{xy}\}$.

We say that a circular planar graph $G$ is a *critical* circular planar graph if the operation of removing any edge or the operation of contracting any edge to a single vertex results in a graph $G'$ such that there is at least one circular pair that is connected through $F$ in $G$ and it is not connected through $F'$ in $G'$ (see [51]).

In [48], the author introduced the notion of *well-connected* graph, which is a circular planar graph in which every circular pair is connected through $F$.

A *well-connected spider graph* $G = (\bar{F}, E)$ with $\ell \geq 0$ circles and $m = 4\ell + 3$ radii is a particular example of a critical circular planar graph, which is the graph corresponding to the following planar embedding. We start by placing a vertex set in the center of a disk $D$ and the $m$ boundary vertices of $\delta(F)$ in $\partial D$. Next, we draw straight lines, referred to as *radii*, from the central vertex to each of the boundary vertices. Then, we draw $\ell$ distinct concentric circumferences contained within the interior of $D$ whose center is the center of $D$. Now, we place a vertex for every intersection point of every circle and radius. The graph's edges are determined by these radii and circles, as shown in Figure 1.5.

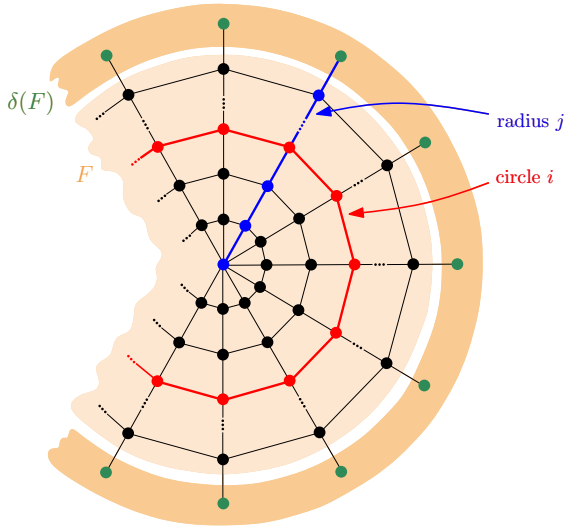


Figure 1.5: Representation of a spider graph.

The arithmetic conditions between the number of circles and radii ensure that the graph is indeed critical and well-connected, (see [54, Proposition 2.3 and Corollary 8.9]).

## 1.3 Electrical networks

In this section we will introduce a discrete vector calculus on Direct Current (DC) and Alternating Current (AC) electrical networks. A DC network is modeled mathematically as a graph with a real positive weight at each edge, which is the inverse of its *resistance*. Several detailed versions of calculus on DC electrical networks have been proposed (see for instance [7, 35, 36]).

For modeling AC networks there are different alternatives, depending on the characteristics of the network. In this work, we study the case of balanced three-phase networks in which all lines are inductive and "short", (*i.e.*, their length is shorter than 80km). In that case, the *susceptance to earth* of the lines can be neglected and the mathematical model of a network is a graph in which each physical connection between a pair of vertices is represented by a single edge characterized by a complex weight with nonnegative real part and nonpositive imaginary part called *admittance*, (see [96, 99]).

Discrete vector calculus on AC electrical networks has been less studied than the one on DC networks. In [30], some of the concepts of a version of calculus in networks with general complex weights are introduced, but without the structure of vector fields. We propose a generalization of the vector calculus and difference operators in [35] to include the case of AC networks.

**Definition 1.3.1.** An *electrical network* is a pair $\Gamma = (V, a)$ where $V$ is a finite nonempty set called *vertex set*, and $a \in \mathscr{C}(V \times V, \mathbb{C})$, called *admittance*, satisfies the following properties:

(i) $a = c - ib$ where $c, b \in \mathscr{C}^+(V \times V)$ and the kernel $c$ is called *conductance* whereas the

kernel $b$ is called *susceptance*.

(ii) $c$ and $b$ are symmetric and $c(x,x) = b(x,x) = 0$, for any $x \in V$.

In the particular case the network is operating in DC, $b = 0$, so the network $\Gamma = (V, c)$ is a real weighted graph. In a DC network, the kernel $r \in \mathscr{C}^+_\infty(V \times V)$ such that for every $(x,y) \in V \times V$, $r(x,y) = 0$ if $x = y$ and $r(x,y) = 1/c(x,y)$ if $x \neq y$ is named *resistance*. Also, we get that $r(x,y) = +\infty$ iff $x \neq y$ and $x \not\sim y$. Given $x, y \in V$, and a path from $x$ to $y$, we define the resistance of the path as the sum of the resistances of all edges in the path. We denote by $d_r(x,y)$ the *resistance distance* in the graph, that is defined as the minimum of the resistances of all existing paths from $x$ to $y$ if $x$ and $y$ belong to the same connected component of $G$ and as $d_r(x,y) = \infty$ otherwise.

An electrical network $\Gamma = (V, a)$ has an associated graph $G(\Gamma) = (V, E(\Gamma))$ called its "*network topology*". The set of edges of the network is $E(\Gamma) = \{e_{xy} \text{ such that } (x,y) \in \mathsf{supp}(a)\}$. Note that $E(\Gamma)$ is well defined because $a(x,y) \neq 0$ iff $a(y,x) \neq 0$. For any $e_{xy} \in E(\Gamma)$, we denote by $a(e_{xy})$ the value $a(x,y) = a(y,x) \neq 0$. Note that $a(x,x) = 0$ for any $x \in V$, so $(V, E(\Gamma))$ is a finite undirected simple graph without loops, *i.e.*, without edges from a vertex to itself. The inverse of the value of the admittance at an edge $e_{xy} \in E$, $\dfrac{1}{a(e_{xy})} = \left(\dfrac{c}{c^2+b^2} + i\dfrac{b}{c^2+d^2}\right)(x,y)$, is called the *impedance* of $e_{xy}$. The real and imaginary parts of the impedance are nonnegative.

All the concepts defined in the previous section can be considered for the graph $G(\Gamma) = (V, E(\Gamma))$ which is a topology of a network $\Gamma$, and we will denote them substituting the dependency of the graph from the dependency of the network. As an example, we will denote by $\mathscr{C}(\Gamma, \mathbb{C})$ the subspace $\mathscr{C}(G(\Gamma), \mathbb{C})$, and we will use the expression *network with boundary* to refer to a network whose topology is a graph with boundary. We will denote by $E$ the set of edges $E(\Gamma)$ when the electrical network $\Gamma$ is clear from the context.

For an AC network $\Gamma = (V, a)$ we consider the two DC networks $\Gamma_c = (V, c)$ and $\Gamma_b = (V, b)$, which we will call the conductance and susceptance networks of $\Gamma$, respectively. Note that $E(\Gamma) = E(\Gamma_c) \cup E(\Gamma_b)$.

For $x \in V$, we denote by $\kappa(x) \in \mathbb{C}$ the *weighted degree* of $x$, *i.e.*, $\kappa(x) = \displaystyle\int_V a(x,y)\, dy$. Given a subset $F \subseteq V$, we denote by $\kappa^F(x) \in \mathbb{C}$ the sum of weights of the edges adjacent to $x$ and to a vertex of $F$, *i.e.*, $\kappa^F(x) = \displaystyle\int_F a(x,y)\, dy$.

**Definition 1.3.2.** Given an electrical network $\Gamma = (V, a)$ with topology $G = (V, E)$, and a subset $F \subseteq V$, we define the *subnetwork* $\Gamma^F = (F, a_{|_{F\times F}})$. Note that its network topology is $G^F$.

### 1.3.1 Difference operators on a network

For an electrical network $\Gamma = (V, a)$, we will consider the derivative and divergence operators (which depend only on the topology of $\Gamma$), and we will also define discrete difference operators

depending on the admittance $a$ which are the discrete analogues (see [35]) to the *gradient*, to the *normal derivative*, and to the *Laplace-Beltrami operator* (see [33]).

We define the *gradient* as $\nabla = a\mathsf{d}$. So, it is the linear map $\nabla\colon \mathscr{C}(V,\mathbb{C}) \longrightarrow X(G)$, which assigns to each $u \in \mathscr{C}(V,\mathbb{C})$ the flow $\nabla u$, such that

$$\nabla u(x) = \sum_{y\sim x} a(x,y)(u(y)-u(x))e_{xy}, \quad \text{for each } x \in V.$$

The *Laplacian* of $\Gamma$ is the endomorphism of $\mathscr{C}(V,\mathbb{C})$ given by $\mathcal{L} = -\mathsf{div}\circ\nabla$. For any $u \in \mathscr{C}(V,\mathbb{C})$ and any $x \in V$, as $\nabla u$ is a flow, from Proposition 1.2.4:

$$\mathcal{L}(u)(x) = \sum_{y\in V} a(x,y)\big(u(x)-u(y)\big).$$

Given a subnetwork $\Gamma^F = (F, a_{|_{F\times F}})$, we denote its Laplacian as $\mathcal{L}^F$. Note that the restriction of the Laplacian to $\mathscr{C}(F,\mathbb{C})$, $\mathcal{L}|_{\mathscr{C}(F,\mathbb{C})}$, is equal to $\mathcal{L}^F$ iff $\Gamma^F$ is a connected component of $\Gamma$ or the union of several of them.

We denote by $\mathcal{L}_c$ and $\mathcal{L}_b$ the Laplacian of the conductance and susceptance (DC) networks of $\Gamma$, respectively. Clearly, $\mathcal{L} = \mathcal{L}_c - i\mathcal{L}_b$.

Several authors have considered a discrete version of the Green identities for DC networks, (see [46, 67]). The next result is a generalization to the case of AC networks.

**Proposition 1.3.3.** *Let $\Gamma = (V,a)$ be an electrical network whose decomposition in connected components is $\Gamma = \Gamma^{V_1} \sqcup ... \sqcup \Gamma^{V_s}$. Given $u, v \in \mathscr{C}(V,\mathbb{C})$ the following properties hold:*

*(i)* First Green Identity*,*

$$\int_V \mathcal{L}(u)\overline{v}dx = \frac{1}{2}\int_{V\times V} a(x,y)\big(u(x)-u(y)\big)\big(\overline{v}(x)-\overline{v}(y)\big)dxdy$$

*(ii)* Second Green Identity*,*

$$\int_V \mathcal{L}(u)\overline{v}dx = \int_V u\mathcal{L}(\overline{v})dx.$$

*(iii)* Gauss' Theorem*,*

$$\int_{V_i} \mathcal{L}(u)dx = 0, \quad \textit{for every } i = 1,...,s.$$

*Proof.* Given $u, v \in \mathscr{C}(V,\mathbb{C})$, by the definition of divergence, we get that

$$\int_V \mathcal{L}(u)\overline{v}dx = -\langle \mathsf{div}(\nabla u), v\rangle = \langle \nabla u, dv\rangle. \tag{1.2}$$

The first Green identity follows applying Lemma 1.2.2 to the last inner product, and considering that when we integrate over $V\times V$, we are summing the quantity $a(x,y)\big(u(x)-u(y)\big)\big(\overline{v}(x)-\overline{v}(y)\big)$ corresponding to each edge $e_{xy}$ twice.

The second identity follows directly from the first one. Gauss' theorem is obtained substituting $v = \chi_{V_i}$ in (1.2).

□

If $\Gamma$ is a DC network, then by Proposition 1.3.3-(i), its Laplacian is a positive semidefinite operator, and by Proposition 1.3.3-(ii), it is self-adjoint.

In the case $\Gamma$ is an AC network, for any $u, v \in \mathscr{C}(V, \mathbb{C})$, we have $\langle \mathcal{L}(u), v\rangle = \langle u, \overline{\mathcal{L}(\overline{v})}\rangle$, so $\mathcal{L}^* = \mathcal{C} \circ \mathcal{L} \circ \mathcal{C}$, and thus the Laplacian is a complex symmetric operator. As $\mathcal{L}_c^* = \mathcal{L}_c$ and $\mathcal{L}_b^* = \mathcal{L}_b$, we have that $\mathcal{L}^* = \mathcal{L}_c + i\mathcal{L}_b$. As a consequence, the real part of the Laplacian is the positive semidefinite operator $\Re(\mathcal{L}) = \mathcal{L}_c$ and the imaginary part of the Laplacian is the negative semidefinite operator $\Im(\mathcal{L}) = -\mathcal{L}_b$.

We define the *energy* of a network [35] as the bilinear form on $\mathscr{C}(V, \mathbb{C})$ given by $\mathcal{E}(u, v) = \langle u, \mathcal{L}(v)\rangle$, that is,

$$\mathcal{E}(u, v) = \int_V u\overline{\mathcal{L}(v)}dx = \frac{1}{2}\int_{V\times V} \overline{a}(x, y)\big(u(x) - u(y)\big)\big(\overline{v}(x) - \overline{v}(y)\big)dxdy.$$

For DC networks, the energy is a positive semidefinite symmetric form, that is, for any $u, v \in \mathscr{C}(V, \mathbb{C})$, we have $\mathcal{E}(u, v) = \mathcal{E}(v, u)$ and $\mathcal{E}(u, u) \geq 0$. Additionally, the restriction of the energy to $\mathscr{C}(V) \times \mathscr{C}(V)$ is a real bilinear form. For AC networks, $\mathcal{E}(u, v) = \langle u, \mathcal{L}_c(v)\rangle + i\langle u, \mathcal{L}_b(v)\rangle = \langle \mathcal{L}^*(u), v\rangle = \mathcal{E}(\overline{v}, \overline{u})$ for any $u, v \in \mathscr{C}(V, \mathbb{C})$; and the real and imaginary parts of $\mathcal{E}(u, u)$ are nonnegative for any $u \in \mathscr{C}(V, \mathbb{C})$.

**Lemma 1.3.4.** *Let $\Gamma = (V, a)$ be an electrical network and $u \in \mathscr{C}(V, \mathbb{C})$. Then, the following statements are equivalent:*

*(i)* *$u$ is constant on each connected component of $\Gamma$.*

*(ii)* $\mathcal{L}(u) = 0$.

*(iii)* $\mathcal{E}(u, u) = 0$.

*Proof.* The implications $(i) \implies (ii)$ and $(ii) \implies (iii)$ are trivial. In order to see that $(iii) \implies (i)$, notice that by the First Green Identity:

$$\mathcal{E}(u, u) = \sum_{\{x,y\}\in E} \overline{a(x, y)}\,|u(x) - u(y)|^2\,.$$

The real and imaginary parts in each summand of the previous expression are nonnegative, so if $\mathcal{E}(u, u) = 0$, then $u(x) = u(y)$ whenever $a(x, y) \neq 0$. □

As a consequence, a basis for the null space of $\mathcal{L}$ is $\{\chi_{V_1}, ..., \chi_{V_s}\}$, where $\Gamma = \Gamma^{V_1} \sqcup ... \sqcup \Gamma^{V_s}$ is the decomposition in connected components of $\Gamma$.

**Remark 1.3.5.** After fixing a labeling $\{x_1, ..., x_n\}$ on the vertex set $V$ of a network $\Gamma = (V, a)$, we denote by $\mathsf{L}$ the matrix corresponding to its combinatorial Laplacian, $\mathcal{L}$. The matrix $\mathsf{L}$ is called the *Admittance matrix* of $\Gamma$ if it is an AC network and the *Laplacian*

*matrix* of $\Gamma$ if it is a DC network. Denoting $a_{jk} \equiv a(x_j, x_k)$, $\mathsf{L}$ is the $n \times n$ singular complex symmetric matrix defined by:

$$\mathsf{L}(x_j, x_k) = \begin{cases} -a_{jk} & \text{if } \{x_j, x_k\} \in E \\ \sum_{t \neq j} a_{jt} & \text{if } j = k \\ 0 & \text{otherwise.} \end{cases} \tag{1.3}$$

If we write an admittance matrix as the sum of its real and imaginary parts, then $\mathsf{L} = \mathsf{L}_c - i\mathsf{L}_b$, where $\mathsf{L}_c$ and $\mathsf{L}_b$ are the Laplacian matrices of the conductance network $\Gamma_c = (V, c)$ and the susceptance network $\Gamma_b = (V, b)$, respectively.

For DC networks, the Laplacian matrix $\mathsf{L}$ is positive semidefinite. Moreover, it is an $M$-matrix, *i.e.* its off-diagonal entries are nonpositive and the real parts of its eigenvalues are nonnegative. Additionally, it is diagonally dominant, *i.e.*, $|\mathsf{L}(x,x)| \geq \sum_{y \neq x} |\mathsf{L}(x,y)|$ for every $x \in V$.

Given a network $\Gamma = (V, a)$, and $F \subset V$, the normal derivative of a function $u \in \mathscr{C}(V, \mathbb{C})$ with respect to $F$ is defined as the function in $\mathscr{C}(\delta(F), \mathbb{C})$ given by

$$\frac{\partial u}{\partial \mathsf{n}_{_F}}(x) = [\nabla u(x), n_{_F}(x)] = \sum_{y \in F} a(x,y)\big(u(x) - u(y)\big), \quad \text{for any } x \in \delta(F).$$

We remark that the normal derivative of a function $u$ with respect to $F$ only depends of the values of $u$ on the interior and exterior boundaries of $F$.

The following result is an extension of Proposition 1.3.3 to the case in which we integrate over a subset of vertices. It is also an extension of a result given in [35] for DC networks.

**Proposition 1.3.6.** *Given $u, v \in \mathscr{C}(V, \mathbb{C})$ and $F \subset V$ the following properties hold:*

*(i)* First Green Identity,

$$\begin{aligned} \int_F \mathcal{L}(u)\overline{v}dx = \; & \frac{1}{2}\int_{(\bar{F}\times\bar{F})\setminus(\delta(F)\times\delta(F))} a(x,y)\big(u(x)-u(y)\big)\big(\overline{v}(x)-\overline{v}(y)\big)dxdy \\ & - \int_{\delta(F)} \frac{\partial u}{\partial \mathsf{n}_{_F}}\overline{v}dx. \end{aligned}$$

*(ii)* Second Green Identity,

$$\int_F \big(\mathcal{L}(u)\overline{v} - u\mathcal{L}(\overline{v})\big)dx = \int_{\delta(F)} \left(u\,\frac{\partial \overline{v}}{\partial \mathsf{n}_{\mathsf{F}}} - \frac{\partial u}{\partial \mathsf{n}_{\mathsf{F}}}\overline{v}\right)dx.$$

*(iii)* Gauss' Theorem,

$$\int_F \mathcal{L}(u)dx = -\int_{\delta(F)} \frac{\partial u}{\partial \mathsf{n}_{_F}}dx.$$

*Proof.* For any $x \in F$, $\mathcal{L}(u)(x) = \sum_{y\in\bar{F}} a(x,y)\big(u(x)-u(y)\big)$, so we get

$$\begin{aligned}\int_F \mathcal{L}(u)\overline{v}dx &= \int_F\int_{\bar{F}} a(x,y)\big(u(x)-u(y)\big)\overline{v}(x)dydx\\ &= \int_{\bar{F}}\int_{\bar{F}} a(x,y)\big(u(x)-u(y)\big)\overline{v}(x)dydx\\ &\quad -\int_{\delta(F)}\int_{\bar{F}} a(x,y)\big(u(x)-u(y)\big)\overline{v}(x)dydx.\end{aligned}$$

Then, on one hand,

$$\int_{\bar{F}}\int_{\bar{F}} a(x,y)\big(u(x)-u(y)\big)\overline{v}(x)dydx = \frac{1}{2}\int_{\bar{F}\times\bar{F}} a(x,y)\big(u(x)-u(y)\big)\big(\overline{v}(x)-\overline{v}(y)\big)dxdy,$$

and on the other hand,

$$\int_{\delta(F)}\int_{\bar{F}} a(x,y)\big(u(x)-u(y)\big)\overline{v}(x)dydx = \int_{\delta(F)}\overline{v}(x)\left(\frac{\partial u}{\partial \mathsf{n}_F}(x)+\int_{\delta(F)} a(x,y)\big(u(x)-u(y)\big)dy\right)dx,$$

so we obtain the first Green identity. The second Green identity and Gauss' theorem follow trivially from the first Green identity. □

Finally, we introduce the following notations and lemma, which are generalizations of the ones in [35] to include the case of AC networks.

Given $F \subset V$ and a kernel $K$, for each $x \in \delta(F)$ and each $y \in V$, we denote by $\frac{\partial K}{\partial \mathsf{n}_x}(x,y)$ the value $\frac{\partial K_y}{\partial \mathsf{n}_F}(x)$; and for each $x \in V$ and each $y \in \delta(F)$, we denote by $\frac{\partial K}{\partial \mathsf{n}_y}(x,y)$ the value $\frac{\partial K^x}{\partial \mathsf{n}_F}(y)$. When $K \in \mathscr{C}(V\times V,\mathbb{C})$, we have $\frac{\partial K}{\partial \mathsf{n}_x} \in \mathscr{C}(\delta(F)\times V,\mathbb{C})$ and $\frac{\partial K}{\partial \mathsf{n}_y} \in \mathscr{C}(V\times\delta(F),\mathbb{C})$. Meanwhile, when $K \in \mathscr{C}(V\times V)$, we have $\frac{\partial K}{\partial \mathsf{n}_x} \in \mathscr{C}(\delta(F)\times V)$ and $\frac{\partial K}{\partial \mathsf{n}_y} \in \mathscr{C}(V\times\delta(F))$.

**Lemma 1.3.7.** *Let $K$ be a complex, respectively real, kernel on $V$, then we have*

$$\frac{\partial^2 K}{\partial \mathsf{n}_x\partial \mathsf{n}_y} = \frac{\partial^2 K}{\partial \mathsf{n}_y\partial \mathsf{n}_x},$$

*and both are complex, respectively real, kernels on $\delta(F)$. In addition, for each $x, y \in \delta(F)$:*

$$\begin{aligned}\frac{\partial^2 K}{\partial \mathsf{n}_x\partial \mathsf{n}_y} = &\ \kappa^F(x)\kappa^F(y)K(x,y) - \kappa^F(x)\int_F a(y,z)K(x,z)dz\\ &-\kappa^F(y)\int_F a(x,z)K(z,y)dz + \int_F\int_F a(x,u)a(y,z)K(u,z)dudz.\end{aligned}$$

*Moreover, $\frac{\partial^2 K}{\partial \mathsf{n}_x\partial \mathsf{n}_y}$ is a symmetric kernel when $K$ is.*

**Remark 1.3.8.** The physical laws governing the current transmission in electrical networks can be stated using the difference operators that we have defined. For AC networks, the potential in the network can be represented by a function $u \in \mathscr{C}(V, \mathbb{C})$. Then, by Ohms' law, $-\nabla u$ represents the flow of electrical current. That is, each of the coefficients in the coordinate basis of $-\nabla u(x)$ is equal to the current flowing from $x$ to each of its neighbours. Also, by Kirchhoff's Current Law, $\mathcal{L}(u)$ is the function assigning to each vertex the current injected at it when the potential at the network is $u$. Then, $u\overline{\mathcal{L}(u)}$ is the function assigning to each vertex the apparent power injected at it when the potential at the network is $u$, and thus $\mathcal{E}(u,u)$ is equal to the total power dissipated at the network when the potential is $u$. For DC networks, the potential in the network can be represented by $u \in \mathscr{C}(V)$ and the rest of results are analogous, with the additional result that the dissipated power in the network is always nonnegative.

## 1.4 Boundary value problems

The objective of this section is to review several results about the *Dirichlet and Poisson problems* on DC networks that can be found in [17, 35, 36], and to extend them to the case of AC networks. We study the following problem.

*Given an electrical network* $\Gamma$, $F \subseteq V$, $h \in \mathscr{C}(F, \mathbb{C})$ *and* $g \in \mathscr{C}(F^c, \mathbb{C})$, *find* $u \in \mathscr{C}(V, \mathbb{C})$ *such that*

$$\mathcal{L}(u) = h \ \text{ on } \ F, \quad u = g \ \text{ on } \ F^c. \tag{1.4}$$

When $F = V$ this is called the *Poisson problem* and when $F \subsetneq V$ this is called the *Dirichlet problem*. We have that $F^c = \delta(F) \sqcup \mathrm{Ext}(F)$, but because the values of the Laplacian of a function at $F$ only depend on the values of the function at $\bar{F}$, the set of solutions of (1.4) only depends on the values of $g$ at $\delta(F)$, so it is called a *boundary value problem on* $F$.

*The associated homogeneous boundary value problem consists in finding* $u \in \mathscr{C}(V, \mathbb{C})$ *such that*

$$\mathcal{L}(u) = 0 \ \text{ on } \ F, \quad u = 0 \ \text{ on } \ F^c. \tag{1.5}$$

**Lemma 1.4.1.** *Let* $\Gamma = \Gamma^{V_1} \sqcup ... \sqcup \Gamma^{V_s}$ *be the decomposition in connected components of* $\Gamma$. *Then, the set of solutions of the homogeneous boundary value problem (1.5) is the vector subspace* $\mathcal{V}$ *of* $\mathscr{C}(F, \mathbb{C})$ *spanned by* $\left\{\chi_{V_i} \text{ such that } V_i \subseteq F\right\}$.

*Proof.* Clearly, any function of $\mathcal{V}$ is a solution of (1.5). Now, let $u \in \mathscr{C}(F, \mathbb{C})$ be a solution of (1.5). Then,

$$\mathcal{E}(u,u) = \int_V u\overline{\mathcal{L}(u)}dx = \int_F u\overline{\mathcal{L}(u)}dx + \int_{F^c} u\overline{\mathcal{L}(u)}dx = 0,$$

so $u$ is a linear combination of $\left\{\chi_{V_1}, ..., \chi_{V_s}\right\}$. As $u = 0$ in $F^c$, $u$ must be equal to zero in each $V_i$ such that $V_i \cap F^c \neq \emptyset$, so $u \in \mathcal{V}$. □

**Proposition 1.4.2.** *Let $\Gamma = (V, a)$ be an electrical network and let $\Gamma = \Gamma^{V_1} \sqcup ... \sqcup \Gamma^{V_s}$ be its decomposition in connected components. Then, (1.4) has a solution if and only if $\int_{V_i} h\, dx = 0$ for each $i$ such that $V_i \subseteq F$. Moreover, if the problem has a solution, then there is a unique solution $v$ such that $\int_{V_i} v\, dx = 0$ for each $i$ such that $V_i \subseteq F$.*

*Proof.* In the case (1.4) has a solution, then, for any solution $u$, the set of all its solutions is $u + \mathcal{V}$.

Consider the problem (1.4) of *finding $u \in \mathscr{C}(V, \mathbb{C})$ such that*

$$\mathcal{L}(u) = h - \mathcal{L}(g) \text{ on } F, \quad u = 0 \text{ on } F^c. \tag{1.6}$$

Then $u$ is a solution to (1.6) iff $u + g$ is a solution to (1.4).

We denote by $\mathscr{M} : \mathscr{C}(F, \mathbb{C}) \longrightarrow \mathscr{C}(F, \mathbb{C})$ the linear operator $\mathscr{M}(u) = \mathcal{L}(u)$ on $F$ for each $u \in \mathscr{C}(F, \mathbb{C})$. Considering the inner product on $\mathscr{C}(F, \mathbb{C})$ induced by the standard one on $\mathscr{C}(V, \mathbb{C})$, we have that, for every $u, v \in \mathscr{C}(F, \mathbb{C})$:

$$\langle \mathscr{M}(u), v\rangle = \int_F \mathscr{M}(u)\overline{v}dx = \int_V \mathcal{L}(u)\overline{v}dx = \int_V u\mathcal{L}(\overline{v})dx = \int_F u\mathscr{M}(\overline{v})dx = \langle u, \overline{\mathscr{M}(\overline{v})}\rangle,$$

so $\mathscr{M}^* = \mathcal{C} \circ \mathscr{M} \circ \mathcal{C}$, and thus $\mathscr{M}$ is a symmetric operator. Now, $\ker(\mathscr{M}) = \mathcal{V}$. Moreover, $u \in \ker(\mathscr{M}^*)$ iff $\mathscr{M}(\overline{u}) = 0$, that is, iff $\overline{u} \in \ker(\mathscr{M})$. As $\overline{u} \in \mathcal{V}$ iff $u \in \mathcal{V}$, we have that $\ker(\mathscr{M}) = \ker(\mathscr{M}^*)$, and, by the Fredholm alternative, $\mathrm{Img}(\mathscr{M}) = \mathcal{V}^\perp$.

Then, (1.6) has a solution iff $\langle h - \mathcal{L}(g), \chi_{V_i}\rangle = 0$ for each $i$ such that $V_i \subseteq F$. This is equivalent to saying $\int_{V_i} h\, dx = \int_{V_i} \mathcal{L}(g)\, dx = 0$ for each $i$ such that $V_i \subseteq F$, and the last equality follows from Gauss' Theorem.

To prove the uniqueness, we see that there is a unique solution $w$ to (1.6) such that $w \in \mathcal{V}^\perp$. This is equivalent to that $v = w + g$ is the only solution to (1.4) satisfying that

$$\int_{V_i} v\, dx = \int_{V_i} w\, dx = 0$$

for each $i$ such that $V_i \subseteq F$.

□

We say that a function $u$ is harmonic on $F$ when $\mathcal{L}(u) = 0$ on $F$. The particular case of (1.4) in which $h = 0$ consists in, given the values of a function at $F^c$, seeking for an extension of the function at $F$ that is harmonic on $F$. In this case, any solution must be constant on each $i$ such that $V_i \subseteq F$, so we get the following result.

**Corollary 1.4.3.** *Given an electrical network $\Gamma$, $F \subseteq V$ and $g \in \mathscr{C}(F^c, \mathbb{C})$, the boundary value problem of finding $u \in \mathscr{C}(V, \mathbb{C})$ such that*

$$\mathcal{L}(u) = 0 \text{ on } F, \quad u = g \text{ on } F^c, \tag{1.7}$$

*always has a solution. Moreover, it has a unique solution that is equal to zero on every connected component of the network that is contained in $F$, that we denote by $u_g$.*

**Remark 1.4.4.** Let $v$ be a solution of (1.7). Then $\frac{\partial v}{\partial \mathsf{n}_F} = \frac{\partial u_g}{\partial \mathsf{n}_F}$, $\mathcal{L}(v) = \mathcal{L}(u_g)$ and $\mathcal{E}(v,v) = \mathcal{E}(u_g, u_g)$.

In [30], a uniqueness result for a Dirichlet problem that is similar to (1.7) was obtained. The problem there is partially more general than (1.7) in the sense that they consider the possibility of adding a Schrödinger potential with some restrictions and the possibility of having negative susceptance, but it is also partially more restrictive than (1.7) in the sense that they only study the problem for connected networks. In the connected case, we obtain the same uniqueness result immediately from Corollary 1.4.3.

**Corollary 1.4.5.** *If $\Gamma$ is a connected network and $h = 0$, then any Dirichlet problem has a unique solution and the set of solutions to the Poisson problem is the set of constant functions on $V$.*

Let $\Gamma = \Gamma^{V_1} \sqcup ... \sqcup \Gamma^{V_s}$ be the decomposition in connected components of $\Gamma$, and $F \subset V$. We denote by $F_0$ the union of the $V_i$ such that $V_i \subseteq F$, and $F_1 = F \setminus F_0$. Analogously to the operator $\mathscr{M}$ defined in the proof of Proposition 1.4.2, we denote by $\mathscr{M}_{F_1} \colon \mathscr{C}(F_1, \mathbb{C}) \longrightarrow \mathscr{C}(F_1, \mathbb{C})$ the linear operator such that for each $u \in \mathscr{C}(F_1, \mathbb{C})$, $\mathscr{M}_{F_1}(u) = \mathcal{L}(u)$ on $F_1$, which is an automorphism.

**Definition 1.4.6.** We define the *Green operator* of $F$ as $\mathscr{J} = {\mathscr{M}_{F_1}}^{-1}$, which is an automorphism of $\mathscr{C}(F_1, \mathbb{C})$. For any $h \in \mathscr{C}(F_1, \mathbb{C})$, $u = \mathscr{J}(h)$ is the unique solution to the boundary problem $\mathcal{L}(u) = h$ on $F_1$ and $u = 0$ on $F^c \sqcup F_0$.

We define the *Poisson operator* of $F$ as the linear operator $\mathscr{K} : \mathscr{C}(F^c, \mathbb{C}) \longrightarrow \mathscr{C}(V \setminus F_0, \mathbb{C})$ such that, for each $g \in \mathscr{C}(F^c, \mathbb{C})$, $\mathscr{K}(g) = u_g$. That is, $\mathscr{K}(g)$ is the unique function satisfying $\mathcal{L}(\mathscr{K}(g)) = 0$ on $F$, $\mathscr{K}(g) = g$ on $F^c$ and $\mathscr{K}(g) = 0$ on $F_0$.

**Lemma 1.4.7.** *The Green operator $\mathscr{J}$ is symmetric with respect to the inner product on $\mathscr{C}(F_1, \mathbb{C})$ induced by the standard one on $\mathscr{C}(V, \mathbb{C})$.*

*Proof.* Given $g, h \in \mathscr{C}(F_1, \mathbb{C})$, we denote $u = \mathscr{J}(g)$ and $v = \mathscr{J}(\overline{h})$. Then we have $\mathcal{L}(u) = g$ and $\mathcal{L}(v) = \overline{h}$ on $F_1$, and thus:

$$\langle \mathscr{J}(g), h \rangle = \int_{F_1} \mathscr{J}(g)\overline{h} dx = \int_V u\mathcal{L}(v) dx = \int_V \mathcal{L}(u) v dx = \int_{F_1} g\, \overline{\mathscr{J}(\overline{h})} dx = \langle g, \overline{\mathscr{J}(\overline{h})} \rangle,$$

so $\mathscr{J}^* = \mathcal{C} \circ \mathscr{J} \circ \mathcal{C}$. □

The kernel $J \in \mathscr{C}(F_1 \times F_1, \mathbb{C})$ associated with the Green operator $\mathscr{J}$ on $F$, is called the *Green kernel*. By the previous lemma, it is symmetric. The matrix associated with $\mathscr{M}_{F_1}$ is $\mathsf{L}(F_1; F_1)$, so the matrix associated with $\mathscr{J}$ is $\mathsf{L}(F_1; F_1)^{-1}$.

We can extend the Poisson operator $\mathscr{K}$ on $F$ to an endomorphism of $\mathscr{C}(V \setminus F_0, \mathbb{C})$ such that the image of any vector in $\mathscr{C}(F_1, \mathbb{C})$ is equal to zero. By the Kernel Theorem, it has an associated kernel $K \in \mathscr{C}((V \setminus F_0) \times F^c, \mathbb{C})$, which is called the *Poisson kernel*.

The following result gives a characterization of the Green and Poisson kernels as solutions of boundary value problems, and a relation between them.

**Proposition 1.4.8.** *For every $y \in F_1$, the function $J_y$ is determined by $\mathcal{L}(J_y) = \varepsilon_y$ on $F_1$. For every $y \in F^c$, the function $K_y$ is determined by $\mathcal{L}(K_y) = 0$ on $F$, $K_y = \varepsilon_y$ on $F^c$ and $K_y = 0$ on $F_0$. Furthermore,*

$$K(x,y) = \varepsilon_y(x) - \left(\frac{\partial J}{\partial \mathsf{n}_y}\right)(x,y), \quad \text{for every } x \in V \setminus F_0 \text{ and } y \in F^c.$$

*Moreover, $\frac{\partial K}{\partial \mathsf{n}_x} \in \mathscr{C}(\delta(F) \times \delta(F), \mathbb{C})$ and, for every $x, y \in \delta(F)$,*

$$\left(\frac{\partial K}{\partial \mathsf{n}_x}\right)(x,y) = \varepsilon_y(x)\kappa^F(x) - \left(\frac{\partial^2 J}{\partial \mathsf{n}_x \partial \mathsf{n}_y}\right)(x,y).$$

*As a consequence, $\frac{\partial K}{\partial \mathsf{n}_x}$ is symmetric on $\mathscr{C}(\delta(F) \times \delta(F), \mathbb{C})$.*

*Proof.* By the correspondence between kernels and operators, for every $y \in F_1$, $J_y = \mathscr{J}(\varepsilon_y)$. As $\mathscr{J}$ is an automorphism, this is equivalent to $\mathcal{L}(J_y) = 0$ on $F$. Similarly, for every $y \in F^c$, $K_y = \mathscr{K}(\varepsilon_y)$ and thus $u = K_y$ is the unique solution of the boundary problem $\mathcal{L}(u) = 0$ on $F$, $u = \varepsilon_y$ on $F^c$ and $u = 0$ on $F_0$. That problem is equivalent to seeking for $v \in \mathscr{C}(F_1, \mathbb{C})$ such that $\mathcal{L}(v) = -\mathcal{L}(\varepsilon_y)$ on $F_1$, in the sense that $K_y = \varepsilon_y - \mathscr{J}(\mathcal{L}(\varepsilon_y)|_{F_1})$.

Now, for every $x \in F_1$, $\mathcal{L}(\varepsilon_y)(x) = \int_V a(x,z)(\varepsilon_y(x) - \varepsilon_y(z))\,dz = -a(x,y)$, so we get:

$$\begin{aligned}\mathscr{J}(\mathcal{L}(\varepsilon_y)|_{F_1}) = \; & -\int_{F_1} J(x,z)a_y(z)dz \\ & \int_{F_1} a(y,z)\,(J(x,y) - J(x,z))\,dz = \left(\frac{\partial J}{\partial \mathsf{n}_y}\right)(x,y).\end{aligned}$$

Now, we define the kernel $\varepsilon \in \mathscr{C}(F^c \times F^c, \mathbb{C})$ as $\varepsilon(x,y) = \varepsilon_y(x)$ for every $x, y \in F^c$. The expression of $\frac{\partial K}{\partial \mathsf{n}_x}$ follows from the fact that, for every $x \in \delta(F)$:

$$\frac{\partial \varepsilon}{\partial \mathsf{n}_x}(x,y) = \frac{\partial \varepsilon_y}{\partial \mathsf{n}_F}(x) = \int_F a(x,z)\,(\varepsilon(x,y) - \varepsilon(x,z))\,dz = \varepsilon_y(x)\kappa^F(x).$$

Clearly, $\frac{\partial \varepsilon}{\partial \mathsf{n}_x} \in \mathscr{C}(\delta(F) \times \delta(F), \mathbb{C})$. Moreover, $\frac{\partial J}{\partial \mathsf{n}_y} \in \mathscr{C}(F_1 \times \delta(F), \mathbb{C})$, so also $\frac{\partial^2 J}{\partial \mathsf{n}_x \partial \mathsf{n}_y} \in \mathscr{C}(\delta(F) \times \delta(F), \mathbb{C})$; and thus $\frac{\partial K}{\partial \mathsf{n}_x} \in \mathscr{C}(\delta(F) \times \delta(F), \mathbb{C})$. The symmetry of this kernel follows from Lemma 1.3.7. □

**Remark 1.4.9.** In the particular case of (1.4) in which $\Gamma$ is a DC electrical network, $h \in \mathscr{C}(F)$ and $g \in \mathscr{C}(F^c)$, we can restrict the problem to seek only for real solutions, *i.e.*, *to seek for $u \in \mathscr{C}(V)$ such that*

$$\mathcal{L}(u) = h \;\text{ on }\; F, \quad u = g \;\text{ on }\; F^c. \tag{1.8}$$

Then, restricting to real function spaces, we can obtain for (1.8) results that are analogous to all the results in the section. As a consequence, in that case, the solution $v$ in Proposition 1.4.2 and the solution $u_g$ in Corollary 1.4.3 are real. Because of that, we can consider the real restrictions of the Green and Poisson operators, that we also denote as $\mathscr{J} : \mathscr{C}(F_1) \longrightarrow \mathscr{C}(F_1)$ and $\mathscr{K} : \mathscr{C}(F^c) \longrightarrow \mathscr{C}(V \setminus F_0)$, respectively. Its associated Green and Poisson kernels are real and also satisfy Lemma 1.4.7 and Proposition 1.4.8, plus the fact that, in addition, $\frac{\partial K}{\partial \mathsf{n}_x} \in \mathscr{C}(\delta(F) \times \delta(F))$.

## 1.5 The Dirichlet-to-Neumann map

Consider an electrical network $\Gamma = (V, a)$ and $F \subset V$. Recall that for any function $g \in \mathscr{C}(F^c, \mathbb{C})$, the Poisson operator gives a solution $\mathscr{K}(g) = u_g \in \mathscr{C}(V, \mathbb{C})$ to (1.7), that is, an extension of $g$ to all $V$ that is harmonic on $F$. This section is devoted to the study of the relationship between $g$ and $\mathcal{L}(u_g)$, which is given by the following linear operator.

**Definition 1.5.1.** Given an AC (respectively DC) electrical network and $F \subset V$, the *Dirichlet-to-Neumann map* is the following endomorphism $\Lambda\colon \mathscr{C}(F^c, \mathbb{C}) \longrightarrow \mathscr{C}(F^c, \mathbb{C})$ (respectively $\Lambda\colon \mathscr{C}(F^c) \longrightarrow \mathscr{C}(F^c)$) defined for any $g \in \mathscr{C}(F^c, \mathbb{C})$ (respectively $g \in \mathscr{C}(F^c)$) as:

$$\Lambda(g) = \frac{\partial u_g}{\partial \mathsf{n}_F} + \mathcal{L}^{F^c}(g) = \mathcal{L}(u_g) = (\mathcal{L} \circ \mathscr{K})(g).$$

Note that, because of Remark 1.4.4, the definition of the Dirichlet-to-Neumann map is independent of the chosen solution of (1.7).

In the literature, the Dirichlet-to-Neumann map is only defined for networks with boundary. For AC networks, it is defined as the function $\Upsilon\colon \mathscr{C}(\delta(F), \mathbb{C}) \longrightarrow \mathscr{C}(\delta(F), \mathbb{C})$ such that, for any $g \in \mathscr{C}(\delta(F), \mathbb{C})$, $\Upsilon(g) = \dfrac{\partial u_g}{\partial \mathsf{n}_F}$. Similarly, for DC networks, it is defined as the function $\Upsilon\colon \mathscr{C}(\delta(F)) \longrightarrow \mathscr{C}(\delta(F))$ such that, for any $g \in \mathscr{C}(\delta(F))$, $\Upsilon(g) = \dfrac{\partial u_g}{\partial \mathsf{n}_F}$. Note that, for networks with boundary, our definition agrees with this one, *i.e.* $\Lambda = \Upsilon$. This is because the subnetwork of $\Gamma$ corresponding to $F^c$ is $\Gamma^{F^c} = (F^c, 0)$, so $E(\Gamma^{F^c}) = \emptyset$ and thus its Laplacian $\mathcal{L}^{F^c}$ is zero.

For DC networks, the Dirichlet-to-Neumann map was considered in [52]. Later, in [10], it is proved that the Dirichlet-to-Robin map, which is a generalization of the Dirichlet-to-Neumann map to the case of a Schrödinger potential, is self-adjoint and positive semidefinite. The characterization of possible Dirichlet-to-Neumann maps of networks with complex weights at the edges whose imaginary parts are not necessarily nonpositive was first derived in [78]. It was later rediscovered independently in [87]. A generalization of the Dirichlet-to-Robin map to these networks with complex weights for certain complex Schrödinger potentials was defined in [30].

The extension of the map to general electrical networks will allow us to introduce in Section 1.7 the effective admittance from this map. This will allow us in Section 3.3 to give a novel physical interpretation to the product of the conductance of an edge by its effective resistance and, as a consequence, to the Algorithm 1 of spectral sparsification of networks.

We can also give the following physical interpretation to the Dirichlet-to-Neumann map. Under the condition that there is zero injected current at the vertices of $F$ for any potential, the values of a potential at $F^c$ uniquely determine the values of that potential at the interior boundary of $F$, and thus, they also uniquely determine the values of injected current at $F^c$. Moreover, the relationship between potential at $F^c$ and injected current at $F^c$ is linear.

In the electrical networks of the real world usually there is a subset of vertices $F$ that

are not associated to any generator or consumer in which there is never injected current, and thus the Dirichlet-to-Neumann map allows us to study the relationship between current and voltage in the rest of the vertices without having to calculate the voltage at $F$. Another practical application of this discrete operator is that, for networks with boundary, it is a mimetic discretization of the continuous Dirichlet-to-Neumann map, that is defined as follows in [6].

Let $\Omega \subseteq \mathbb{R}^n$ be a bounded connected open set with $n \geq 2$ and a bounded measurable conductivity $\sigma$ which satisfies $\lambda \geq \sigma \geq \lambda^{-1}$ almost everywhere in $\Omega$ for some $\lambda > 0$. Given a potential $g \in H^{1/2}(\partial\Omega)$ in the trace space on the boundary $\partial\Omega$, the induced potential $u_g$ on $\Omega$ solves the Dirichlet problem of finding $u \in H^1(\Omega)$ such that

$$\nabla \cdot (\sigma \nabla u) = 0 \quad \text{in } \Omega, \quad u|_{\partial\Omega} = g.$$

The Dirichlet-to-Neumann map, (see [6]), is defined as the operator $\Lambda\colon H^{1/2}(\partial\Omega) \longrightarrow H^{1/2}(\partial\Omega)$ such that

$$\Lambda_\sigma(g) = \left(\sigma \frac{\partial u_g}{\partial \mathsf{n}}\right)\Big|_{\partial\Omega},$$

for every $g \in H^{1/2}(\partial\Omega)$, where $\mathsf{n}$ denotes the outer unit normal vector to $\partial\Omega$.

Roughly speaking, $H^1(\Omega)$ is the subset of the Hilbert space of square-integrable functions $L^2(\Omega)$ whose weak derivatives belong to $L^2(\Omega)$, and therefore with weak gradient in $L^2(\Omega)$. These functions can be extended to functions on $\partial\Omega$. The set of these extensions is $H^{1/2}(\partial\Omega)$, which is a subspace of functions of $L^2(\partial\Omega)$ which have certain regularity. The consideration of these spaces allows the variational treatment of the problem and the proof that there is a solution (in $H^1(\Omega)$). The detailed definition and properties of these spaces can be found in [3, 31].

The knowledge of the properties of the discrete Dirichlet-to-Neumann operator will allow us to study the discrete problem analogous to *Calderón's inverse conductivity problem*, which will be the objective of Chapter 2.

The bilinear form on $\mathscr{C}(F^c, \mathbb{C})$ associated to the Dirichlet-to-Neumann operator is given, for every $g, h \in \mathscr{C}(F^c, \mathbb{C})$, by:

$$\langle h, \Lambda(g)\rangle = \int_V h\overline{\Lambda(g)}dx = \langle u_h, \mathcal{L}(u_g)\rangle = \mathcal{E}(u_h, u_g).$$

By the First Green identity, and considering that $\mathcal{L}(u_g) = 0$ on $F$, we have that

$$\begin{aligned}\langle h, \Lambda(g)\rangle &= \int_{\delta(F)} u_h \overline{\frac{\partial u_g}{\partial \mathsf{n}_F}}dx + \int_{F^c} h\overline{\mathcal{L}^{F^c}(g)}dx \\ &= \frac{1}{2}\int_{V\times V} \overline{a}(x,y)\big(u_h(x) - u_h(y)\big)\big(\overline{u_g}(x) - \overline{u_g}(y)\big)dxdy.\end{aligned}$$

**Proposition 1.5.2.** *Let $\Gamma = \Gamma^{V_1} \sqcup \ldots \sqcup \Gamma^{V_s}$ be the decomposition in connected components of $\Gamma$, and $F \subset V$. The Dirichlet-to-Neumann map $\Lambda$ is symmetric, singular, its real part is*

*positive semidefinite and its imaginary part is negative semidefinite. Moreover, its null space is the set of functions that are constant on each $V_i \cap F^c$ that is not empty. Furthermore, the symmetric kernel $N \in \mathscr{C}(F^c \times F^c, \mathbb{C})$ of $\Lambda$ is:*

$$N = L|_{F^c \times F^c} - \frac{\partial^2 J}{\partial \mathsf{n}_x \partial \mathsf{n}_y}.$$

*Proof.* For every $g, h \in \mathscr{C}(F^c, \mathbb{C})$, we have that

$$\begin{aligned}\langle \Lambda(g), h\rangle - \langle g, \overline{\Lambda(\overline{h})}\rangle &= \int_V \Lambda(g)\overline{h} - g\Lambda(\overline{h})dx \\ &= \int_{\delta(F)} \left( \frac{\partial u_g}{\partial \mathsf{n}_\mathsf{F}} u_{\overline{h}} - u_g \frac{\partial u_{\overline{h}}}{\partial \mathsf{n}_\mathsf{F}} \right) dx + \int_{F^c} \left( \mathcal{L}^{F^c}(g)\overline{h} - g\mathcal{L}^{F^c}(\overline{h}) \right) dx = 0,\end{aligned}$$

where the integral in $\delta(F)$ is equal to zero by the Second Green Identity on $F$, and the integral in $F^c$ is equal to zero by the Second Green Identity on the whole subnetwork $\Gamma^{F^c}$. As a consequence, $\Lambda^* = \mathcal{C} \circ \Lambda \circ \mathcal{C}$, so $\Lambda$ is symmetric.

On the other hand, for any $g \in \mathscr{C}(F^c, \mathbb{C})$, it is satisfied that

$$\begin{aligned}\langle \Lambda(g), g\rangle &= \overline{\mathcal{E}(u_g, u_g)} = \frac{1}{2}\int_{V\times V} a(x,y)\big|u_g(x) - u_g(y)\big|^2 dxdy \\ &= \frac{1}{2}\int_{V\times V} c(x,y)\big|u_g(x) - u_g(y)\big|^2 dxdy \\ &\quad -i\frac{1}{2}\int_{V\times V} b(x,y)\big|u_g(x) - u_g(y)\big|^2 dxdy.\end{aligned}$$

Considering that $\langle \Lambda^*(g), g\rangle = \overline{\langle g, \Lambda^*(g)\rangle} = \overline{\langle \Lambda(g), g\rangle}$; it is clear that $\langle \Re(\Lambda)(g), g\rangle \geq 0$ and $\langle \Im(\Lambda)(g), g\rangle \leq 0$.

Now, as in the previous section, if we denote by $F_0$ the union of the $V_i$ such that $V_i \subseteq F$, then $F_1 = F \setminus F_0$ is the union of the $V_i$ such that $V_i \cap F^c \neq \emptyset$. For any $g \in \mathscr{C}(F^c, \mathbb{C})$, $\Lambda(g) = 0$ iff $\mathcal{L}(u_g) = 0$ iff $u_g$ is constant at each $V_i$. If the last condition holds, it is clear that $g$ is constant on each $V_i \cap F^c$ such that $V_i \subseteq F_1$. Suppose now that $g = \sum_{i:V_i\subseteq F_1} k_i \chi_{V_i \cap F^c}$ with each $k_i \in \mathbb{C}$. Next, we will prove that for this $g$, $u_g$ is piecewise constant on each $V_i$, which is enough to demonstrate the claim in the proposition about the null space of $\Lambda$.

By definition, $u_g$ is the unique solution to the boundary problem of finding $u \in \mathscr{C}(V \setminus F_0, \mathbb{C})$ such that $\mathcal{L}(u) = 0$ on $F$ and $u = g$ on $F^c$. We consider the equivalent problem of seeking for $v \in \mathscr{C}(F_1, \mathbb{C})$ such that $\mathcal{L}(v) = -\mathcal{L}(g)$ on $F_1$.

The unique solution to this last problem is $v = \sum_{i:V_i\subseteq F_1} k_i \chi_{V_i \cap F}$, because

$$\mathcal{L}\Big(\sum_{i:V_i\subseteq F_1} k_i \chi_{V_i\cap F}\Big) = \sum_{i:V_i\subseteq F_1} k_i \mathcal{L}(\chi_{V_i\cap F}) = \sum_{i:V_i\subseteq F_1} k_i \mathcal{L}(\chi_{V_i} - \chi_{V_i\cap F^c}) = -\mathcal{L}(g).$$

Then, $u_g = \sum_{i:V_i\subseteq F_1} k_i \chi_{V_i\cap F} + g = \sum_{i:V_i\subseteq F_1} k_i \chi_{V_i}$, so $u_g$ is piecewise constant on each $V_i$.

On the other hand, denoting as $L^{F^c}$ the kernel of $\mathcal{L}^{F^c}$, by the definition of $\Lambda$, we have that $N = L^{F^c} + \frac{\partial K}{\partial \mathsf{n}_x}$. As a consequence, from Proposition 1.4.8, we get that for every $x, y \in F^c$:

$$N(x,y) = L^{F^c}(x,y) + \left(\frac{\partial K}{\partial \mathsf{n}_x}\right)(x,y) = L^{F^c}(x,y) + \varepsilon_y(x)\kappa^F(x) - \left(\frac{\partial^2 J}{\partial \mathsf{n}_x \partial \mathsf{n}_y}\right)(x,y).$$

For every $x, y \in F^c$, we have that

$$L^{F^c}(x,y) = L^{F^c}(\varepsilon_y)(x) = \int_{F^c} a(x,z)(\varepsilon_y(x) - \varepsilon_y(z))\, dz,$$

$$L(x,y) = \mathcal{L}(\varepsilon_y)(x) = \int_{V} a(x,z)(\varepsilon_y(x) - \varepsilon_y(z))\, dz,$$

so $L(x,y) = L^{F^c}(x,y)$ except when $x = y \in \delta(F)$, for which $L(x,x) = L^{F^c}(x,x) + \kappa^F(x)$. Therefore, we obtain the desired expression of the kernel $N$. □

**Corollary 1.5.3.** *If $\Gamma$ is a DC network, then the Dirichlet-to-Neumann map $\Lambda$ is self-adjoint and positive semidefinite. Moreover, $N \in \mathscr{C}(F^c \times F^c)$.*

**Remark 1.5.4.** After fixing a labeling $\{x_1, ..., x_n\}$ on the vertex set $V$ of a network $\Gamma = (V, a)$, we denote by $\mathsf{N} \in \mathscr{M}_{|F^c|\times|F^c|}(\mathbb{C})$ the matrix corresponding to the Dirichlet-to-Neumann map, $\Lambda$, which is named the *response matrix* of $\Gamma$. It is a singular complex symmetric matrix.

We can write a response matrix as $\mathsf{N} = \Re(\mathsf{N}) + i\Im(\mathsf{N})$, the sum of its real and imaginary parts, with the property that $\Re(\mathsf{N})$ is positive semidefinite and $\Im(\mathsf{N})$ is negative semidefinite.

As a consequence, for every $x \in F^c$, $\mathsf{N}(x,x) = -\sum_{y\neq x} \mathsf{N}(x,y)$ has a nonnegative real part and a nonpositive imaginary part.

For DC networks, the response matrix $\mathsf{N}$ is real, positive semidefinite and its diagonal entries are nonnegative.

Moreover, applying Lemma 1.3.7 to the kernel $J$ associated to the Green operator (whose matrix is $\mathsf{L}(F_1;F_1)^{-1}$), we get that the matrix of $\frac{\partial^2 J}{\partial \mathsf{n}_x \partial \mathsf{n}_y}$ is $\mathsf{L}(F^c;F_1)\mathsf{L}(F_1;F_1)^{-1}\mathsf{L}(F^c;F_1)^T$, because $J$ is a kernel on $F_1$, and thus the first three terms in the right side of the equation of that lemma are equal to zero.

Therefore,

$$\mathsf{N} = \mathsf{L}(F^c;F^c) - \mathsf{L}(F^c;F_1)\mathsf{L}(F_1;F_1)^{-1}\mathsf{L}(F^c;F_1)^T.$$

Thus $\mathsf{N}$ is equal to the Schur complement of $\mathsf{L}(F_1;F_1)$ of $\mathsf{L}\big((V\setminus F_0);(V\setminus F_0)\big)$, which is denoted as $\mathsf{L}\big((V\setminus F_0);(V\setminus F_0)\big)/\mathsf{L}(F_1;F_1)$, (see [51]).

## 1.6 Monotonicity on DC networks

In this section we will review some results of monotonicity of real functions on DC networks (Propositions 1.6.1, 1.6.2, 1.6.3 and 1.6.4), that can be found in [9] and [35]. This will allow

us to prove additional properties (see Proposition 1.6.5, Lemma 1.6.7 and Proposition 1.6.8) of the Dirichlet-to-Neumann map of a DC network.

The results in this section rely on the order of $\mathbb{R}$ and on the fact that the restriction of the Laplacian of a DC network to the space of real functions $\mathscr{C}(V)$ is an endomorphism of $\mathscr{C}(V)$, so they can not be generalized to AC networks. In fact, we show a counterexample to Proposition 1.6.5 in the AC case.

Let $\Gamma = (V, c)$ be a DC network and $F \subseteq V$. We say that a function $u \in \mathscr{C}(V)$ is *superharmonic* (respectively *subharmonic*) on $F$ when $\mathcal{L}(u) \geq 0$ (respectively $\mathcal{L}(u) \leq 0$) on $F$. Also, we say that a function $u \in \mathscr{C}(V)$ is *strictly superharmonic* (respectively *strictly subharmonic*) on $F$ when $\mathcal{L}(u) > 0$ (respectively $\mathcal{L}(u) < 0$) on $F$.

**Proposition 1.6.1** (Hopf's minimum principle)**.** *Let $\Gamma = (V, c)$ be a DC network, $F \subseteq V$ a connected subset, and $u \in \mathscr{C}(V)$ superharmonic on $F$. If there is $x^* \in F$ such that $u(x^*) = \min_{y \in \bar{F}} \{u(y)\}$, then $u$ is constant on $\bar{F}$ and it is harmonic on $F$.*

*Proof.* As $c$ is nonnegative,

$$0 \leq \mathcal{L}(u)(x^*) = \int_{\bar{F}} c(x^*, y)(u(x^*) - u(y))dy \leq 0.$$

So $u(y) = u(x^*)$ whenever $c(x, y) > 0$, that is, for any $y \sim x$. We can iterate this argument evaluating the Laplacian at any vertex $y \in F$ for which we know that $u(y) = u(x^*)$, until we get that $u = u(x^*)$ on $\bar{F}$. As a consequence, $\mathcal{L}(u) = 0$ on $F$.

□

The two following results are consequences of Hopf's minimum principle.

**Proposition 1.6.2** (Monotonicity Principle)**.** *Let $\Gamma = (V, c)$ be a DC network, $F \subseteq V$ a connected subset, and $u \in \mathscr{C}(V)$ superharmonic on $F$. If $\delta(F) = \emptyset$, then $u$ is constant on $\bar{F}$ and it is harmonic on $F$. Moreover, if $\delta(F) \neq \emptyset$ and $u \geq 0$ on $\delta(F)$, then either $u > 0$ on $F$ or $u = 0$ on $\bar{F}$.*

*Proof.* The result in the case that $\delta(F) = \emptyset$ is a straightforward consequence of Gauss' Theorem.

Now, in the case that $\delta(F) \neq \emptyset$ and $u \geq 0$ on $\delta(F)$, if there exists a vertex $x^* \in F$ such that $u(x^*) = 0$, then $u(x^*) = \min_{y \in \bar{F}} \{u(y)\}$, so by Hopf's minimum principle, $u = 0$ in $\bar{F}$. □

**Proposition 1.6.3** (Minimum Principle)**.** *Let $\Gamma = (V, c)$ be a DC network, $F \subset V$ a connected subset such that $\delta(F) \neq \emptyset$, and $u \in \mathscr{C}(V)$ superharmonic on $F$. Then:*

$$\min_{y \in \bar{F}} \{u(y)\} = \min_{y \in \delta(F)} \{u(y)\},$$

*and the equality holds if and only if $u$ is constant on $\bar{F}$.*

*Proof.* We define the function $v = u - \min_{y\in\delta(F)} \{u(y)\}\chi_{\bar{F}} \in \mathscr{C}(V)$. As $\mathcal{L}(\chi_{\bar{F}}) = 0$ on $F$, $v$ is superharmonic on $F$. The function $v$ is also nonnegative on $\delta(F)$, so we obtain the result applying Proposition 1.6.2 to $v$. □

In the next result we prove that a strictly superharmonic function on $F$ can not have a local minimum in $F$, as in the continuous vector calculus.

**Proposition 1.6.4.** *Let $\Gamma = (V, c)$ be a DC network, $F \subset V$ and $u \in \mathscr{C}(V)$ strictly superharmonic on $F$. Then, for any $x \in F$, there exists $y \in \bar{F}$ such that $y \sim x$ and $u(y) < u(x)$.*

*Proof.* Let $x \in F$ and suppose that for every vertex $y \in \bar{F}$ adjacent to $x$, we have $u(x) \leq u(y)$. Then we arrive to the following contradiction:

$$0 < \mathcal{L}(u)(x) = \int_{\bar{F}} c(x, y)(u(x) - u(y))dy \leq 0.$$

□

As a consequence of the Minimum Principle, we obtain the following property for the Dirichlet-to-Neumann map of any DC network.

**Proposition 1.6.5.** *Let $\Gamma = (V, c)$ be a DC network, $F \subset V$, and let $\Lambda\colon \mathscr{C}(F^c) \longrightarrow \mathscr{C}(F^c)$ be the Dirichlet-to-Neumann map of $\Gamma$ and $F$, whose kernel is $N \in \mathscr{C}(F^c \times F^c)$. Then, for any $x, y \in F^c$ such that $x \neq y$, we have that $N(x, y) \leq 0$. Moreover, $N(x, y) < 0$ if and only if $x \sim y$ or $x$ and $y$ are connected through $F$.*

*Proof.* Given $x, y \in F^c$ such that $x \neq y$, we have that

$$N(x, y) = \Lambda(\varepsilon_y)(x) = \frac{\partial u_{\varepsilon_y}}{\partial \mathsf{n}_{F}}(x) + \mathcal{L}^{F^c}(\varepsilon_y)(x).$$

On one hand, $\mathcal{L}^{F^c}(\varepsilon_y)(x) \leq 0$ and $\mathcal{L}^{F^c}(\varepsilon_y)(x) < 0$ iff $x \sim y$. On the other hand, as $K(x, y) = \varepsilon_y(x) = 0$, we get:

$$\frac{\partial u_{\varepsilon_y}}{\partial \mathsf{n}_{F}}(x) = \frac{\partial K}{\partial \mathsf{n}_{x}}(x, y) = \sum_{z\in F} c(x, z)\big(K(x, y) - K(z, y)\big) = -\sum_{z\in F} c(x, z)K(z, y).$$

By Proposition 1.4.8, if $x \notin \delta(F)$ or $y \notin \delta(F)$, $\frac{\partial u_{\varepsilon_y}}{\partial \mathsf{n}_{F}}(x) = 0$. Now, for every $z \in F$ such that $z \sim x$, we denote by $H_z \subseteq F$ the connected component of $F$ that contains the vertex $z$. For any $z \in F$ such that $z \sim x$, $x \in \delta(H_z) \neq \emptyset$ and $u_{\varepsilon_y} \geq 0$ on $\delta(H_z)$, so we get that $K(z, y) = u_{\varepsilon_y}(z) \geq 0$ applying the Monotonicity Principle to $u_{\varepsilon_y}$, which is harmonic on $F$. As a consequence, $N(x, y) \leq 0$.

Moreover, for any $z \in F$ such that $z \sim x$, by the Minimum Principle, $K(z, y) > 0$ iff $y \in \delta(H_z)$. Given that $x$ and $y$ are connected through $F$ iff there exists $z \in F$ with $z \sim x$ such that $y \in \delta(H_z)$, we finish the proof.

□

As a consequence of Corollary 1.5.3 and Proposition 1.6.5, for DC networks, the response matrix $\mathsf{N}$ has the same properties as a Laplacian matrix. It is a symmetric and diagonally dominant $M$-matrix, such that $\mathsf{N}(x,x) = -\sum_{y\neq x}\mathsf{N}(x,y)$ for each $x \in F^c$. In fact, it is the Laplacian matrix of the *Kron reduction* of the network, (see [58, 60]).

**Definition 1.6.6.** Let $\Gamma = (V,c)$ be a DC network, let $F \subset V$, and let $\Lambda_F$ be the Dirichlet-to-Neumann map of $\Gamma$ and $F$, whose kernel is $N$. The *Kron reduction of* $\Gamma$ *with respect to* $F$ is the DC network $\Gamma_{\Lambda_F} = (F^c, c^{\Lambda_F})$ whose conductance kernel $c^{\Lambda_F} \in \mathscr{C}^+(F^c \times F^c)$ is defined for each $x, y \in F^c$ as $c^{\Lambda_F}(x,y) = -N(x,y)$ if $x \neq y$ and as $c^{\Lambda_F}(x,y) = 0$ if $x = y$.

**Lemma 1.6.7.** *Let $\Gamma = (V,c)$ be a DC network, let $\Gamma = \Gamma^{V_1} \sqcup \ldots \sqcup \Gamma^{V_s}$ be its decomposition in connected components, let $F \subset V$, let $\Lambda_F$ be the Dirichlet-to-Neumann map of $\Gamma$ and $F$, and let $\Gamma_{\Lambda_F} = (F^c, c^{\Lambda_F})$ be the Kron reduction of $\Gamma$ with respect to $F$. Then, the set of edges of $\Gamma_{\Lambda_F}$ is $E(\Gamma_{\Lambda_F}) = E\big(\Gamma^{F^c}\big) \cup \{e_{xy}$ such that $x, y \in \delta(F)$ and $x$ and $y$ are connected through $F\}$. Moreover, the Laplacian of the network is $\Lambda_F$ and the connected components of $\Gamma_{\Lambda_F}$ are the sets $V_i \cap F^c$ that are nonempty.*

*Proof.* The fact that $\Lambda_F$ is the Laplacian of the network follows trivially from the definition of Kron reduction. The statement about the set of edges is a consequence of Proposition 1.6.5. From Proposition 1.5.2, the null space of $\Lambda_F$ is the set of functions that are constant on each $V_i \cap F^c$ that is not empty, so those sets are the connected components of $\Gamma_{\Lambda_F}$. □

The last result implies that the operation of taking the Kron reduction is closed on the set of DC networks. In the next result we prove that, given any two subsets $H$ and $F$ such that $H \subset F \subset V$, the operation of doing the Kron reduction with respect to $F$ is equivalent to the composition of doing the Kron reduction with respect to $H$ and doing the Kron reduction of the result with respect to $F \setminus H$. This composition property has been studied in the literature from the properties of the Schur complement, (see [50, 58]). Nevertheless, we provide a different proof using discrete vector calculus tools.

**Proposition 1.6.8.** *Let $\Gamma = (V,c)$ be a DC network, let $H \subset F \subset V$, let $\Lambda_F$ and $\Lambda_H$ be the Dirichlet-to-Neumann maps of $\Gamma$ and $F$ and of $\Gamma$ and $H$, respectively. Let $\Gamma_{\Lambda_F} = (F^c, c^{\Lambda_F})$ and $\Gamma_{\Lambda_H} = (H^c, c^{\Lambda_H})$ be the Kron reductions of $\Gamma$ with respect to $F$ and with respect to $H$, respectively. We denote as $\Sigma_{F\setminus H}$ the Dirichlet-to-Neumann map of $\Gamma_{\Lambda_H} = (H^c, c^{\Lambda_H})$ and $F \setminus H$; and we denote as $\big(\Gamma_{\Lambda_H}\big)_{\Sigma_{F\setminus H}} = (F^c, c^{\Sigma_{F\setminus H}})$ the Kron reduction of $\Gamma_{\Lambda_H}$ with respect to $F \setminus H$. Then:*

$$\big(\Gamma_{\Lambda_H}\big)_{\Sigma_{F\setminus H}} = \Gamma_{\Lambda_F}.$$

*Proof.* The set of vertices of $\big(\Gamma_{\Lambda_H}\big)_{\Sigma_{F\setminus H}}$ and $\Gamma_{\Lambda_F}$ are equal, so it is sufficient to prove that $\Sigma_{F\setminus H} = \Lambda_F$.

As $\Gamma_{\Lambda_H}$ is a DC network with set of vertices $H^c$ and Laplacian $\Lambda_H$, by definition of the Dirichlet-to-Neumann map, we have $\Sigma_{F\setminus H} = \Lambda_H \circ \Xi$, where $\Xi$ is the Poisson operator of $F \setminus H$ in the network $\Gamma_{\Lambda_H}$. The set $F^c$ is the complementary of $F \setminus H$ in $H^c$, so $\Xi$ is the linear operator $\Xi\colon \mathscr{C}(F^c, \mathbb{C}) \longrightarrow \mathscr{C}(H^c \setminus \big((F \setminus H)_0\big), \mathbb{C})$ such that for any $g \in \mathscr{C}(F^c, \mathbb{C})$, $u = \Xi(g)$ is the unique solution of the boundary problem:

$$\Lambda_H(u) = 0 \ \text{ on } \ F \setminus H, \quad u = g \ \text{ on } \ F^c, \quad u = 0 \ \text{ on } \ (F \setminus H)_0. \tag{1.9}$$

Now, we fix a function $g \in \mathscr{C}(F^c, \mathbb{C})$. By definition, the Laplacian $\Lambda_H$ is equal to $\Lambda_H = \mathcal{L} \circ \mathscr{K}_H$, where $\mathscr{K}_H$ is the Poisson operator of $H$ in the network $\Gamma$. Moreover, $\Lambda_H$ is an operator on $H^c$, so $\Lambda_H(\Xi(g)) = \mathcal{L}\big((\mathscr{K}_H \circ \Xi)(g)\big) = 0$ on $F$. Since $F^c \subset H^c$, we get that $(\mathscr{K}_H \circ \Xi)(g) = \Xi(g) = g$ on $F^c$.

The set $(F \setminus H)_0$ in (1.9) stands for the set of connected components of the network $\Gamma_{\Lambda_H}$ that are contained in $F \setminus H$. Let $\Gamma = \Gamma^{V_1} \sqcup ... \sqcup \Gamma^{V_s}$ be the decomposition of $\Gamma$ in its connected components. The set $(F \setminus H)_0$ is equal to the union of the nonempty $V_i \cap (F \setminus H)$ such that $V_i \subseteq F$. That is, $(F \setminus H)_0$ is the union of the $V_i \cap (F \setminus H)$ such that $V_i \subseteq F_0$ and $V_i \not\subseteq H_0$. Now, $\mathscr{K}_H$ is the Poisson operator of $H$, so $(\mathscr{K}_H \circ \Xi)(g) = 0$ on $H_0$, and because $(F \setminus H)_0 \subseteq H^c$, we also have that $(\mathscr{K}_H \circ \Xi)(g) = \Xi(g) = 0$ on $(F \setminus H)_0$. Since $\mathcal{L}\big((\mathscr{K}_H \circ \Xi)(g)\big) = 0$ on $F$, the function $(\mathscr{K}_H \circ \Xi)(g)$ must be constant on each connected component $V_i \subseteq F_0$. Whether a connected component $V_i \subseteq F_0$ is contained in $H_0$ or not, there is at least one vertex of $V_i$ such that $(\mathscr{K}_H \circ \Xi)(g)$ is equal to zero, so we get $(\mathscr{K}_H \circ \Xi)(g) = 0$ on $F_0$. As a consequence, $u = (\mathscr{K}_H \circ \Xi)(g)$ is a solution of the boundary value problem:

$$\mathcal{L}(u) = 0 \ \text{ on } \ F, \quad u = g \ \text{ on } \ F^c, \quad u = 0 \ \text{ on } \ F_0. \tag{1.10}$$

But (1.10) has a unique solution, which is $\mathscr{K}_F(g)$, where $\mathscr{K}_F$ is the Poisson operator of $F$ in the network $\Gamma$. Then, $(\mathscr{K}_H \circ \Xi)(g) = \mathscr{K}_F(g)$ for every $g \in \mathscr{C}(F^c, \mathbb{C})$, which implies that $(\mathscr{K}_H \circ \Xi) = \mathscr{K}_F$. As a consequence, $\Sigma_{F \setminus H} = \mathcal{L} \circ (\mathscr{K}_H \circ \Xi) = \mathcal{L} \circ \mathscr{K}_F = \Lambda_F$. □

In the case of an AC network, $\Gamma = (V, a)$, if we take $F \subset V$, and $\Lambda_F$ is the Dirichlet-to-Neumann map of $\Gamma$ and $F$, with kernel $N = \Re(N) + i\Im(N) \in \mathscr{C}(V \times V, \mathbb{C})$, whose real and imaginary parts are $\Re(N), \Im(N) \in \mathscr{C}(V \times V)$, respectively; we can define the Kron reduction of the network if and only if the following property is satisfied:

$$\Re(N)(x, y) \leq 0, \ \text{ and } \ \Im(N)(x, y) \geq 0 \ \text{ for any } \ x, y \in F^c \ \text{ such that } \ x \neq y. \tag{1.11}$$

If (1.11) holds, we can give the analogous definition to Definition 1.6.6 for the AC case. That is, the *Kron reduction of* $\Gamma$ *with respect to* $F$ is the AC network $\Gamma_{\Lambda_F} = (F^c, a^{\Lambda_F})$ whose admittance kernel $a^{\Lambda_F} \in \mathscr{C}(F^c \times F^c, \mathbb{C})$ is defined for each $x, y \in F^c$ as $a^{\Lambda_F}(x, y) = -N(x, y)$ if $x \neq y$ and as $a^{\Lambda_F}(x, y) = 0$ if $x = y$.

Property (1.11) assures that we can write $a^{\Lambda_F} = c^{\Lambda_F} - ib^{\Lambda_F}$ where $c^{\Lambda_F}, b^{\Lambda_F} \in \mathscr{C}^+(V \times V)$ are the conductance and susceptance kernels of $\Gamma_{\Lambda_F}$, so the Kron reduction is indeed an AC network. Nevertheless, there is no result analogous to Proposition 1.6.5 for the case of AC networks that ensures that (1.11) holds for every AC network and every subset, as we can see in the following counterexample.

**Example 1.6.9.** Let $\Gamma = (V, a)$ be the AC spider network in Figure 1.6, which has $\ell = 0$ circles and $m = 3$ radii. We consider the labeling $V = \{x_1, ..., x_4\}$, and the subset $F = \{x_4\}$, which only contains the central node.

The Admittance matrix of $\Gamma$ is:

$$\mathsf{L} = \begin{bmatrix} -i & 0 & 0 & i \\ 0 & -i & 0 & i \\ 0 & 0 & 10 & -10 \\ i & i & -10 & 10 - 2i \end{bmatrix}.$$

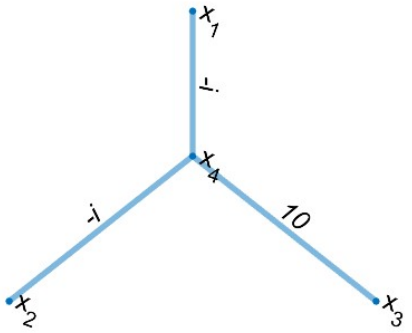


Figure 1.6: AC spider network which does not satisfy (1.11).

The response matrix associated with the Dirichlet-to-Neumann map of $\Gamma$ and $F$ can be calculated as the following Schur complement:

$$\mathsf{N} = \mathsf{L}(V;V)/\mathsf{L}(F;F) = \begin{bmatrix} -i & 0 & 0 \\ 0 & -i & 0 \\ 0 & 0 & -10 \end{bmatrix} - (10-2i)^{-1} \begin{bmatrix} i \\ i \\ -10 \end{bmatrix} \begin{bmatrix} i & i & -10 \end{bmatrix} =$$

$$\frac{5+i}{52} \begin{bmatrix} -1-10i & 1 & 10i \\ 1 & -1-10i & 10i \\ 10i & 10i & -20i \end{bmatrix} =$$

$$\frac{1}{52} \begin{bmatrix} 5-51i & 5+i & -10+50i \\ 5+i & 5-51i & -10+50i \\ -10+50i & -10+50i & 20-100i \end{bmatrix}.$$

Note that the kernel $N$ associated to the Dirichlet-to-Neumann map satisfies $N(x_1, x_2) = 5+i$, so (1.11) does not hold, and thus $N$ is not the kernel of the Laplacian of a network.

As a conclusion, the operation of taking the Kron reduction is not closed on the set of AC networks.

## 1.7 Effective admittance

**Definition 1.7.1.** Let $\Gamma = (V, a)$ be an electrical network, and let $x, y \in V$ be a pair of vertices. We denote by $\Lambda$ the Dirichlet-to-Neumann map of $\Gamma$ and the set $F = V \setminus \{x, y\}$. We define the effective admittance between $x$ and $y$ as:

$$a^e(x, y) = \Lambda(\varepsilon_x)(x) = \Lambda(\varepsilon_y)(y).$$

If $\Gamma$ is a DC network, the *effective admittance* is also called *effective conductance* between $x$ and $y$, and it is denoted by $c^e(x, y)$.

Recall that, for an AC, respectively DC, network, the Dirichlet-to-Neumann map $\Lambda\colon \mathscr{C}(\{x,y\},\mathbb{C}) \longrightarrow \mathscr{C}(\{x,y\},\mathbb{C})$, respectively $\Lambda\colon \mathscr{C}(\{x,y\}) \longrightarrow \mathscr{C}(\{x,y\})$ is associated with the Dirichlet problem of, for any $g \in \mathscr{C}(\{x,y\},\mathbb{C})$, respectively $g \in \mathscr{C}(\{x,y\})$, finding $u \in \mathscr{C}(V,\mathbb{C})$ such that

$$\mathcal{L}(u) = 0 \quad \text{on} \quad V \setminus \{x,y\} \quad \text{and} \quad u = g \quad \text{on} \quad \{x,y\}.$$

As a consequence, a physical meaning of the effective admittance between $x$ and $y$, is that it is the injected current that appears at $x$ when we fix a potential equal to 1 at $x$, a potential equal to 0 at $y$, and there is no injected current at any vertex of $V \setminus \{x,y\}$.

**Lemma 1.7.2.** *The effective admittance, respectively conductance, between the vertices $x$ and $y$ is nonzero if and only if $x$ and $y$ belong to the same connected component of the network and $x \neq y$.*

*Proof.* Let $\Gamma = \Gamma^{V_1} \sqcup \ldots \sqcup \Gamma^{V_s}$ be the decomposition in connected components of the network $\Gamma$. By Proposition 1.5.2, $a^e(x,y) = \Lambda(\varepsilon_x)(x) = -\Lambda(\varepsilon_x)(y)$, so $a^e(x,y) = 0$ iff $\Lambda(\varepsilon_x) = 0$. This is satisfied if and only if $\varepsilon_x$ is constant on each $V_i \cap \{x,y\}$ that is not empty, and thus if and only if $x$ and $y$ belong to different connected components of the network or $x = y$. □

Analogously to the definition of resistance, for a DC network we define the *effective resistance* as the kernel $r^e \in \mathscr{C}^+_\infty(V \times V)$ such that for every $(x,y) \in V \times V$, $r^e(x,y) = 0$ if $x = y$ and $r^e(x,y) = 1/c^e(x,y)$ if $x \neq y$. Note that $r^e(x,y) = +\infty$ iff $x$ and $y$ belong to different connected components of the network.

Now, let $x, y \in V$ be vertices of a network $\Gamma$ and let $N$ be the kernel of the Dirichlet-to-Neumann map $\Lambda$ of $\Gamma$ and $F = V \setminus \{x,y\}$. We have that $N(x,y) = -N(x,x)$, so (1.11) holds. Because of that, both in the case of an AC or a DC network, we can define the Kron reduction of $\Gamma$ with respect to $F$, $\Gamma_\Lambda = (\{x,y\}, c^\Lambda)$. If $x = y$, $\Gamma_\Lambda = (\{x\}, 0)$, so the graph associated with $\Gamma_\Lambda$ has one vertex and zero edges. If $x \neq y$, $c^\Lambda(x,y) = -N(x,y) = a^e(x,y)$, so $E(\Gamma_\Lambda) = \emptyset$ iff $x$ and $y$ belong to different connected components of the network.

Therefore, when there is only injected current at $x$ and $y$ and $x$ and $y$ belong to the same connected component, the relationship between potential and current in $\{x,y\}$ is equivalent to the relationship given by a network of a single edge between $x$ and $y$ whose admittance is the effective admittance between $x$ and $y$.

The following result is a straightforward consequence of Proposition 1.6.8.

**Corollary 1.7.3.** *The effective conductance between every pair of vertices of a Kron reduction of a network is the same as in the original network.*

Finally, recall that

$$a^e(x,y) = \Lambda(\varepsilon_x)(x) = \frac{\partial u_{\varepsilon_x}}{\partial \mathsf{n}_{_F}}(x) + \mathcal{L}^{F^c}(\varepsilon_x)(x).$$

On one hand, $\mathcal{L}^{F^c}(\varepsilon_x)(x) = a(x,y)$. On the other hand, we consider the network obtained from $\Gamma$ by removing the edge $e_{xy}$, *i.e.*, the network $\Gamma \setminus e_{xy} = (V, a_{\setminus e_{xy}})$ such that $a_{\setminus e_{xy}} = a$ in

$\big(V \times V\big) \setminus \{(x,y),(y,x)\}$ and $a(x,y) = a(y,x) = 0$. In that network, the effective admittance between $x$ and $y$ is equal to:

$$a^e_{\setminus e_{xy}}(x,y) = \frac{\partial u_{\varepsilon_x}}{\partial \mathsf{n}_{_F}}(x),$$

that is, the function $u_{\varepsilon_x}$ and its normal derivative with respect to $F$ do not change if we remove the edge $e_{xy}$. As a consequence,

$$a^e(x,y) = a^e_{\setminus e_{xy}}(x,y) + a(x,y), \tag{1.12}$$

where $a^e_{\setminus e_{xy}}(x,y)$ and $a(x,y)$ have nonnegative real part and nonpositive imaginary part. In particular, if $\Gamma$ is a DC network, we can write

$$c^e(x,y) = c^e_{\setminus e_{xy}}(x,y) + c(x,y), \tag{1.13}$$

and we have that $c^e(x,y) \geq c(x,y)$.

From 1.12, the effective admittance between $x$ and $y$ is the sum of the admittance between $x$ and $y$ and the effective admittance corresponding to the rest of paths between $x$ and $y$ through the rest of vertices of the network. In particular, $a^e(x,y) = a^e_{\setminus e_{xy}}(x,y)$ iff $x \not\sim y$ and $a^e(x,y) = a(x,y)$ iff $e_{xy}$ is a bridge, *i.e.*, if the removal of $e_{xy}$ creates a new connected component in the network, or equivalently, if $x$ and $y$ are not connected through $V \setminus \{x,y\}$.

# Chapter 2

# The inverse conductance problem

The objective of this chapter is to obtain a stable algorithm for the solution of the inverse conductance problem. The inverse conductance problem corresponds to the discrete version of the well established *Calderón problem* in the (plane) continuous setting and in fact our algorithm can be seen as the last step in the solution of this problem, namely the *reconstruction step*. Specifically, the inverse conductance problem can be understood as part of the *numerical reconstruction of conductivity*, whose objective is to obtain an approximation of the conductivity from a finite number of (voltage and current) measurements.

As we mention in the previous chapter, given a bounded connected open set $\Omega \subseteq \mathbb{R}^n$ with $n \geq 2$, given a bounded measurable conductivity $\sigma$ which satisfies $\lambda \geq \sigma \geq \lambda^{-1}$ almost everywhere in $\Omega$ for some $\lambda > 0$, and given a potential $g$ belonging to $H^{1/2}(\partial\Omega)$, the trace space on the boundary $\partial\Omega$, the induced potential $u_g$ on $\Omega$ solves the Dirichlet problem of finding $u \in H^1(\Omega)$ such that

$$\nabla \cdot (\sigma \nabla u) = 0 \quad \text{in } \Omega, \quad u|_{\partial\Omega} = g.$$

The Dirichlet-to-Neumann map is the operator $\Lambda_\sigma \colon H^{1/2}(\partial\Omega) \longrightarrow H^{1/2}(\partial\Omega)$ defined as

$$\Lambda_\sigma(g) = \left( \sigma \frac{\partial u_g}{\partial \mathsf{n}} \right) \Big|_{\partial\Omega},$$

for every $g \in H^{1/2}(\partial\Omega)$, where $\mathsf{n}$ denotes the outer unit normal vector to $\partial\Omega$.

The Dirichlet-to-Neumann map is the key tool to solve the so-called *Inverse conductivity problem*, also known as Calderón's problem, which is stated as follows, (see [34]).

**Problem 2.0.1** (Calderón's problem)**.** *Let $\Omega \subseteq \mathbb{R}^n$ be a bounded connected open set with $n \geq 2$ and an unknown bounded measurable conductivity $\sigma$ which satisfies $\lambda \geq \sigma \geq \lambda^{-1}$ almost everywhere in $\Omega$ for some $\lambda > 0$. Let $\Lambda_\sigma \colon H^{1/2}(\partial\Omega) \longrightarrow H^{1/2}(\partial\Omega)$ be the (continuous) Dirichlet-to-Neumann map operator. The problem consists in determining $\sigma$ from $\Lambda_\sigma$.*

A good summary of the problem origins and the different steps of its resolution can be found in [15, 98].

The discrete version of Calderón's problem, called the *Inverse conductance problem* is concerned with the recovery of the conductance of a given network from the response matrix. Of course, this (discrete) inverse problem is not limited to the realm of numerical reconstruction of conductivities, but makes sense in its own right and can be posed on arbitrary graphs and networks. It was proposed in the last decade of the past century mainly by the Seattle school, led by E.B. Curtis and J. Morrow. The explanation in terms of discrete vector calculus, mimicking the continuous formulation, is more recent, dating back to the last ten years and is based on the work of the MAPTHE group in Barcelona. In fact, if $\Gamma$ is a network with boundary, *i.e.*, $\Gamma = (\bar{F}, c)$, the Dirichlet-to-Neumann map is a mimetic discretization of the continuous Dirichlet-to-Neumann map, (as stated in Section 1.5) and hence the resolution of the discrete problem can be interpreted as the reconstruction step of the continuous one. Therefore, with the notations introduced in Section 1.5, in this chapter, we study the following problem, (see [7, 8, 10, 54]).

**Problem 2.0.2** (Inverse conductance problem)**.** *Let $\Gamma = (V, c)$ be a DC electrical network with unknown conductance $c$, but with a known topology, $G(\Gamma) = (V, E(\Gamma))$. Let $F \subset V$ and let $\Lambda$ be the Dirichlet-to-Neumann map of $\Gamma$ and $F$. The problem consists in determining $c$ from $\Lambda$.*

## 2.1 Background of the problem

The (continuous) inverse conductivity problem has received a lot of attention since its introduction in 1980. There are abundant papers dedicated to it, such as [5, 6, 23, 24, 26, 32, 34, 86, 97].

Two of the most studied aspects are the uniqueness of its solution, and in the cases where there is a unique solution, the construction of an algorithm to obtain it. In the case of dimension $n = 2$, the solution was proved to be unique in [13]. Moreover, an algorithm to recover the conductivity in this case was obtained in [12]. In the case of dimension $n \geq 3$, the question of uniqueness in general remains open to this date, although some authors have proved that the solution is unique if further regularity assumptions are added to the problem. For instance, in [40] the uniqueness of the problem was proved if the conductivity and the surface are Lipschitz continuous. Furthermore, an algorithm to recover the solution under this hypothesis was obtained in [39].

Even when the conductivity $\sigma$ can be uniquely obtained from the Dirichlet-to-Neumann map $\Lambda_\sigma$, the solution $\sigma$ does not depend continuously on $\Lambda_\sigma$ in general, so the problem is ill-posed, (see [6, 15]). Because of that, several authors have investigated if knowing some *a priori* information about $\sigma$ makes the problem stable. For example, in [14, 75] for the case of dimension $n = 2$ and in [5] for the case $n \geq 3$, the authors proved that if it is *a priori* known that $\sigma$ is bounded for a certain suitable norm, then $\sigma$ depends continuously on $\Lambda_\sigma$, but with this *a priori* hypothesis we only have the so-called *logarithmic stability*. Therefore, the problem still exhibits a bad numerical behavior, which represents a severe obstruction for the reconstruction step.

In that line of research, we highlight the paper [6] by Alessandrini and Vessella, where they proved that if it is *a priori* known that there is a known partition of the set $\Omega$ with a bounded

number of connected subsets satisfying some additional hypothesis such that the conductivity is piecewise constant on that partition, (that is, $\sigma$ is equal to an unknown constant value at each subset), then Calderón's problem becomes Lipschitz stable. Furthermore, the Lipschitz constant grows exponentially with the number of subsets in the partition, as demonstrated in [77, 85]. In order to improve the stability of the recovery process, there are authors that have used regularization methods, mainly of *Tikhonov* type, (see [61, 76, 86]). Other authors have used machine learning techniques, (see [41]).

The (discrete) inverse conductance problem has gathered relatively less attention than its continuous counterpart, with papers such as [8, 10, 30, 45, 51, 65, 66]. Additionally, several authors have studied the problem with the goal of obtaining an approximate solution to Calderón's problem, (see [23, 24, 26, 27, 28, 62]).

The situation in the research about this problem is analogous to the one in the continuous problem. On one hand, there are works that study the uniqueness of the problem, also known as the *identification problem*, which depends on the graph associated to the electrical network $G(\Gamma)$. To the best of our knowledge, the statement of this problem for general networks appeared in [47], and was solved under some monotonicity hypothesis, see also [22]. In these works, the authors emphasize the need to formulate network problems using an operational calculus that allows following the developments of the continuum. In fact, the background of most of the authors comes from the field of PDEs. The used operators are the gradient, the normal derivative and the Laplacian, which are sufficient to describe the analogue of the Dirichlet-to-Neumann map and to use the variational approach. The most general framework including the consideration of general (discrete) elliptic operators and a complete vector calculus was presented in [20], where again under monotonicity hypothesis, similar results to the mentioned papers were obtained.

The extension of Problem 2.0.2 to the case of recovering the admittance $a$ in an AC network was raised in [30]. In this paper, the authors also consider cases in which the imaginary part of $a$ is not nonpositive (which we do not consider in Definition 1.3.1), *i.e.* the authors extend the problem to the case in which each edge has a complex weight with positive real part. For this extension, they give a criterion to identify the graphs for which the problem has a unique solution for almost all networks with that topology.

In previous works (see [52, 53, 54, 55]), Curtis and Morrow proved that the inverse conductance problem has a unique solution when the network topology is a critical planar graph, and thus, in particular, when it is a well-connected spider graph. They also introduced an explicit method to recover the conductance of a well-connected spider network from a finite number of elementary algebraic operations, which is called the *layer peeling method*. This method was generalized in [10] to include the case in which there is a Schrödinger potential at the vertices.

There are other network topologies for which the the solution of the inverse conductance problem is also known to be unique and there is an explicit method similar to layer peeling to obtain the conductance, including the $n \times n$ grids (see [11]), and any tree without vertices of combinatorial degree two, (see [66]). The method introduced in the last reference also allows to identify which tree is the network topology up to vertices of combinatorial degree two, although the method is only valid for trees, because it exploits the fact that the effective resistance between any two nodes coincides with the resistance distance between them.

An alternative line of research in the construction of explicit algorithms for solving the inverse conductance problem for some topologies is related to the study of certain Grassmannians. In that line, in [71], an algorithm is proposed to solve the problem for a certain family of networks called standard networks. The values of the solution are obtained as a biratio of Pfaffians constructed from the response matrix. A related algorithm, which works for any well-connected electrical network can be found in [65], although the only example of network in which the conductances are computed is a well-connected spider network with $m = 3$ boundary nodes.

Despite being finite-dimensional, the inverse conductance problem is also severely ill-posed in general, (see [54]). Among the explicit methods to recover the conductance mentioned so far, the ones in well-connected spider networks and in grids (in [10, 11, 52, 53, 54, 55]) are known to be ill-posed for networks of medium or large size; and for the rest of the methods (in [65, 66, 71]) the stability is not studied and the computational examples of recovery presented are only in networks with small size.

Several authors, (see [45]), have developed numerical methods with regularization to recover an approximate solution of the inverse conductance problem with more stability than the mentioned explicit methods. In [45], the inverse problem is reformulated to obtain an equivalent problem in which the goal is to estimate a potential at the vertex set. Then, the problem is solved utilizing a discrete version of the inverse Born series with regularization. The method is tested in $12 \times 12$ grids. In the experiments, the method converges when the deviation from a constant potential is small; and the method diverges otherwise.

Some of the works that solve the discrete inverse problem to approximate the continuous one have also contributed to the study of the stability of the discrete problem and the development of numerical methods to solve it. L. Borcea alongside several collaborators have written several papers in which they approximate the continuous problem using well-connected spider networks, including [23, 24, 26, 27, 28]. In [27], the authors propose to formulate the discrete problem as an optimization problem which includes a Tikhonov-type regularization and to solve it with an optimization method. The regularization term penalizes the deviation from a reference conductance whose value has to be known and fixed *a priori*. The experimental results of the method are carried out in networks with moderate size (with 29 or less vertices in the boundary). In the rest of those works ([23, 24, 26, 28]), the conductance is recovered using the layer peeling algorithm ([55]). In order to have stability, the authors limit the size of the networks, choosing the topology with greatest number of boundary nodes such that the algorithm does not yield negative values for the conductance; which generally has fewer than 11 boundary nodes.

In other works, the continuous problem is approximated solving the discrete one in grids. For example, in [24, 25], the discrete problem is solved using an algorithm that converges to the real network if and only if it is asymptotically close to a reference network that has to be known and fixed *a priori*. In [62], the authors solve the discrete problem using a discrete analogous to the complex geometric optics approach. They also use these solutions to obtain a stability estimate for the discrete problem, which is in $|\log(error)|^{\alpha}$, for some $\alpha < 0$, where *error* stands for the error in the Dirichlet-to-Neumann map, *i.e.*, the problem is exponentially unstable.

In the recent work [38], the authors explore whether knowing *a priori* the hypothesis

that the conductance is piecewise constant on a partition with few subsets makes the discrete inverse conductance problem stable. This hypothesis, called the "*piecewise constant conductance hypothesis*", mimics the hypothesis of piecewise constant conductivity considered in [6]. They propose to formulate the problem as a polynomial optimization problem, with a regularization term *à la Tikhonov* that penalizes the deviation with respect to that hypothesis. The authors present numerous experimental examples in which it is possible to solve the inverse conductance problem with stability in well-connected spider networks satisfying that hypothesis with up to $m = 47$ boundary vertices, which are larger than the networks considered in the previous literature.

Moreover, this work is extended by the same authors in the paper [37]. In that work, they show that the approach in [38] can be used to solve the inverse conductance problem with stability even in some cases in which the piecewise constant conductance hypothesis is not exactly satisfied by the real network. Moreover, they study the variation of the error in the recovered conductance with respect to the penalty parameter, and they use techniques of sum of squares of polynomials to seek for a guarantee that the obtained numerical solution of the polynomial optimization problem is a global minimum.

The rest of the chapter is dedicated to review and extend the results of [37, 38] about the inverse conductance problem in well-connected spider networks.

## 2.2 Ill-posedness of the inverse conductance problem

The aim of this section is to prove that the inverse conductance recovery problem is intrinsically severely ill-posed, in order to emphasize the importance of reformulating the problem and seeking for methods that allow us to recover the conductance with stability. This section is a review of [38, Section 2].

We conduct several tests in which we compute the Dirichlet-to-Neumann map of a well-connected spider network, and then we apply the algorithm in [10] to solve the inverse conductance problem. We recover a conductance that, when the number of boundary vertices is high, widely differs from the one of the original network. This is due to the ill-posedness of the problem: despite the fact that the algorithm is based on explicit formulas, any error in the entries of the response matrix (which are stored with finite precision) could be amplified several orders of magnitude in the algorithm.

For the sake of completeness we give here the highlights of the algorithm of [10] that are mainly based on finding solutions of a battery of overdetermined boundary value problems. Each step requires the information obtained in the last one.

Let $\Gamma = (\bar{F}, c)$ be a DC well-connected spider network and let $A, B \subset \delta(F)$ nonempty subsets such that $A \cap B = \emptyset$. Moreover we denote by $R$ the set $R = \delta(F) \setminus (A \sqcup B)$, so $\delta(F) = A \sqcup B \sqcup R$ is a partition of $\delta(F)$. We remark that $R$ can be an empty set. For any $f \in \mathscr{C}(F)$, $g \in \mathscr{C}(A \sqcup R)$ and $h \in \mathscr{C}(A)$, the *overdetermined partial Dirichlet–Neumann boundary value problem on $F$ with data $f, g, h$* consists in finding a function $u \in \mathscr{C}(\bar{F})$ such

that

$$\mathcal{L}_q(u) = f \ \text{ on } \ F, \qquad \frac{\partial u}{\partial \mathsf{n}_{\mathsf{F}}} = h \ \text{ on } \ A \quad \text{and} \quad u = g \ \text{ on } \ A \sqcup R. \tag{2.1}$$

In Figure 2.1 we show the representation of a general overdetermined boundary problem. We fix a labeling in the vertex set of $\Gamma$, and we denote by $\mathsf{L}$ its Laplacian matrix, by $\mathsf{N}$ its

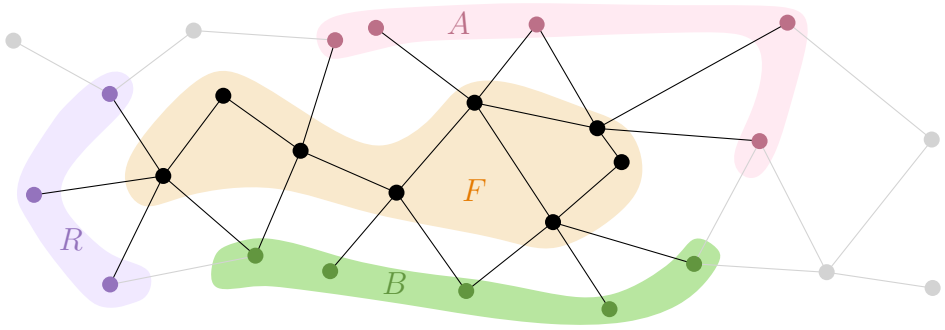


Figure 2.1: Boundary partition in an overdetermined boundary value problem.

response matrix, and by $\mathsf{f}$, $\mathsf{g}$ and $\mathsf{h}$ the vectors associated with $f$, $g$ and $h$, respectively. In [10] the authors proved the existence and uniqueness of a solution to this problem for any data $f \in \mathscr{C}(F)$, $g \in \mathscr{C}(A \sqcup R)$, $h \in \mathscr{C}(A)$ iff $|A| = |B|$ and $\mathsf{N}(A;B)$ is invertible. Moreover, if $u \in \mathscr{C}(\bar{F})$ is the unique solution of the overdetermined partial boundary value problem (2.1), then its associated vector $\mathsf{u}$ satisfies

$$\mathsf{u}(B) = -\mathsf{N}(A;B)^{-1} \cdot \Big(\mathsf{L}(A;F) \cdot \mathsf{L}(F;F)^{-1} \cdot \mathsf{f} + \mathsf{N}(A;A \sqcup R) \cdot \mathsf{g} - \mathsf{h}\Big),$$

$$\mathsf{u}(F) = \mathsf{L}(F;F)^{-1} \cdot \Big(\mathsf{f} - \mathsf{L}(F;B) \cdot \mathsf{u}(B) - \mathsf{L}(F;A \sqcup R) \cdot \mathsf{g}\Big)$$

and, clearly, $\mathsf{u}(A \sqcup R) = \mathsf{g}$.

We consider also the what we called boundary spike formula. If $x \in R$ has a unique neighbour $y \in F$, then

$$c(x,y) = \mathsf{N}(x;x) - \mathsf{N}(x;B) \cdot \mathsf{N}(A;B)^{-1} \cdot \mathsf{N}(A;x).$$

Once we get the value for the conductances on the boundary edges, and taking advantage of the null zone for the solution of Problem (2.1) when $f = 0$, $h = 0$ and $g = \varepsilon_z$, for each $z \in A \sqcup R$, we can recover the value of the solution on the set of vertices that are at distance 1 from the boundary. Then, the process follows alternating the knowledge of the conductance and the function value from the boundary to the interior vertex.

The following example refers to the case of well-connected spider networks, as represented in Figure 2.2.

**Example 2.2.1** ([38]). *For $m = 7, 11, 15, 19, 23, 27, 31$ and 35, we start from the well-connected spider network with $m$ radii and constant conductance $c = 1$. In all cases, we compute the response matrix $\mathsf{N}$ of the network, and from it we recover the conductance $c'$ using the explicit formulas from [10]. The algorithm has been implemented in Matlab.*

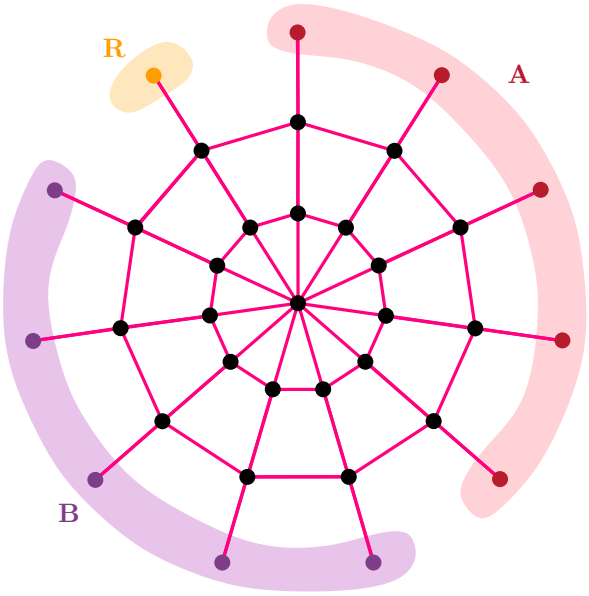


Figure 2.2: The boundary partition in a well-connected spider network.

In Figure 2.3 we show the logarithm of the error in the recovered conductance in the Euclidean norm, $\log(||c'-c||)$, for all values of $m$, where log stands for the decimal logarithm, and the norm of $c'-c \in \mathscr{C}(\Gamma) = \mathscr{C}(G(\Gamma))$ is the one defined in Remark 1.2.3. Moreover, Table 2.1 displays the error on the conductances. We see that the error is almost zero for $m = 7$ and increases approximately exponentially with $m$ from $m = 7$ to $m = 23$. The error keeps increasing with $m$ for $m \geq 23$.

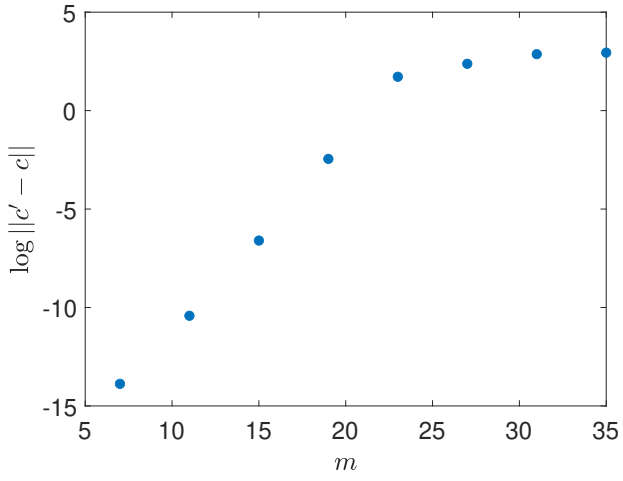


Figure 2.3: Logarithm of the error in the recovered conductance.

We show the recovered conductance for $m = 19$ and for $m = 23$ in Figures 2.4 and 2.5, respectively. In both figures, the width of each edge is proportional to the absolute value of the recovered conductance $c'$. For the sake of clarity, the values displayed on each edge have been rounded to the nearest integer within the graphical illustrations.

Table 2.1: Error in the recovered conductance.

| $m$ | 7 | 11 | 15 | 19 | 23 | 27 | 31 | 35 |
|---|---|---|---|---|---|---|---|---|
| $\|\|c' - c\|\|$ | $1 \cdot 10^{-14}$ | $4 \cdot 10^{-11}$ | $3 \cdot 10^{-7}$ | $4 \cdot 10^{-3}$ | $5 \cdot 10^{2}$ | $2 \cdot 10^{3}$ | $7 \cdot 10^{3}$ | $9 \cdot 10^{3}$ |

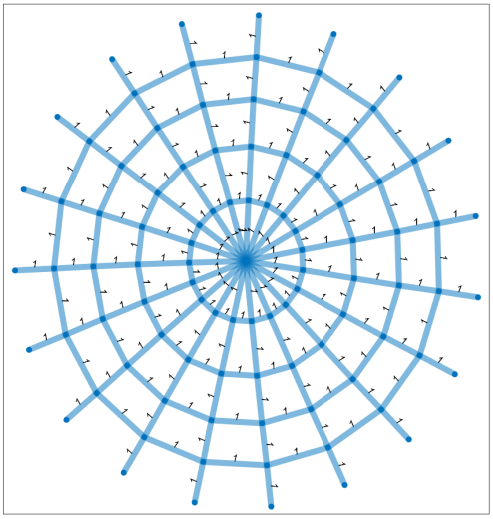

Figure 2.4: Recovered network with $m = 19$ radii in Example 1.

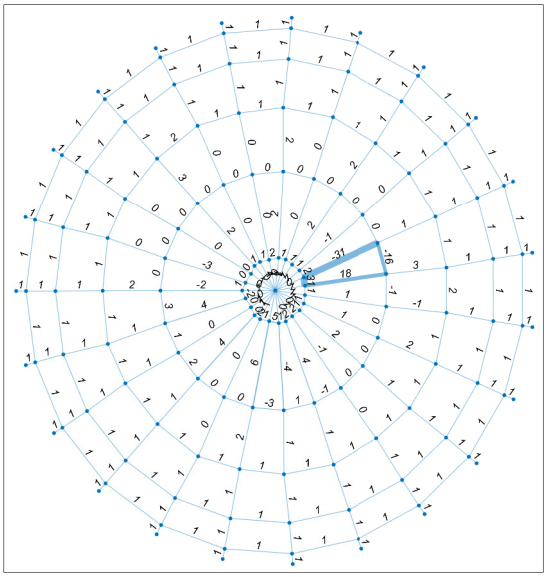

Figure 2.5: Recovered network with $m = 23$ radii in Example 1.

The error for $m = 19$ is approximately $3.5 \cdot 10^{-3}$, and we see that the nearest integer to the value of the recovered conductance at every edge is equal to the true value $c = 1$. However, the error for the next bigger network, the one with $m = 23$, is approximately $5.2 \cdot 10$. We can see that the value of the recovered conductance is very far from 1 and in some cases even negative, especially in edges that are far from the boundary. For example there is an edge with conductance close to $-31$.

As a conclusion of the performed tests, the recovery of the conductance of a well-connected spider network is unstable except for small networks. Moreover, the big discrepancies appear on edges that are far away from the boundary. This situation is analogous to the one that appears in the continuous Calderón inverse conductivity problem, which is severely ill-posed, and the instabilities increase as we move farther away from the boundary, (see [26]).

## 2.3 Stable reformulation: the discrete piecewise constant conductance hypothesis

Calderón's problem is ill-posed, but in [6] it was shown that if the hypothesis that the conductivity is piecewise constant on a partition of the set $\Omega$ with a bounded number of connected subsets is *a priori* known, then the problem becomes Lipschitz stable. As in the previous section we have seen that its discrete counterpart is analogously ill-posed, we propose to translate this hypothesis to the discrete setting and to study the conductance recovery knowing *a priori* this hypothesis. This section is a review and extension of [38, Section 3].

In the discrete case, we say that a conductance is *piecewise constant* on a partition $E = E_1 \sqcup \cdots \sqcup E_s$ if it is constant on each $E_i$. Of course, as the number of edges is finite, any conductance is inherently piecewise constant on some partition. In this work, we understand that a *piecewise constant conductance hypothesis* holds if and only if $s$, the number of subsets in the partition, satisfies $s \ll |E|$. Note that we do not require for any $j = 1, ..., s$ that the subnetwork with edge set $E_j$ and whose vertex set is the set of vertices of the network which are joined by edges of $E_j$ is connected. Therefore this discrete hypothesis can be seen as a generalization of the strict discrete analogue of the hypothesis in [6] for the continuous problem in which the subsets of the partition must be connected.

As demonstrated in the preceding section, even when considering the extreme scenario where the real conductance satisfies the hypothesis with $s = 1$, it has been observed that the explicit recovery methods that solve the general inverse conductance problem lead to instabilities. That is due to the fact that the methods do not use the information of the hypothesis of being piecewise constant on a particular partition: they do not enforce that the solution must satisfy the hypothesis, nor penalize the deviation with respect to the hypothesis in the recovery process.

Consequently, it becomes imperative to develop alternative algorithms that ensure stability. Our proposal is to reformulate the inverse problem as a polynomial optimization problem that includes the deviation in the recovered conductance with respect to being piecewise con-

stant on a given partition as a penalty. We formulate the problem for any possible partition $E = E_1 \sqcup \cdots \sqcup E_s$ of the set of edges of the real network $\Gamma = (\bar{F}, c)$, whether its conductance $c$ is piecewise constant on this partition or not. In the case in which $s \ll |E|$, the penalty term penalizes the deviation with respect to a *piecewise constant conductance hypothesis*.

### 2.3.1 Polynomial optimization problem

The polynomial optimization problem that we propose to solve the discrete inverse problem can be stated as follows.

**Problem 2.3.1.** *[[38]] Let $\Gamma = (\bar{F}, c)$ be a well-connected spider DC network with known set of edges $E(\Gamma)$ but unknown conductance $c$, let $N$ be the kernel of the Dirichlet-to-Neumann map of $\Gamma$ and $F$, let $E(\Gamma) = E_1 \sqcup \cdots \sqcup E_s$ be a partition and let $\mu \geq 0$ be a penalty parameter. We denote by $\Gamma' = (\bar{F}, c')$ the DC network that we want to recover, which must satisfy $E(\Gamma') \subseteq E(\Gamma)$. We define another unknown DC network $\Gamma_\omega = (\bar{F}, \omega)$ such that $E(\Gamma_\omega) \subseteq E(\Gamma)$ and $\omega$ is piecewise constant on $E_1 \sqcup \cdots \sqcup E_s$. For each $z \in \delta(F)$, we define a function $u_z \in \mathscr{C}(V)$ such that $u_z = \varepsilon_z$ on $\delta(F)$. The problem consists in determining values of the variables*

(i) $c'(e_{xy})$ $(= c'(x,y) = c'(y,x))$ *for all* $e_{xy} \in E(\Gamma)$;

(ii) $\omega(E_j)$ *for all* $j = 1, \ldots, s$;

(iii) $u_z(x)$ *for all* $x \in F$ *and* $z \in \delta(F)$,

*which minimize the objective function*

$$\begin{aligned} p = &\int_{\delta(F)\times\delta(F)} \left( N(x,z) - \int_V c'(x,y)\,(u_z(x) - u_z(y))\,dy \right)^2 dxdz \\ &+ \mu \sum_{j=1}^{s} \sum_{e_{xy}\in E_j} (c'(x,y) - \omega(E_j))^2 \end{aligned} \tag{2.2}$$

*subject to the constraints*

$$g_x^z := \int_V c'(x,y)\,(u_z(x) - u_z(y))\,dy = 0 \tag{2.3}$$

*for all $x \in F$ and $z \in \delta(F)$; and $c'(e_{xy}) \geq 0$ for all $e_{xy} \in E$.*

Let $c'$ be a fixed feasible value for the conductance in the problem, and we denote by $\mathcal{L}'$, $\Lambda'$ and $N'$ the Laplacian, the Dirichlet-to-Neumann map and the kernel of the Dirichlet-to-Neumann map of the recovered network $\Gamma' = (\bar{F}, c')$, respectively. Then, for any $x \in F$ and $z \in \delta(F)$ we have that $g_x^z = \mathcal{L}'(u_z)(x)$. Because of that, the constraints (2.3) are equivalent to that, for each $z \in \delta(F)$, $u_z \in \mathscr{C}(V)$ is a solution to the boundary value problem (1.7) for $g = \varepsilon_z$, that is, the boundary value problem of finding $u \in \mathscr{C}(V)$ such that

$$\mathcal{L}'(u) = 0 \ \text{ on } \ F, \quad u = \varepsilon_z \ \text{ on } \ \delta(F), \tag{2.4}$$

Now, for each $x, z \in \delta(F)$, the evaluation at $x$ of the normal derivative of $u_z$ with respect to $F$ in $\Gamma'$ is equal to

$$\frac{\partial u_z}{\partial \mathsf{n}_{\mathsf{F}}}(x) = \int_V c'(x,y)\,(u_z(x) - u_z(y))\,dy = \int_F c'(x,y)\,(u_z(x) - u_z(y))\,dy,$$

and as a consequence of Remark 1.4.4, we have that

$$\frac{\partial u_z}{\partial \mathsf{n}_{\mathsf{F}}}(x) = \frac{\partial u_{\varepsilon_z}}{\partial \mathsf{n}_{\mathsf{F}}}(x) = \Lambda'(\varepsilon_z)(x) = N'(x,z).$$

Then, the objective function (2.2) can be rewritten as

$$p = ||\mathsf{N}' - \mathsf{N}||_{\mathrm{Fr}}^2 + \mu||c' - \omega||^2, \tag{2.5}$$

so a solution of Problem 2.3.1 minimizes the squared Frobenius norm of the difference between the response matrix $\mathsf{N}'$ of the recovered network and $\mathsf{N}$ plus a penalty term which is the squared norm (defined in Remark 1.2.3) of the difference between the recovered conductance and any piecewise constant conductance on $E = E_1 \sqcup \cdots \sqcup E_s$ multiplied by the penalty parameter $\mu$. In the context of Tikhonov-like regularization methods the parameter $\mu$ is often called regularization parameter (see [61, 76, 86]).

**Remark 2.3.2.** In Problem 2.3.1, we allow the possibility that $c'(x,y) = 0$ for some $e_{xy} \in E(\Gamma)$, and thus $E(\Gamma') \subsetneq E(\Gamma)$. As we have discussed, this is not a problem for the objective function $p$ to satisfy (2.5), even if some subset of vertices of $F$ is isolated in $\Gamma'$. Nevertheless, if we know *a priori* a value $\lambda > 0$ such that $c(e_{xy}) \geq \lambda$ for all $e_{xy} \in E(\Gamma)$, we can slightly modify the formulation of the problem, adding the restriction $c'(e_{xy}) \geq \lambda$ for all $e_{xy} \in E$ if we want to ensure that the topology of $\Gamma'$ and $\Gamma$ are the same. In that case, $\Gamma'$ is a network with boundary, so $u_z = u_{\varepsilon_z}$ for each $z \in \delta(F)$. Note that this *a priori* information is analogous to the known lower bound for the conductivity in the formulation of Calderón's problem.

We define the function $f : [0,\infty] \longrightarrow [0,\infty]$ which assigns to each $\mu$ the value of the minimum of $p$ in a solution to Problem 2.3.1, *i.e.*,

$$f(\mu) = \min_{\{c',\omega\}} \left\{||\mathsf{N}' - \mathsf{N}||_{\mathrm{Fr}}^2 + \mu||c' - \omega||^2\right\}.$$

We also define $h$ as the minimum value of $||\mathsf{N}' - \mathsf{N}||_{\mathrm{Fr}}^2$ among the conductances $c'$ that are piecewise constant on the partition $E = E_1 \sqcup \cdots \sqcup E_s$. Note that, for every $\mu$, we have that

$$f(\mu) \leq \min_{\{c',\omega : c' = \omega\}} \left\{||\mathsf{N}' - \mathsf{N}||_{\mathrm{Fr}}^2 + \mu||c' - \omega||^2\right\} = h.$$

By the last inequality, for every $\mu$, the evaluation of the term $\mu||c' - \omega||^2$ in a solution to Problem 2.3.1 must be lower than or equal to $h$. Then, for any $\mu > 0$, we have that

$$f(\mu) = \min_{\left\{c',\omega:\ ||c'-\omega|| \leq \sqrt{\frac{h}{\mu}}\right\}} \left\{||\mathsf{N}' - \mathsf{N}||_{\mathrm{Fr}}^2 + \mu||c' - \omega||^2\right\}.$$

From that expression, we see that the limit case of $\mu \to \infty$ corresponds with enforcing the hypothesis that the recovered conductance is piecewise constant on $E = E_1 \sqcup \cdots \sqcup E_s$

and minimizing the difference between $\mathsf{N}'$ and $\mathsf{N}$. The limit of $f(\mu)$ when $\mu \to \infty$ is equal to $h$. The case $\mu = 0$ corresponds with minimizing the difference between $\mathsf{N}'$ and $\mathsf{N}$ ignoring the piecewise constant hypothesis.

A solution to the Problem 2.3.1 must be a stationary point of the Lagrangian function of the optimization problem. In particular, if $\mu > 0$, for each $j = 1, \ldots, s$, the partial derivative of $\sum_{e_{xy} \in E_j} (c'(x,y) - \omega(E_j))^2$ with respect to the variable $\omega(E_j)$ must be equal to zero, so

$$\omega(E_j) = \frac{1}{|E_j|} \sum_{e_{xy} \in E_j} c'(x,y). \tag{2.6}$$

Therefore, the $\omega(E_1), \ldots, \omega(E_s)$ variables can be removed from the optimization problem by substituting in (2.2) each of the variables $\omega(E_j)$ with (2.6). Clearly, if $\mu = 0$, the objective function $p$ does not depend on the variables $\omega(E_1), \ldots, \omega(E_s)$, so we can remove them from the problem.

We remark that unlike other regularization methods to solve the discrete inverse conductance problem, as the ones in [24, 25, 27], ours has not used a reference conductance known *a priori*. Here, the $s$ constant values of the conductance $\omega$, which appear in the penalty term, are not fixed. On the contrary, they are considered as unknowns in the objective function.

In a well-connected spider network with $m = 4\ell + 3$ boundary vertices it is easy to check that there are $|E| = \binom{m}{2}$ edges and $n = \dfrac{m^2 + m + 4}{4}$ vertices. So, the number of variables of Problem 2.3.1, after removing $\omega(E_1), \ldots, \omega(E_s)$, is equal to

$$r = |E| + m(n - m) = \frac{m(m^2 - m + 2)}{4} = (4\ell + 3)(4\ell^2 + 5\ell + 2).$$

In particular, for the example 2.2.1 the number of variables goes from 77 corresponding to $\ell = 1$ to 10430 corresponding to $\ell = 8$.

We denote by $J = \left\langle g_x^z \text{ such that } x \in V,\ z \in \delta(F) \right\rangle$ the ideal generated by the quadratic polynomials in (2.3), and we denote by $V(J) \subset \mathbb{R}^r$ the real vanishing set of $J$. Then, Problem 2.3.1 can be rewritten as finding a global minimum of the quartic $p$ in the semialgebraic set

$$A = \left([0, \infty]^{|E|} \times \mathbb{R}^{r - |E|}\right) \cap V(J).$$

For $\mu = 0$, Problem 2.3.1 has a unique solution $\hat{t} \in A$, with $p(\hat{t}) = 0$. In the solution, we have that the recovered conductance is the real one, $c' = c$, because $\Gamma$ is the unique network with this topology whose response matrix is exactly $\mathsf{N}$. For every $z \in \delta(F)$, the value of $u_z$ in the solution is $u_z = u_{\varepsilon_z}$, which is the unique solution to (2.4). For any $\mu > 0$, if $c$ is piecewise constant on the partition $E = E_1 \sqcup \cdots \sqcup E_s$, then Problem 2.3.1 also has the same unique solution (with $p(\hat{t}) = 0$ and $c' = \omega = c$).

For any $\mu > 0$, if $c$ is not piecewise constant on the partition $E = E_1 \sqcup \cdots \sqcup E_s$, then a solution $\hat{t} \in A$ to Problem 2.3.1 must satisfy $p(\hat{t}) > 0$, because the recovered network with $c' = c$ is the unique with $||\mathsf{N}' - \mathsf{N}||_{\text{Fr}} = 0$, but for this network $||c' - \omega|| > 0$, (see [37]).

### 2.3.2 Problem resolution

Using a numerical optimization method, such as an interior point algorithm, we can obtain an approximation $t^* \in A$ to a local minimum of $p$ in $A$. In Section 2.4, we will discuss several examples of how the recovered conductance $c'$ in the computed $t^* \in A$ approximates the real conductance $c$ when $c$ is piecewise constant on the partition $E = E_1 \sqcup \cdots \sqcup E_s$. Sections 2.5 and 2.6 are dedicated to discuss several examples of how $c'$ approximates $c$ when $c$ is not piecewise constant on the partition.

We denote by $\Gamma_1 = (\bar{F}, \chi_{_E})$ the DC network with the same topology as $\Gamma$ such that $\chi_{_E}(e_{xy}) = 1$ for every $e_{xy} \in E(\Gamma)$. As an initial guess for the interior point algorithm we choose a constant conductance, $c^0\chi_{_E}$, on the spider graph. The value of $c^0 > 0$ is determined as the one such that the response matrix of $(\bar{F}, c^0\chi_{_E})$ is the closest to $\mathsf{N}$ in the Frobenius norm.

**Proposition 2.3.3.** *Consider a network with boundary $\Gamma = (\bar{F}, c)$ and its response matrix $\mathsf{N}$. Then, the network $\Gamma_0 = (\bar{F}, c^0\chi_{_E})$ with the same set of edges $E$ as $\Gamma$ and constant conductance $c^0 > 0$ at all edges whose response matrix is the closest to $\mathsf{N}$ in the Frobenius norm satisfies that*

$$c^0 = \frac{\operatorname{tr}(\mathsf{N}_1\mathsf{N})}{||\mathsf{N}_1||^2_{\mathrm{Fr}}} = \operatorname{argmin}_{x>0}\left\{||\mathsf{N} - x\mathsf{N}_1||^2_{\mathrm{Fr}}\right\},$$

*where $\mathsf{N}_1$ is the response matrix of the unweighted network $\Gamma_1 = (\bar{F}, \chi_{_E})$.*

**Proof.** If $\mathsf{L}_1$ is the Laplacian matrix of $\Gamma_1$, then

$$\mathsf{N}_1 = \mathsf{L}_1(\delta(F);\delta(F)) - \mathsf{L}_1(\delta(F);F)\mathsf{L}_1(F;F)^{-1}\mathsf{L}_1(\delta(F);F)^T.$$

For any $x > 0$, the Laplacian matrix of the network with set of edges $E$ and constant conductance equal to $x$ is $x\mathsf{L}_1$ and hence, its response matrix is $x\mathsf{N}_1$. On the other hand,

$$||\mathsf{N} - x\mathsf{N}_1||^2_{\mathrm{Fr}} = x^2||\mathsf{N}_1||^2_{\mathrm{Fr}} - 2x\operatorname{tr}(\mathsf{N}_1\mathsf{N}) + ||\mathsf{N}||^2_{\mathrm{Fr}}$$

whose minimum is attained at $c^0 = \dfrac{\operatorname{tr}(\mathsf{N}_1\mathsf{N})}{||\mathsf{N}_1||^2_{\mathrm{Fr}}}$. Moreover each term in the diagonal of $\mathsf{N}_1\mathsf{N}$ is positive, since $\mathsf{N}_1$ and $\mathsf{N}$ are both $M$-matrices. Therefore, $c^0 > 0$. □

**Remark 2.3.4.** *In the case of a well-connected spider, if $m \geq 7$, then*

$$\mathsf{N}_1 = (\mathsf{I} - \mathsf{J}(\delta(F^c);\delta(F^c))$$

*where $\mathsf{J} = \mathsf{L}_1(F;F)^{-1}$, is the matrix associated with the Green operator of the network $\Gamma_1$ on $F$, $\mathscr{J}$; and if $m = 3$, then*

$$\mathsf{N}_1 = \frac{1}{3}\begin{pmatrix} 2 & -1 & -1 \\ -1 & 2 & -1 \\ -1 & -1 & 2 \end{pmatrix}.$$

**Remark 2.3.5.** For each $z \in \delta(F)$ and each $x \in F$, we choose as an initial guess for the variable $u_z(x)$ the unique value which is compatible with satisfying all the constraints (2.3) when $c' = c^0\chi_{_E}$. That is, denoting by $\mathcal{L}_0$ the Laplacian of $\Gamma_0$, for each $z \in \delta(F)$, the initial

guess for $u_z$ is the unique solution to the boundary value problem of finding $u \in \mathscr{C}(V)$ such that

$$\mathcal{L}_0(u) = 0 \ \text{ on } \ F, \quad u = \varepsilon_z \ \text{ on } \ \delta(F).$$

As a consequence, the initial guess for the variable $u_z(x)$ is equal to

$$\big( -\mathsf{L}_1(F;F)^{-1} \cdot \mathsf{L}_1(\delta(F);F)^T \big)(x,z).$$

For computing the experiments in the next sections, we write the proposed optimization problem in MATLAB using Casadi [101], an open-source software tool that provides a symbolic framework suited for numerical optimization, and we obtain an approximate solution of it using the interior-point solver IPOPT [102], an open-source software package for large-scale nonlinear optimization. The tolerance used in IPOPT is equal to $10^{-8}$.

## 2.4 Stable recovery of piecewise constant conductances

In this section, we present numerical examples of the resolution of Problem 2.3.1 in the case in which we aim to recover the conductance of a well-connected spider network $\Gamma = (\bar{F}, c)$ knowing its topology, its Dirichlet-to-Neumann map and a partition $E(\Gamma) = E_1 \sqcup \cdots \sqcup E_s$ such that the real conductance $c$ is really piecewise constant on the partition. This section is a review of [38, Section 3].

In this case, as discussed in the previous section, for any value of the penalty parameter $\mu \geq 0$, the problem has a unique solution $\hat{t} \in A$ with $p(\hat{t}) = 0$, in which the recovered conductance is the real one, and using a numerical optimization method we obtain $t^* \in A$, an approximation of a local minimum of $p$ in $A$. In all the tested experiments, for any value of $\mu$, any network $\Gamma = (\bar{F}, c)$, and any partition, the evaluation of $p$ at $t^*$ has a very small value $p(t^*) \approx p(\hat{t}) = 0$, which is usually lower than the tolerance of the numerical optimization method. That means that in every case we recover a network whose response matrix $\mathsf{N}'$ is very close to the one of $\Gamma$, $\mathsf{N}$.

Nevertheless, because of the ill-posedness of the inverse conductance problem, this does not guarantee that $t^* \in A$ is close to $\hat{t} \in A$, (nor that the recovered conductance $c'$ is close to $c$). In fact, when $\mu = 0$, we obtain results similar to those of Example 2.2.1, in the sense that usually $t^*$ is an approximation of a local minimum which is very far from $\hat{t}$, and $c'$ is very far from $c$, and the instability increases with the size of the network. This is expected, because we are not using any information *a priori* or regularization.

The values of the conductance of any well-connected spider network at the edges are rational functions of the entries of its response matrix, (see [54]), and therefore the inverse conductance problem is locally Lipschitz stable. As a consequence, given $\lambda > 0$, there is a constant $M$ such that for any two networks $\Gamma_1 = (\bar{F}, c_1)$ and $\Gamma_2 = (\bar{F}, c_2)$ with the topology of $\Gamma$ such that $\lambda \geq c_1(x,y) \geq \lambda^{-1}$ and $\lambda \geq c_2(x,y) \geq \lambda^{-1}$ for every $e_{xy} \in E(\Gamma)$, then

$$||c_1 - c_2|| \leq M ||\mathsf{N}_1 - \mathsf{N}_2||_{\mathrm{Fr}},$$

where $\mathsf{N}_1$ and $\mathsf{N}_2$ are the response matrices of $\Gamma_1$ and $\Gamma_2$, respectively. In the experiments, alongside with the error in the recovered conductance $||c' - c||$, we compute the quotient $\dfrac{||c' - c||}{||\mathsf{N}' - \mathsf{N}||_{\text{Fr}}}$, which is a lower bound of the Lipschitz constant.

In Calderón's inverse problem the Lipschitz stability constant depends on the partition in which the conductivity is piecewise constant, as well as in the bounds of the conductivity and the set on which the conductivity is defined. It is expected that the constant will diverge as the number of subsets in the partition goes to infinity [6].

By analogy, in the discrete setting, when the recovered conductance $c'$ is approximately piecewise constant on the partition $E(\Gamma) = E_1 \sqcup \cdots \sqcup E_s$, (on which $c$ is piecewise constant), we expect that the stability of the problem depends on $m$, $s$ and the partition. We also expect the problem becomes unstable as $s \to |E|$, that is, when the piecewise constant conductance hypothesis is false. Note that in the limit $s = |E|$, each edge is in a different subset of the partition, so the penalty term is meaningless.

In the next example we see that when the value of $\mu > 0$ is big enough, and the *piecewise constant conductance hypothesis* holds for $c$, that is, when $c$ is piecewise constant on $E(\Gamma) = E_1 \sqcup \cdots \sqcup E_s$ with $s \ll |E|$, in all the tests we recover the real conductance almost exactly, so $t^*$ is an approximation of $\hat{t}$. This example provides experimental results that suggest that when the piecewise constant conductance hypothesis is true and known *a priori*, the inverse conductance problem becomes well-posed.

**Example 2.4.1.** *For each* $m = 7, 11, 15, 19, 23, 27, 31, 35,\ 39, 43$ *and* $47$*, and for each* $s = 1, \ldots, 10$*, we generate* $10$ *well-connected spider networks with* $m$ *radii, each with a conductance which is piecewise constant on a (possibly different) random partition with* $s$ *subsets. For the case* $m = 3$*, we do the same, but only for* $s = 1, 2$ *and* $3$*, because the total number of edges of the graph is* $3$*.*

*For each combination of values of* $m$ *and* $s$*, for each of the* $10$ *networks, the value of the conductance at each subset of the partition is sampled from the uniform distribution in the interval* $[1, 100]$*. The total number of tested networks is* $1130$*. According with the comments in the preceding section, the number of variables in the above tests goes from* $77$ *corresponding to* $m = 7$ *to* $25427$ *corresponding to* $m = 47$*.*

For each network with conductance $c$, we compute its response matrix $\mathsf{N}$, we recover the conductance $c'$, we compute the error $||c' - c||$, and we compute the quotient $\dfrac{||c' - c||}{||\mathsf{N}' - \mathsf{N}||_{\text{Fr}}}$. In Table 2.2, we show the maximum error in the recovered conductance in the 10 networks with each combination of values of $m$ and $s$. Analogously, we show in Table 2.3 the maximum $\dfrac{||c' - c||}{||\mathsf{N}' - \mathsf{N}||_{\text{Fr}}}$ in the 10 networks with each combination of values of $m$ and $s$.

To recover the conductance of all networks, we choose a value of $\mu = 1$ as penalty parameter in our problem. With this value, in all the experiments, we obtain a solution such that the evaluation of the quartic $p$ at it is lower than $1.3746 \cdot 10^{-13}$, the evaluation of the deviation with respect to the hypothesis of being piecewise constant, $||c' - \omega||^2$, is lower than $9.1998 \cdot 10^{-14}$, and the deviation in the response matrix with respect to the data, $||\mathsf{N}' - \mathsf{N}||^2_{\text{Fr}}$, is lower than $4.5463 \cdot 10^{-14}$.

Table 2.2: Maximum error in the recovered conductance with one significant digit.

| $m\backslash s$ | 1 | 2 | 3 | 4 | 5 | 6 | 7 | 8 | 9 | 10 |
|---|---|---|---|---|---|---|---|---|---|---|
| 3 | $2\cdot10^{-10}$ | $8\cdot10^{-10}$ | $1\cdot10^{-9}$ | | | | | | | |
| 7 | $1\cdot10^{-8}$ | $1\cdot10^{-10}$ | $6\cdot10^{-6}$ | $1\cdot10^{-9}$ | $2\cdot10^{-8}$ | $1\cdot10^{-8}$ | $4\cdot10^{-7}$ | $9\cdot10^{-8}$ | $4\cdot10^{-7}$ | $1\cdot10^{-6}$ |
| 11 | $3\cdot10^{-9}$ | $5\cdot10^{-9}$ | $4\cdot10^{-10}$ | $3\cdot10^{-8}$ | $2\cdot10^{-8}$ | $9\cdot10^{-9}$ | $9\cdot10^{-8}$ | $3\cdot10^{-8}$ | $3\cdot10^{-7}$ | $4\cdot10^{-7}$ |
| 15 | $5\cdot10^{-8}$ | $4\cdot10^{-10}$ | $3\cdot10^{-8}$ | $2\cdot10^{-9}$ | $8\cdot10^{-8}$ | $6\cdot10^{-9}$ | $2\cdot10^{-7}$ | $2\cdot10^{-8}$ | $1\cdot10^{-7}$ | $8\cdot10^{-8}$ |
| 19 | $2\cdot10^{-8}$ | $2\cdot10^{-9}$ | $2\cdot10^{-8}$ | $2\cdot10^{-9}$ | $2\cdot10^{-8}$ | $2\cdot10^{-8}$ | $2\cdot10^{-8}$ | $4\cdot10^{-8}$ | $2\cdot10^{-7}$ | $1\cdot10^{-6}$ |
| 23 | $3\cdot10^{-8}$ | $1\cdot10^{-8}$ | $5\cdot10^{-9}$ | $2\cdot10^{-8}$ | $1\cdot10^{-8}$ | $7\cdot10^{-9}$ | $1\cdot10^{-6}$ | $3\cdot10^{-7}$ | $1\cdot10^{-7}$ | $9\cdot10^{-8}$ |
| 27 | $2\cdot10^{-7}$ | $4\cdot10^{-8}$ | $9\cdot10^{-8}$ | $1\cdot10^{-6}$ | $2\cdot10^{-7}$ | $6\cdot10^{-8}$ | $5\cdot10^{-7}$ | $9\cdot10^{-8}$ | $1\cdot10^{-7}$ | $4\cdot10^{-7}$ |
| 31 | $2\cdot10^{-7}$ | $2\cdot10^{-8}$ | $4\cdot10^{-8}$ | $3\cdot10^{-7}$ | $7\cdot10^{-9}$ | $3\cdot10^{-8}$ | $3\cdot10^{-8}$ | $1\cdot10^{-7}$ | $4\cdot10^{-8}$ | $2\cdot10^{-7}$ |
| 35 | $1\cdot10^{-7}$ | $3\cdot10^{-8}$ | $1\cdot10^{-7}$ | $7\cdot10^{-8}$ | $1\cdot10^{-7}$ | $7\cdot10^{-8}$ | $7\cdot10^{-7}$ | $1\cdot10^{-7}$ | $1\cdot10^{-7}$ | $8\cdot10^{-7}$ |
| 39 | $1\cdot10^{-7}$ | $1\cdot10^{-8}$ | $7\cdot10^{-9}$ | $5\cdot10^{-8}$ | $1\cdot10^{-6}$ | $7\cdot10^{-7}$ | $4\cdot10^{-7}$ | $8\cdot10^{-7}$ | $9\cdot10^{-8}$ | $4\cdot10^{-8}$ |
| 43 | $3\cdot10^{-7}$ | $4\cdot10^{-7}$ | $2\cdot10^{-8}$ | $1\cdot10^{-7}$ | $6\cdot10^{-8}$ | $3\cdot10^{-8}$ | $9\cdot10^{-7}$ | $4\cdot10^{-8}$ | $4\cdot10^{-8}$ | $2\cdot10^{-7}$ |
| 47 | $1\cdot10^{-7}$ | $4\cdot10^{-8}$ | $5\cdot10^{-8}$ | $5\cdot10^{-7}$ | $9\cdot10^{-8}$ | $5\cdot10^{-7}$ | $4\cdot10^{-7}$ | $7\cdot10^{-7}$ | $3\cdot10^{-8}$ | $6\cdot10^{-7}$ |

Table 2.3: Maximum $\frac{||c'-c||}{||\mathsf{N}'-\mathsf{N}||_{\mathrm{Fr}}}$ in the recovered conductance with one significant digit.

| $m\backslash s$ | 1 | 2 | 3 | 4 | 5 | 6 | 7 | 8 | 9 | 10 |
|---|---|---|---|---|---|---|---|---|---|---|
| 3 | $1\cdot10^{0}$ | $4\cdot10^{-1}$ | $7\cdot10^{0}$ | | | | | | | |
| 7 | $3\cdot10^{0}$ | $4\cdot10^{0}$ | $2\cdot10^{2}$ | $3\cdot10^{1}$ | $1\cdot10^{2}$ | $2\cdot10^{2}$ | $8\cdot10^{1}$ | $6\cdot10^{2}$ | $1\cdot10^{2}$ | $7\cdot10^{2}$ |
| 11 | $4\cdot10^{0}$ | $8\cdot10^{0}$ | $9\cdot10^{0}$ | $1\cdot10^{1}$ | $7\cdot10^{1}$ | $7\cdot10^{1}$ | $3\cdot10^{1}$ | $7\cdot10^{1}$ | $8\cdot10^{2}$ | $1\cdot10^{2}$ |
| 15 | $5\cdot10^{0}$ | $5\cdot10^{0}$ | $4\cdot10^{1}$ | $1\cdot10^{1}$ | $5\cdot10^{1}$ | $1\cdot10^{1}$ | $5\cdot10^{1}$ | $6\cdot10^{1}$ | $1\cdot10^{2}$ | $8\cdot10^{1}$ |
| 19 | $5\cdot10^{0}$ | $6\cdot10^{0}$ | $7\cdot10^{0}$ | $1\cdot10^{1}$ | $8\cdot10^{0}$ | $3\cdot10^{1}$ | $6\cdot10^{1}$ | $9\cdot10^{1}$ | $2\cdot10^{2}$ | $8\cdot10^{1}$ |
| 23 | $6\cdot10^{0}$ | $7\cdot10^{0}$ | $1\cdot10^{1}$ | $4\cdot10^{1}$ | $1\cdot10^{1}$ | $2\cdot10^{1}$ | $2\cdot10^{1}$ | $3\cdot10^{1}$ | $2\cdot10^{1}$ | $2\cdot10^{1}$ |
| 27 | $7\cdot10^{0}$ | $7\cdot10^{0}$ | $3\cdot10^{1}$ | $8\cdot10^{0}$ | $1\cdot10^{1}$ | $2\cdot10^{1}$ | $8\cdot10^{1}$ | $2\cdot10^{1}$ | $8\cdot10^{1}$ | $7\cdot10^{1}$ |
| 31 | $7\cdot10^{0}$ | $8\cdot10^{0}$ | $9\cdot10^{0}$ | $9\cdot10^{0}$ | $2\cdot10^{1}$ | $2\cdot10^{1}$ | $6\cdot10^{1}$ | $5\cdot10^{1}$ | $6\cdot10^{1}$ | $4\cdot10^{1}$ |
| 35 | $8\cdot10^{0}$ | $9\cdot10^{0}$ | $1\cdot10^{1}$ | $1\cdot10^{1}$ | $1\cdot10^{1}$ | $1\cdot10^{1}$ | $1\cdot10^{1}$ | $1\cdot10^{1}$ | $3\cdot10^{1}$ | $1\cdot10^{1}$ |
| 39 | $8\cdot10^{0}$ | $1\cdot10^{1}$ | $1\cdot10^{1}$ | $1\cdot10^{1}$ | $1\cdot10^{1}$ | $1\cdot10^{1}$ | $1\cdot10^{1}$ | $5\cdot10^{1}$ | $2\cdot10^{1}$ | $2\cdot10^{1}$ |
| 43 | $8\cdot10^{0}$ | $1\cdot10^{1}$ | $1\cdot10^{1}$ | $1\cdot10^{1}$ | $1\cdot10^{1}$ | $1\cdot10^{1}$ | $1\cdot10^{1}$ | $1\cdot10^{1}$ | $1\cdot10^{1}$ | $3\cdot10^{1}$ |
| 47 | $9\cdot10^{0}$ | $1\cdot10^{1}$ | $1\cdot10^{1}$ | $1\cdot10^{1}$ | $1\cdot10^{1}$ | $1\cdot10^{1}$ | $2\cdot10^{1}$ | $2\cdot10^{1}$ | $3\cdot10^{1}$ | $4\cdot10^{1}$ |

We see in Table 2.2 that we recover the conductance of all networks with an error lower than $6.0250\cdot10^{-6}$, which is much lower than the norm of the real conductances. In Table 2.3, we see that in all cases the error in the conductance is lower than 833 times the error in the response matrix with respect to the data, $||\mathsf{N}'-\mathsf{N}||_{\mathrm{Fr}}$.

As a note, we have done the same experiment for a wide range of different positive values of $\mu$, recovering in all cases the conductances with very low error. The recovery only becomes unstable when the network is large and $\mu\to0$, because we obtain solutions such that the evaluation of the quartic $p=||\mathsf{N}'-\mathsf{N}||^2_{\mathrm{Fr}}+\mu||c'-\omega||^2$ is almost zero, but the value $||c'-\omega||^2$ is very high, so the conductance is far from being piecewise constant.

In all 1130 cases, the fact that the deviation with respect to the piecewise constant hypothesis is very low gives us a stable recovery of the conductances. As the partition is different in general for the 10 networks with the same value of $m$ and $s$, we get quite different errors recovering them, but we see that in general, the maximum of the ratio $\dfrac{||c'-c||}{||\mathsf{N}'-\mathsf{N}||_{\mathrm{Fr}}}$ increases with $s$, as expected. For example, in the case $m=7$ and $s=10$, $s$ is almost half of the total number of edges ($|E|=21$), and the ratio is equal to $7\cdot10^2$. However, for $m=35$ and $s=10$, that represents almost the 2% of the edges, the ratio equals 10.

All the computations have been performed on a personal laptop with Intel(R) Core(TM)

i5-1035G1 CPU and 8GB RAM. For the biggest case $m = 47$ the number of variables, for each one of the 100 test performed, is 25427 and the computation time is approximately 1/2 hour. The experiments conducted show that the method remains stable as $m$ increases. But the variation of $s$ is critical, as we will see in the next experiment.

We consider an example of recovery of piecewise constant conductances in networks with the same value of radii $m = 11$ and all possible number of subsets of the partition $s$ to see how the stability varies with $s$.

**Example 2.4.2.** *We set* $m = 11$*, and for each* $s = 1, \dots, |E| = 55$*, we generate* 100 *different spider networks with* 11 *radii and piecewise constant conductance whose values at each subset of the partition is sampled from the uniform distribution in the interval* $[1, 100]$*.*

As in Example 2.4.1, we set $\mu = 1$, we compute its response matrix $\mathsf{N}$, we recover the conductance $c'$, we compute the error $||c' - c||$, and we compute the quotient $\dfrac{||c' - c||}{||\mathsf{N}' - \mathsf{N}||_{\text{Fr}}}$. In Figure 2.6, we show the logarithm of the maximum error in the recovered conductance in the 100 networks with each value of $s$. Analogously, we show in Figure 2.7 the logarithm of the maximum $\dfrac{||c' - c||}{||\mathsf{N}' - \mathsf{N}||_{\text{Fr}}}$ in the 100 networks with each value of $s$.

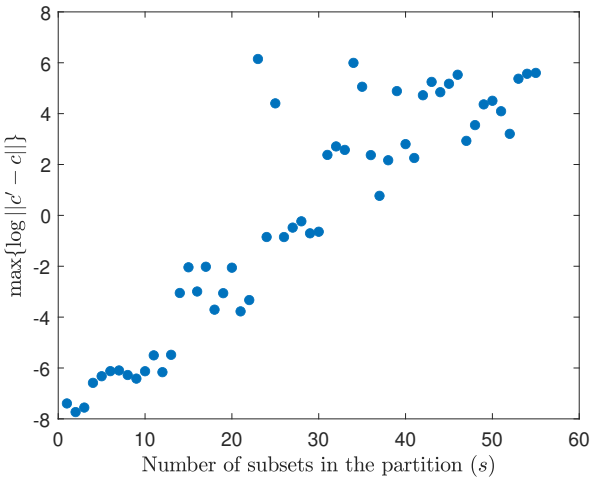


Figure 2.6: Maximum of the logarithm of the error in the recovered conductances of 100 networks with $m = 11$ and $s = 1, \dots, 55$. (Example 2.4.2).

In this example, we see that there is a strong linear dependence between the logarithm of the maximum of the ratio $\dfrac{||c' - c||}{||\mathsf{N}' - \mathsf{N}||_{\text{Fr}}}$ and $s$, which is in agreement with the results obtained in [6, 85] about exponential behaviour of the Lipschitz constant with respect to the number of regions where the conductivity is constant. The line in Figure 2.7 shows the linear regression between the number of subsets in a partition and the logarithm of the maximum ratio. It has been computed using Matlab and the results show a value of R-squared equal to 0.938 with a p-value of $1.22 \cdot 10^{-33}$.

In every case, we are able to recover a network with a low value of $||\mathsf{N}' - \mathsf{N}||_{\text{Fr}}$, so we see that the error $||c' - c||$ is low when $s \ll |E|$. In particular, we see that for values of $s$

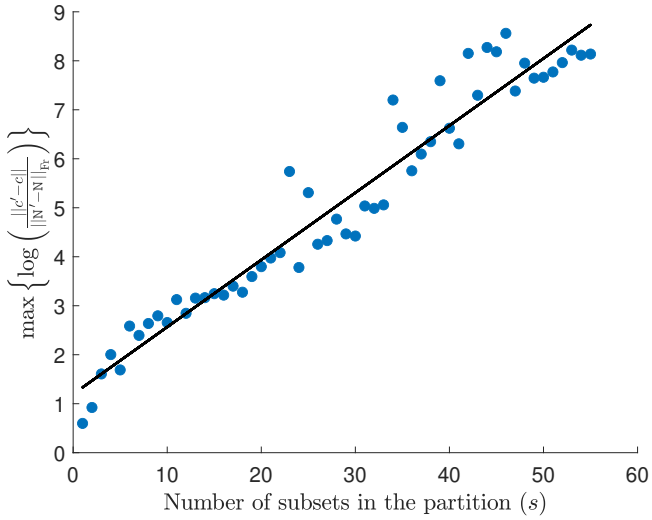


Figure 2.7: Maximum $\log\left(\frac{||c'-c||}{||\mathsf{N}'-\mathsf{N}||_{\mathrm{Fr}}}\right)$ in recovered conductance of 100 networks with $m = 11$ and $s = 1, \ldots, 55$. (Example 2.4.2).

between 1 and 13, the error in the recovered conductances is very low in all the networks. Besides, for values of $s$ between 14 and 22, the error is greater in some cases, but smaller than the norm of the real conductances. Finally, for $s > 23$, there are networks in which the recovered conductances have a great error.

We finish this work by considering again the test of Example 2.2.1 but with our approach. These results will show the robustness of our method, since as we will see all the cases are stable and even if we perturb the response matrix we can recover the conductance.

**Example 2.4.3.** *For $m = 7, 11, 15, 19, 23, 27, 31$, 35, 39, 43 and 47, we start from the well-connected spider network with $m$ radii and constant conductance $c = 1$. In all cases, we compute the response matrix $\mathsf{N}$ of the network, and from it we recover the conductance $c'$ obtaining an approximation to Problem 2.3.1 with $s = 1$. Additionally, for each $m$ we repeat 10 times the process of adding random perturbations to each entry of $\mathsf{N}$ sampled from a uniform distribution in each of the intervals $[-10^{-8}, 10^{-8}]$, $[-10^{-7}, 10^{-7}]$ and $[-10^{-1}, 10^{-1}]$, and then recovering the conductance with the perturbed matrix.*

As in Example 2.4.1, we set $\mu = 1$, we recover the conductance $c'$, we compute the error $||c' - c||$, and we compute the quotient $\dfrac{||c' - c||}{||\mathsf{N}' - \mathsf{N}||_{\mathrm{Fr}}}$. In the first row of Table 2.4 we show the error in the recovered conductance in the unperturbed case. As we see the error is very small, especially in comparison with the results displayed in Table 2.1. We can initially see that for $m = 7, 11$ the error is smaller in the explicit case, however for $m$ bigger or equal than 15, when the explicit case becomes unstable, not only the error is smaller with our algorithm but also the recovered value accurately approximates the spider network with constant conductance 1, see Figure 2.8 for the case $m = 23$. In this last case, observe that the maximum error in the conductance values is $1.4 \cdot 10^{-8}$.

In the rest of the entries of Table 2.4 we show, for each network and each interval of

perturbation, the maximum error in the 10 recovered networks. Moreover, in Table 2.5, we display the maximum of the values of $\frac{||c' - c||}{||\mathsf{N}' - \mathsf{N}||_{\text{Fr}}}$. As we can see the results are similar to the ones obtained by considering the unperturbed $\mathsf{N}$, except for the case where the magnitude of the perturbation is $10^{-1}$. In this case, the error is much bigger but still comparable with the magnitude of the perturbation performed. Besides, the value for the conductance is close enough to 1, see Figure 2.9. This also shows the robustness of our algorithm. We can compare these results in Table 2.4 with the ones obtained in [55, Section 13], where a similar experiment was conducted only for $m = 15$. There, the authors perturbed the entries of $\mathsf{N}$ randomly by terms of magnitude $10^{-8}$ obtaining the conductance values with an error of up to 0.5. Also, the authors perturbed the entries of $\mathsf{N}$ randomly by terms of magnitude $10^{-7}$ obtaining several negative values in the conductance. In contrast, using our algorithm the maximum error in the conductance of an edge is $1.1 \cdot 10^{-8}$ for perturbations of order of magnitude $10^{-8}$; and the maximum error in the conductance is $8.7 \cdot 10^{-8}$ for perturbations of order of magnitude $10^{-7}$. We have continued this experiment with perturbations of order of magnitude $10^{-1}$, obtaining a conductance whose maximum error is $7.8 \cdot 10^{-2}$.

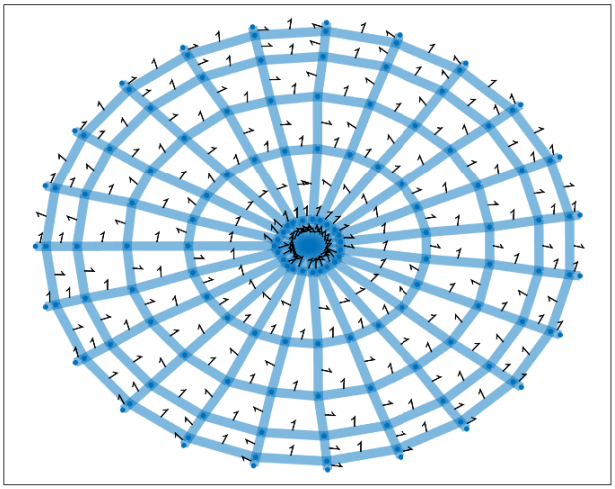

Figure 2.8: Recovered network with $m = 23$ radii in Example 2.4.3.

Table 2.4: Maximum error in the recovered conductance with one significant digit.

| Interval $\backslash m$ | 7 | 11 | 15 | 19 | 23 | 27 | 31 | 35 | 39 | 43 | 47 |
|---|---|---|---|---|---|---|---|---|---|---|---|
| Unperturbed | $2 \cdot 10^{-8}$ | $4 \cdot 10^{-8}$ | $9 \cdot 10^{-8}$ | $1 \cdot 10^{-7}$ | $2 \cdot 10^{-7}$ | $3 \cdot 10^{-7}$ | $4 \cdot 10^{-7}$ | $5 \cdot 10^{-7}$ | $6 \cdot 10^{-7}$ | $8 \cdot 10^{-7}$ | $9 \cdot 10^{-7}$ |
| $[-10^{-8}, 10^{-8}]$ | $4 \cdot 10^{-8}$ | $6 \cdot 10^{-8}$ | $1 \cdot 10^{-7}$ | $2 \cdot 10^{-7}$ | $3 \cdot 10^{-7}$ | $4 \cdot 10^{-7}$ | $4 \cdot 10^{-7}$ | $6 \cdot 10^{-7}$ | $7 \cdot 10^{-7}$ | $8 \cdot 10^{-7}$ | $1 \cdot 10^{-6}$ |
| $[-10^{-7}, 10^{-7}]$ | $3 \cdot 10^{-7}$ | $4 \cdot 10^{-7}$ | $5 \cdot 10^{-7}$ | $6 \cdot 10^{-7}$ | $6 \cdot 10^{-7}$ | $1 \cdot 10^{-6}$ | $7 \cdot 10^{-7}$ | $7 \cdot 10^{-7}$ | $9 \cdot 10^{-7}$ | $1 \cdot 10^{-6}$ | $2 \cdot 10^{-6}$ |
| $[-10^{-1}, 10^{-1}]$ | $3 \cdot 10^{-1}$ | $4 \cdot 10^{-1}$ | $4 \cdot 10^{-1}$ | $4 \cdot 10^{-1}$ | $3 \cdot 10^{-1}$ | $8 \cdot 10^{-1}$ | $9 \cdot 10^{-1}$ | $9 \cdot 10^{-1}$ | $6 \cdot 10^{-1}$ | $8 \cdot 10^{-1}$ | $8 \cdot 10^{-1}$ |

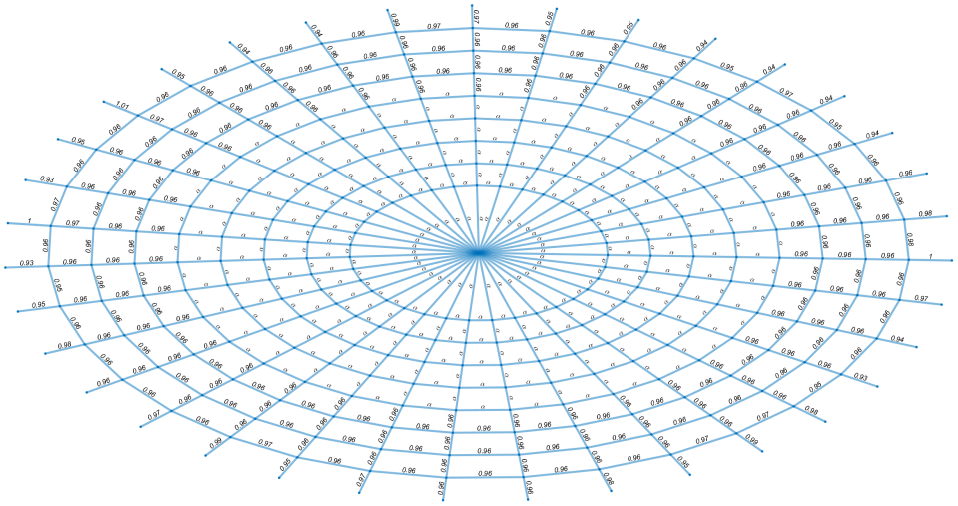

Figure 2.9: Recovered network with $m = 35$ radii in Example 2.4.3 and perturbations in the interval $[-10^{-1}, 10^{-1}]$. ($\alpha = 0.96$).

Table 2.5: Maximum $\frac{||c'-c||}{||\mathsf{N}'-\mathsf{N}||_{\mathrm{Fr}}}$ in the recovered conductance with two significant digits.

| Interval $\backslash m$ | 7 | 11 | 15 | 19 | 23 | 27 | 31 | 35 | 39 | 43 | 47 |
|---|---|---|---|---|---|---|---|---|---|---|---|
| Unperturbed | 2.8 | 3.9 | 4.7 | 5.4 | 6.0 | 6.6 | 7.1 | 7.6 | 8.0 | 8.5 | 8.9 |
| $[-10^{-8}, 10^{-8}]$ | 2.7 | 4.8 | 5.1 | 5.7 | 6.3 | 6.7 | 7.6 | 7.8 | 8.1 | 8.7 | 9.0 |
| $[-10^{-7}, 10^{-7}]$ | 2.5 | 3.4 | 3.9 | 4.6 | 4.9 | 5.5 | 5.8 | 6.2 | 6.8 | 7.3 | 7.8 |
| $[-10^{-1}, 10^{-1}]$ | 2.5 | 3.4 | 3.8 | 4.1 | 4.2 | 5.1 | 5.5 | 5.7 | 5.4 | 6.1 | 6.4 |

## 2.5 Error Variation with respect to the penalty parameter

This section is a review of [37, Section 2]. The formulation of Problem 2.3.1 introduces the deviation with respect to the piecewise constant hypothesis as a penalty rather than imposing the hypothesis and minimizing the difference between $\mathsf{N}'$ and $\mathsf{N}$. As $\mu \to \infty$, the formulation of the problem corresponds with this last scenario.

As discussed in the previous section, in the case that the real conductance $c$ is piecewise constant on the partition $E = E_1 \sqcup \cdots \sqcup E_s$, with $s \ll |E|$, the solution of the problem is almost equal for every $\mu > 0$, recovering a conductance that is very close to $c$, except when $\mu \to 0$, that is when the problem becomes unstable. Therefore, in that case, the penalty formulation for any value of $\mu$ that is big enough gives almost the same experimental results as the approach of imposing the hypothesis and minimizing the difference between $\mathsf{N}'$ and $\mathsf{N}$.

Nevertheless, the penalty formulation has the advantage of making possible to consider

intermediate values of $\mu \in (0, \infty)$ that allow us to obtain a good approximation to the conductance avoiding the instabilities in cases in which the conductance is not piecewise constant on the partition $E = E_1 \sqcup \cdots \sqcup E_s$, as we can see in the following example.

**Example 2.5.1.** *We consider the DC spider network $\Gamma = (\bar{F}, c)$ with $m = 19$ radii, see Figure 2.10, and we show how the error in recovering the conductance varies with $\mu$ when a piecewise constant conductance hypothesis which does not hold in the network is used.*

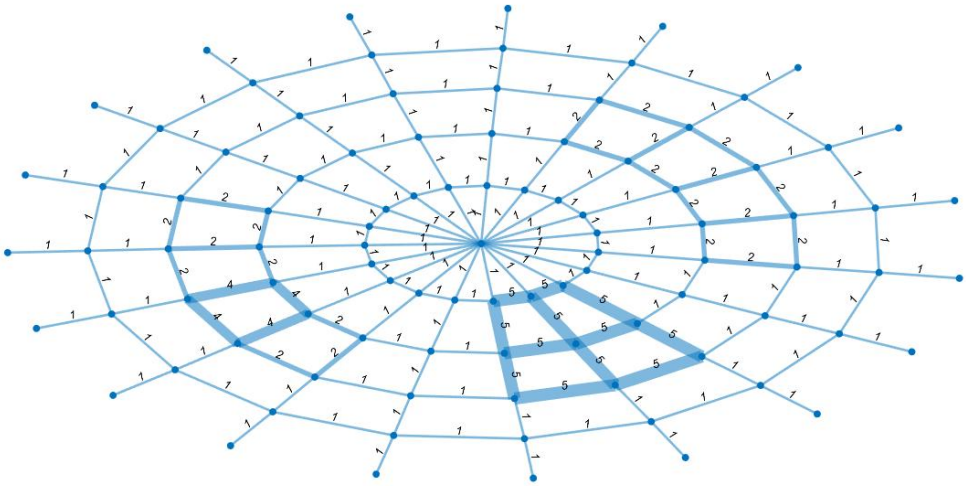

Figure 2.10: Well-connected spider network $\Gamma$ with $m = 19$.

The conductance is piecewise constant on a partition $E = E_1 \sqcup E_2 \sqcup E_3 \sqcup E_4$, with $c(E_1) = 1$, $c(E_2) = 5$, $c(E_3) = 2$ and $c(E_4) = 4$.

We run our algorithm assuming that the conductance is piecewise constant on a different partition $E = A_1 \sqcup A_2 \sqcup A_3$, with $A_1 = E_1$, $A_2 = E_2$ and $A_3 = E_3 \sqcup E_4$.

We obtain a numerical approximation to a local minimum of Problem 2.3.1 with this false hypothesis for the following 498 values of $\mu$: $\mu = 0$, $\mu = 10^{-10}j$, $\mu = 10^{-8}j$, $\mu = 10^{-6}j$, $\mu = 10^{-4}j$ and $10^{-2}j$ for $j = 1, 2, ..., 99$, $\mu = 1$ and $\mu = 10^5$. The error in the recovered conductances $||c' - c||$ is shown in Figure 2.11 for the values such that $\mu \leq 5 \cdot 10^{-7}$ with a linear interpolation. Additionally, the error $||c' - c||$ is shown in Figure 2.12 in a logarithmic scale with a linear interpolation for all the positive values except $\mu = 10^5$, for which the recovered conductance is almost equal to the one recovered with $\mu = 1$. In all figures, the recovered values of the conductances have been rounded with one decimal digit for the sake of clarity.

For $\mu = 0$, we obtain the network in Figure 2.13. The error is 7.8519, which is much higher than for any of the other values of $\mu$. Despite in this case we have the minimum difference with respect to the data $||\mathsf{N}' - \mathsf{N}||_{\text{Fr}} = 5.9512 \cdot 10^{-6}$, and thus also this is the solution at which the evaluation of $p$ is minimum (equal to $3.5417 \cdot 10^{-11}$), the recovered

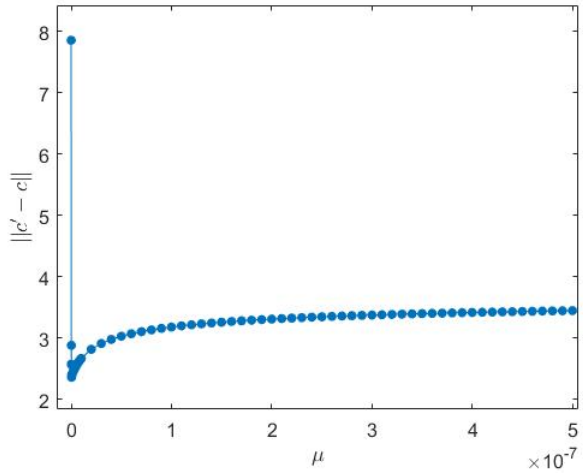


Figure 2.11: Error in the recovered conductance as a function of $\mu$.

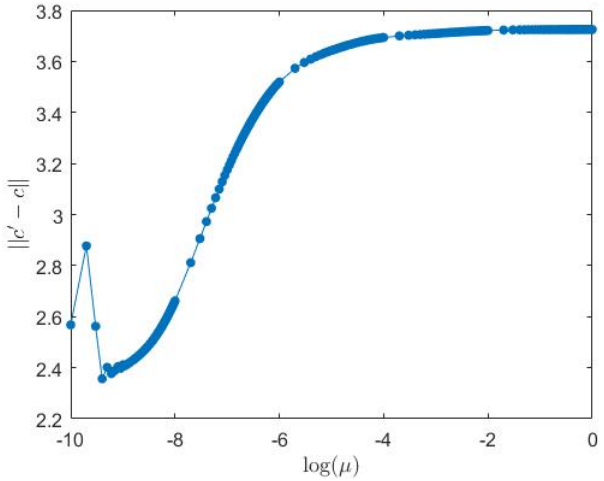


Figure 2.12: Error in the recovered conductance as a function of $\log(\mu)$.

network differs a lot from the real one, being $\max|c - c'| = 2.9997$, because the inverse conductance problem without regularization is ill-posed.

When we recover the conductance for the problem with a positive value of $\mu$, the error decreases drastically, and in $\mu = 4 \cdot 10^{-10}$ the error is minimum, $||c' - c|| = 2.3567$. In Figure 2.14, we show the recovered network for this value. Despite the error in the data, $||\mathsf{N}' - \mathsf{N}||_{\text{Fr}} = 1.0791 \cdot 10^{-5}$, is greater than for $\mu = 0$, the recovered conductance is much closer to the real one, with $\max|c - c'| = 1.3334$. The evaluation of $p$ is equal to $2.6808 \cdot 10^{-9}$.

For $\mu > 4 \cdot 10^{-10}$, the error monotonically increases with $\mu$. From $\mu = 4.7 \cdot 10^{-1}$ onwards, the recovered conductance almost does not vary with $\mu$, being almost piecewise constant on the partition $E = A_1 \sqcup A_2 \sqcup A_3$, with $c'(A_1) = 0.9999$, $c'(A_2) = 5.0145$ and $c'(A_3) = 2.1943$. The error is $||c' - c|| = 3.7250$. The deviation with respect to the data is maximum, $||\mathsf{N}' - \mathsf{N}||_{\text{Fr}} = 0.0078$, the evaluation of $p$ is equal to $6.0897 \cdot 10^{-5}$, and $\max|c - c'| = 1.8057$.

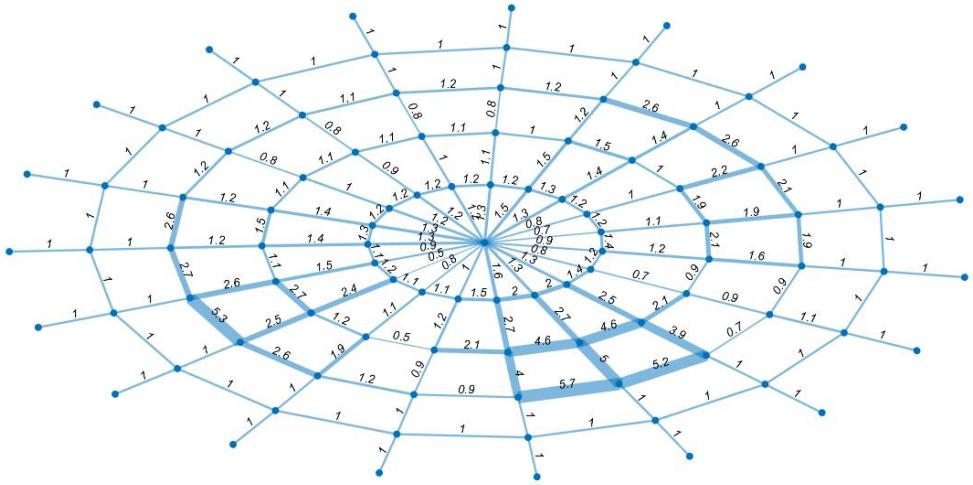

Figure 2.13: Recovered network with $\mu = 0$.

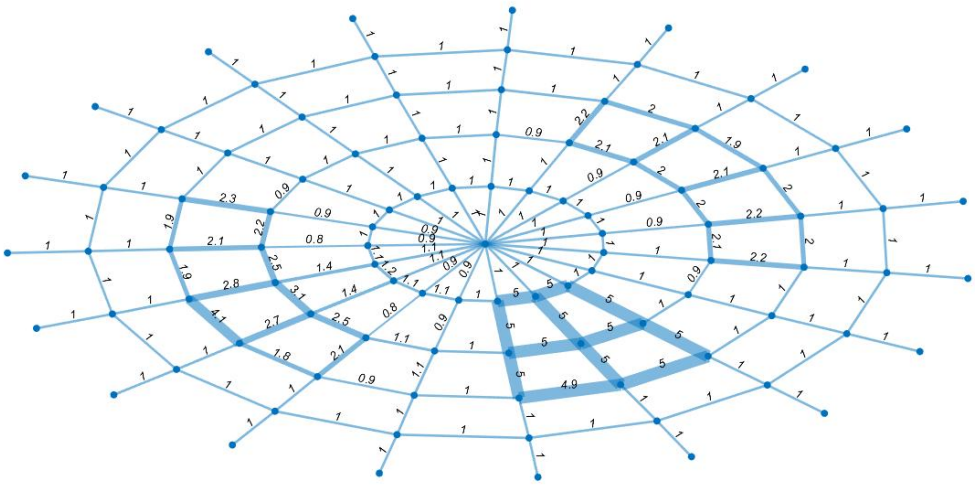

Figure 2.14: Recovered network with $\mu = 4 \cdot 10^{-10}$.

The recovered conductance for $\mu = 10^5$ can be seen in Figure 2.15, and in Table 2.6 there is a summary of the results for this value of $\mu$, and also for $\mu = 0$ and for the value of $\mu$ with minimum error.

This example illustrates that if we consider a piecewise constant conductance hypothesis on a given partition that does not suit the real network, but the real conductance is not far from a piecewise constant conductance in this partition, the error in the recovered conductance is lower when introducing the penalization ($\mu > 0$) than if we do not use it

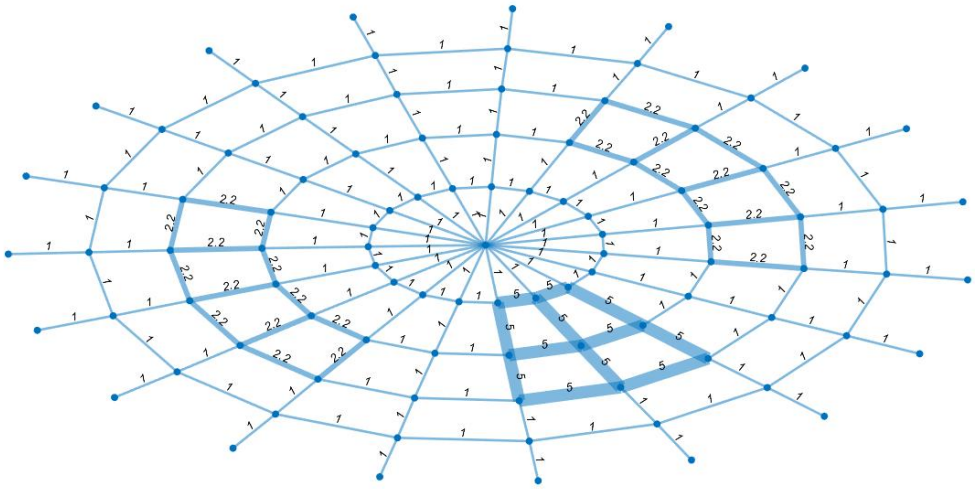

Figure 2.15: Recovered network with $\mu = 10000$.

Table 2.6: Error in the recovered conductance for different values of $\mu$.

| $\mu$ | $\|\|c - c'\|\|$ | $\max\{\|c - c'\|\}$ | $\|\|\mathsf{N}' - \mathsf{N}\|\|_{\text{Fr}}$ |
|---|---|---|---|
| 0 | 7.8519 | 2.9997 | $5.9512 \cdot 10^{-6}$ |
| $4 \cdot 10^{-10}$ | 2.3567 | 1.3334 | $1.0791 \cdot 10^{-5}$ |
| $10^5$ ($\mu \to \infty$) | 3.7250 | 1.8057 | $7.8037 \cdot 10^{-3}$ |

($\mu = 0$).

These results support using a penalty term in our formulation of Problem 2.3.1 and will be useful in many applied inverse conductance problems. From an applied perspective, it is reasonable to work with a piecewise constant conductance hypothesis that may not be entirely accurate but closely approximates reality. This can be intentional, such as when using an approximate piecewise constant model, or unintentional, because we are recovering a network whose conductance should be piecewise constant on a partition under normal circumstances, but may exhibit perturbations in certain unknown edges.

In the given example, we achieve the minimum error for an intermediate value of $\mu \in (0, \infty)$ for which there is a compromise between deviating with respect to the data $\mathsf{N}$ and with respect to the piecewise constant conductance hypothesis.

In the solution with $\mu = 4 \cdot 10^{-10}$, we see that the recovered conductance $c'$ is close to being constant on $A_1$ and on $A_2$, on which the real conductance is constant, while $c'$ is far from being piecewise constant on $A_3$, and the value of $c'$ at any edge of $E_3$ is lower than the value of $c'$ at any edge of $E_4$. This suggests the idea of choosing a finer partition than the original one for the subsets on which the solution is far from being constant. Then, we would recover the conductance again Problem 2.3.1 by considering this refined partition seeking a solution with a lower error.

## 2.6 Optimality guarantees of the recovered conductances

This section is a review of [37, Section 3]. In the previous section we have shown an example in which obtaining an approximation to a local minimum $t^* \in A$ of Problem 2.3.1 with a value $\mu > 0$ and a partition $E = E_1 \sqcup \cdots \sqcup E_s$ with $s \ll |E|$ such that $c$ is not piecewise constant on it allow us to recover an approximation of $c$ with some stability. Recall that, in this case of a false *piecewise constant conductance hypothesis*, a solution $\hat{t} \in A$ to Problem 2.3.1 must satisfy $p(\hat{t}) > 0$. In this case, we do not know *a priori* the value of $p(\hat{t})$, so we can not tell whether $t^*$ is an approximation of a global minimum or not just from the value of $p(t^*)$, even if the recovery is stable. Nevertheless, we can apply techniques of Sum of Squares (SOS) decompositions of polynomials [81] to this problem to try to find a guarantee that $t^*$ is an approximation to a global minimum, and as a consequence, an approximation to a solution to Problem 2.3.1.

SOS decompositions are relaxations used in polynomial optimization to obtain a lower bound for a real polynomial in a real algebraic set. We say that a polynomial is SOS if it can be written as a sum of squares of real polynomials and we denote by $I(V(J))$ the ideal of polynomials vanishing on $V(J)$. We denote by $t$ the vector containing all the variables of Problem 2.3.1, and we define the coordinate ring of the algebraic set $V(J)$ as the quotient ring $\mathbb{R}[t]/I(V(J))$. We formulate the following SOS problem, which is a particular case of the main problem studied in [56].

**Problem 2.6.1.** *Given a bound $d \in \mathbb{N}$, a quartic $p$, an algebraic set $V(J)$, and a value $z \geq 0$, is there any polynomial $q$ such that*

$$p(t) - z = q(t) \text{ in } \mathbb{R}[t]/I(V(J)); q \text{ is SOS, and } deg(q) \leq 2d?$$

Let $z = p(t^*)$ for $t^* \in A$ and suppose that Problem 2.6.1 has an affirmative answer for $p$, $V(J)$, $z$ and some $d$, then $p(t) \geq z$ in $V(J)$. Therefore, $t^*$ is a global minimum of $p$ in $A$ and thus a solution to Problem 2.3.1. In Example 2.6.2, we will show a network in which we are able to guarantee that a minimum to Problem 2.3.1 is global by finding an affirmative answer to Problem 2.6.1.

It could be possible that there is a global minimum $t^* \in A$ to Problem 2.3.1 such that Problem 2.6.1 has a negative answer for $V(J)$, $z = p(t^*)$ and any $d$, because for most algebraic varieties there exist nonnegative polynomials which are not SOS in the coordinate ring. Nevertheless, $p - p(t^*)$ in $V(J)$ can always be approximated by SOS polynomials, and the minimum degree of those polynomials depends on the closeness of the approximation [56], (see also [73] for more details).

Given a Gröbner basis of $I(V(J))$, Problem 2.6.1 reduces to a semidefinite program (SDP) [56]. It is equivalent to find a symmetric positive semidefinite matrix $Q$ such that the normal form of $p - z - u^T Q u$ in the Gröbner basis is zero, where u is a vector whose entries are the standard monomials corresponding to the Gröbner basis, (that is, the monomials which are not divisible by any leading term of the polynomials in that basis) with degree at most $d$, see [81].

In general, it is computationally complex to determine a Gröbner basis of the real radical $I(V(J))$ of $J$. Alternatively, we can check if $p - z$ is sum of squares in $\mathbb{R}[t]/J$, which is a

SDP problem that only requires a Gröbner basis of $J$, and obtaining an affirmative answer to this problem is a sufficient condition for obtaining an affirmative answer to Problem 2.6.1, because the evaluation of a polynomial which is equal to $p-z$ in $\mathbb{R}[t]/J$ at any point of $V(J)$ is equal to the evaluation of $p-z$ at that point.

Even with the relaxation of the above paragraph, the computation of a Gröbner basis of the ideal $J$ is computationally expensive when $J$ is the ideal of a spider network of a medium or large number of radii, because the number of variables of Problem 2.3.1 and the number of polynomials in (2.3) increase with the number of radii. Nevertheless, the ideal $J$ depends only on the number of radii, and it does not depend on the Dirichlet-to-Neumann matrix nor on the partition used in Problem 2.3.1, so once a Gröbner basis of $J$ corresponding to a number of radii is computed, it could be used to check if a local minimum of any case of Problem 2.3.1 in a spider network with this number of radii is a global minimum.

**Example 2.6.2.** *We consider the spider network $\Gamma = (\bar{F}, c)$ with $m = 3$ radii in Figure 2.16, we recover its conductance using a piecewise constant conductance hypothesis which does not hold in the network, and we check if the obtained solution is a global minimum of Problem 2.3.1.*

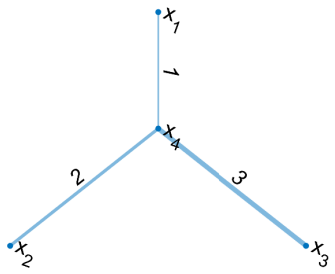


Figure 2.16: Real network with $m = 3$.

In the real network, we have $c(x_1, x_4) = 1$, $c(x_2, x_4) = 2$ and $c(x_3, x_4) = 3$. The Laplacian matrix of $\Gamma$ is

$$\mathsf{L} = \begin{pmatrix} 1 & 0 & 0 & -1 \\ 0 & 2 & 0 & -2 \\ 0 & 0 & 3 & -3 \\ -1 & -2 & -3 & 6 \end{pmatrix},$$

and its Dirichlet-to-Neumann matrix is

$$\mathsf{N} = \frac{1}{6} \begin{pmatrix} 5 & -2 & -3 \\ -2 & 8 & -6 \\ -3 & -6 & 9 \end{pmatrix}.$$

We set $\mu = 1$ and we obtain a numerical approximation to a local minimum of Problem 2.3.1 under the hypothesis that the conductance is piecewise constant on $E = E_1 \sqcup E_2$, with $E_1 = \{e_{x_2x_4}, e_{x_1x_4}\}$ and $E_2 = \{e_{x_3x_4}\}$; which is false in $\Gamma$. In Problem 2.3.1, we do not include

the variable $\omega(E_2)$, nor the term $(c'(x_3,x_4)-\omega(E_2))^2$ in $p$, since as $E_2$ only has one edge, in the solution we will have $\omega(E_2)=c'(x_3,x_4)$ trivially. The problem is to minimize

$$\begin{aligned}p=&\left(c'(x_1,x_4)-c'(x_1,x_4)u_{x_1}(x_4)-\tfrac{5}{6}\right)^2+\left(-c'(x_2,x_4)u_{x_1}(x_4)+\tfrac{1}{3}\right)^2\\&+\left(-c'(x_3,x_4)u_{x_1}(x_4)+\tfrac{1}{2}\right)^2+\left(-c'(x_1,x_4)u_{x_2}(x_4)+\tfrac{1}{3}\right)^2\\&+\left(c'(x_2,x_4)-c'(x_2,x_4)u_{x_2}(x_4)-\tfrac{4}{3}\right)^2+\left(-c'(x_3,x_4)u_{x_2}(x_4)+1\right)^2\\&+\left(-c'(x_1,x_4)u_{x_3}(x_4)+\tfrac{1}{2}\right)^2+\left(-c'(x_2,x_4)u_{x_3}(x_4)+1\right)^2\\&+\left(c'(x_3,x_4)-c'(x_3,x_4)u_{x_3}(x_4)-\tfrac{3}{2}\right)^2+\left(c'(x_1,x_4)-\omega(E_1)\right)^2+\left(c'(x_2,x_4)-\omega(E_1)\right)^2.\end{aligned}$$

subject to

$$\begin{cases}g_4^1:=-c'(x_1,x_4)+(c'(x_1,x_4)+c'(x_2,x_4)+c'(x_3,x_4))u_{x_1}(x_4)=0\\g_4^2:=-c'(x_2,x_4)+(c'(x_1,x_4)+c'(x_2,x_4)+c'(x_3,x_4))u_{x_2}(x_4)=0\\g_4^3:=-c'(x_3,x_4)+(c'(x_1,x_4)+c'(x_2,x_4)+c'(x_3,x_4))u_{x_3}(x_4)=0,\end{cases}$$

and $c(x,y)\geq 0$ for all $e_{xy}\in E$.

Using an interior point method, we obtain a local minimum $t^*$ such that $p(t^*)=0.1995$, and the values of all the variables in $t^*$ are $c'(x_1,x_4)=1.1486$, $c'(x_2,x_4)=1.5765$, $c'(x_3,x_4)=3.4764$, $\omega(E_1)=1.3625$, $u_{x_1}(x_4)=0.1852$, $u_{x_2}(x_4)=0.2542$ and $u_{x_3}(x_4)=0.5606$.

We define the ideal $J=\langle g_4^1,g_4^2,g_4^3\rangle$. We choose the degree reverse lexicographic order with $c'(x_1,x_4)>c'(x_2,x_4)>c'(x_3,x_4)>u_{x_1}(x_4)>u_{x_2}(x_4)>u_{x_3}(x_4)$, and we compute the Gröbner basis $J=\langle h_1,h_2,h_3,h_4,h_5,h_6\rangle$ of $J$ with respect to that monomial order using the *gbasis* function in Matlab. The polynomials of the basis are

$$\begin{cases}h_1=c'(x_2,x_4)-c'(x_1,x_4)+c'(x_3,x_4)+c'(x_1,x_4)u_{x_1}(x_4)-c'(x_2,x_4)u_{x_2}(x_4)\\-2c'(x_2,x_4)u_{x_3}(x_4)-c'(x_3,x_4)u_{x_3}(x_4),\\h_2=c'(x_2,x_4)u_{x_1}(x_4)-c'(x_2,x_4)+c'(x_2,x_4)u_{x_2}(x_4)+c'(x_2,x_4)u_{x_3}(x_4),\\h_3=c'(x_3,x_4)u_{x_1}(x_4)-c'(x_3,x_4)+c'(x_2,x_4)u_{x_3}(x_4)+c'(x_3,x_4)u_{x_3}(x_4),\\h_4=c'(x_1,x_4)u_{x_2}(x_4)-c'(x_2,x_4)+c'(x_2,x_4)u_{x_2}(x_4)+c'(x_2,x_4)u_{x_3}(x_4),\\h_5=c'(x_3,x_4)u_{x_2}(x_4)-c'(x_2,x_4)u_{x_3}(x_4),\\h_6=c'(x_1,x_4)u_{x_3}(x_4)-c'(x_3,x_4)+c'(x_2,x_4)u_{x_3}(x_4)+c'(x_3,x_4)u_{x_3}(x_4).\end{cases}$$

Then, we solve Problem 2.6.1 for $p$, $z=p(t^*)$ and $d=2$, but with the relaxation that consists in substituting the coordinate ring $\mathbb{R}[t]/I(V(J))$ by $\mathbb{R}[t]/J$. That is, we check if there is a symmetric positive semidefinite matrix $Q$ such that the normal form of $p-0.1995-u^TQu$ in $\langle h_1,h_2,h_3,h_4,h_5,h_6\rangle$ is null, where $u$ is a vector whose entries are the standard monomials with degree at most 2 corresponding to $\langle h_1,h_2,h_3,h_4,h_5,h_6\rangle$.

Using the function *findbound* from *SOOSTOOLS*, a toolbox of Matlab for solving sum of squares programs [80], and the SDP solver SeDuMi [103], we obtain an affirmative answer to the raised question.

Therefore, $p - 0.1995$ is SOS in $\mathbb{R}[t]/J$, so $p \geq 0.1995$ in $A$ and thus we have been able to guarantee that $t^*$ is a global minimum of $p$ in $A$ and thus a solution to Problem 2.3.1 without needing a Gröbner basis of $I(V(J))$.

# Chapter 3

# Simultaneous recovery of the topology and admittance of a network

In this chapter we study the inverse problem of simultaneously recovering the admittance of an AC network $\Gamma$, respectively the conductance of a DC network $\Gamma$, and the topology of $\Gamma$ from a set of measurements of voltage and its corresponding power injected at all vertices. Recall that, as mentioned in Remark 1.3.8, if $\Gamma$ is an AC network, at a given time, the potential at the vertices can be represented by $u \in \mathscr{C}(V, \mathbb{C})$, and the power injected at the vertices is equal to $s = u\overline{\mathcal{L}(u)} \in \mathscr{C}(V, \mathbb{C})$, where $\mathcal{L}$ is the Laplacian of $\Gamma$. Similarly, if $\Gamma$ is a DC network, the potential at the vertices can be represented by $u \in \mathscr{C}(V)$, and the power injected at the vertices is equal to $s = u\mathcal{L}(u) \in \mathscr{C}(V)$. These equations relating voltage and power are called the *power flow equations*, (see [79]).

**Remark 3.0.1.** In order to avoid possible faults in the operation of an electrical network, voltages are usually maintained close to a reference value, that is chosen to be $u = 1$ in appropriate units (see [79]). In this chapter we will fix minimum and maximum values of voltage $0 < |u|_{\min} \leq |u|_{\max}$. Later, in the experiments, we will use $|u|_{\min} = 0.9$ and $|u|_{\max} = 1.1$.

Throughout the chapter we always assume that given $m \in \mathbb{N}^*$ and $\boldsymbol{u} \in \mathscr{C}(V, \mathbb{C}^m)$, respectively $\boldsymbol{u} \in \mathscr{C}(V, \mathbb{R}^m)$, the components of $\boldsymbol{u}$ are $u_1, \ldots, u_m \in \mathscr{C}(V, \mathbb{C})$, respectively $u_1, \ldots, u_m \in \mathscr{C}(V)$, *i.e.* $\boldsymbol{u} = (u_1, \ldots, u_m)$. We denote its real and imaginary parts as $\Re(\boldsymbol{u}) = (\Re(u_1), ..., \Re(u_m)) \in \mathscr{C}(V, \mathbb{R}^m)$ and $\Im(\boldsymbol{u}) = (\Im(u_1), ..., \Im(u_m)) \in \mathscr{C}(V, \mathbb{R}^m)$.

In this chapter, for any kernel $a \in \mathscr{C}(V \times V, \mathbb{C})$ that is symmetric and satisfies that $a(x, x) = 0$ for any $x \in V$, we denote by $\mathcal{L}_a$ the endomorphism of $\mathscr{C}(V, \mathbb{C})$ defined as

$$\mathcal{L}_a(u)(x) = \sum_{y \in V} a(x, y) \big(u(x) - u(y)\big)$$

for any $u \in \mathscr{C}(V, \mathbb{C})$ and any $x \in V$. Note that if $a$ is the admittance of an electrical network $\Gamma = (V, a)$, then $\mathcal{L}_a$ is the Laplacian of $\Gamma$, that is, $\mathcal{L}_a = -\mathsf{div} \circ (a\mathsf{d})$.

Moreover, for any $a \in \mathscr{C}(V \times V, \mathbb{C})$ that is symmetric and satisfies that $a(x, x) = 0$ for any $x \in V$, we denote by $\mathscr{P}_a \colon \mathscr{C}(V, \mathbb{C}^m) \times \mathscr{C}(V, \mathbb{C}^m) \longrightarrow \mathscr{C}(V, \mathbb{C}^m)$ the function defined for

each $(\boldsymbol{v}, \boldsymbol{w}) = ((v_1, ..., v_m), (w_1, ..., w_m)) \in \mathscr{C}(V, \mathbb{C}^m) \times \mathscr{C}(V, \mathbb{C}^m)$ as

$$\mathscr{P}_a(\boldsymbol{v}, \boldsymbol{w}) = (v_1\overline{\mathcal{L}_a(w_1)}, ..., v_m\overline{\mathcal{L}_a(w_m)}).$$

Of course, when $a$ is a real kernel, $\mathscr{P}_a(\boldsymbol{v}, \boldsymbol{w}) \in \mathscr{C}(V, \mathbb{R}^m)$ for every $\boldsymbol{u}, \boldsymbol{v} \in \mathscr{C}(V, \mathbb{R}^m)$. Also, if $a$ is the admittance of an AC network, respectively a DC network, then for any $\boldsymbol{u} \in \mathscr{C}(V, \mathbb{C}^m)$, respectively $\boldsymbol{u} \in \mathscr{C}(V, \mathbb{R}^m)$, the j-th component of the function $\mathscr{P}_a(\boldsymbol{u}, \boldsymbol{u})$ is equal to the power injected at the network when the potential is $u_j$, for any $j = 1, ..., m$.

We denote as $E(K_V)$ the set of edges of the complete graph on $V$, *i.e.* the set of all possible edges on the vertex set $V$. In an applied situation, one of the main causes that the system operators of a network $\Gamma$ may not know its topology $(V, E(\Gamma))$ is the existence of lines which have a switch whose status is unknown, so they do not know whether their corresponding edges belong to $E(\Gamma)$ or not, (see [2]). In general, we formulate the inverse problem with the *a priori* information that there is a set $E \subseteq E(K_V)$ of edges which are candidates to belong to $E(\Gamma)$, and we know that the edges in $E(K_V) \setminus E$ do not exist in the network topology. Note that, the particular case in which $E = E(K_V)$, corresponds with the framework in which we do not have any *a priori* information about $E(\Gamma)$.

**Problem 3.0.2.** *Let $V$ be a finite set of vertices, let $E$ be a set of edges, let $0 < |u|_{\min} \leq |u|_{\max}$ be positive values, let $m \in \mathbb{N}^*$ and let $\boldsymbol{u}, \boldsymbol{s} \in \mathscr{C}(V, \mathbb{C}^m)$, respectively $\boldsymbol{u}, \boldsymbol{s} \in \mathscr{C}(V, \mathbb{R}^m)$, such that $|u|_{\min} \leq |u_j| \leq |u|_{\max}$ for all $j = 1, \ldots, m$. Determine an AC, respectively a DC, electrical network $\Gamma = (V, a)$ with set of edges $E(\Gamma) \subseteq E$ such that $\boldsymbol{s} = \mathscr{P}_a(\boldsymbol{u}, \boldsymbol{u})$.*

The pair $(\boldsymbol{u}, \boldsymbol{s})$ is usually called *the data pair* or *the data set* and hence we always understand that for any $j = 1, \ldots, m$, $u_j$ represents a measurement of voltage and $s_j$ represents its corresponding measurement of power. Therefore for any $j = 1, \ldots, m$ we have that $u_j(z) \neq 0$ for all $z \in V$, since $0 < |u|_{\min} \leq |u_j|$.

Several authors have formulated different problems of recovering the topology and admittance of a network, starting from different data; and they have proposed methods to solve these problems. For instance, as mentioned in Section 2 in the context of the inverse conductance problem, in [66] the authors introduced a method which recovers the conductance and the topology up to vertices of combinatorial degree two of any tree from its Dirichlet-to-Neumann map.

In [2], the application of a least squares approach to solve two problems is discussed: the first one concerns the admittance estimation alongside voltage estimation from a known topology, and the second one consists of the voltage estimation alongside detection of errors in the network topology determined by a given admittance. However, in that paper, the simultaneous recovery of topology and admittance is not discussed.

An iterative method is proposed in [72] to recover simultaneously the topology and admittance of a network from power and voltage data, starting at each step from an estimated admittance and then calculating the current flow in each edge, removing an edge if its conductance and susceptance have a value below a given threshold. Nevertheless, relying only on the values of the admittance to decide if an edge can be removed from a network can lead us to an error, as we show in Example 3.6.1. The method proposed in [57] also estimates both the topology and admittance of a network from power and voltage data, but only in the particular case of distribution networks which operationally are a tree.

In [88], it is shown that the problem of simultaneously recovering the topology and admittance of an electrical network from power and voltage data at all nodes is often ill-posed, sometimes even having multiple solutions. Instead of recovering a network with the best fit to the data, the author formulates a problem of seeking a network which fits the data up to a given tolerance and whose topology is sparse, *i.e.*, with few edges. The author proposes an algorithm to solve this problem, which combines, in an iterative procedure, the resolution of nonnegative linear regression problems, and techniques of spectral sparsification of networks. The algorithm is tested on several electrical networks.

The objective of this chapter is to review the results from [88] from a perspective of discrete vector calculus on networks.

## 3.1 Ill-posedness of the problem

This section is a review of [88, Section 3]. Problem 3.0.2 is ill-posed in general, often having multiple solutions. For example, in the following example, we show a case in which, under the restriction that the power injected at a node is zero at a certain vertex for all the $s_j$ functions in the data pair $(\boldsymbol{u}, \boldsymbol{s})$, then there are multiple solutions for any choice of $(\boldsymbol{u}, \boldsymbol{s})$. Recall that this restriction is common in networks of the real world, in which there are vertices which are not associated to any generator or consumer of power.

**Example 3.1.1.** Let $\Gamma = (V, c)$ be the DC electrical network which is the weighted path in Figure 3.1, with vertex set $V = \{x, y, z\}$, with set of edges $E(\Gamma) = \{e_{xy}, e_{yz}\}$, whose conductance values are $c(x, y) = c(y, x) > 0$ and $c(y, z) = c(z, y) > 0$, respectively; and with Laplacian $\mathcal{L}$. Let $(\boldsymbol{u}, \boldsymbol{s})$ be a data pair satisfying the power flow equations, that is, $\boldsymbol{s} = \mathscr{P}_c(\boldsymbol{u}, \boldsymbol{u}) = \big(u_1\mathcal{L}(u_1), \ldots, u_m\mathcal{L}(u_m)\big)$, and moreover that $\boldsymbol{s}(y) = \boldsymbol{0}$.


Figure 3.1: Electrical network in Example 3.1.1.

We have that for each $j = 1, ..., m$, $u_j$ is harmonic on $y$, because $u_j(y) \neq 0$. By Gauss' Theorem, $\mathcal{L}(u_j)(x) = I_j$, $\mathcal{L}(u_j)(y) = 0$ and $\mathcal{L}(u_j)(z) = -I_j$, for some $I_j \in \mathbb{R}$. Then, each $u_j$ must be equal to $u_j(x) = \frac{I_j}{c(x,y)} + \zeta_j$, $u_j(y) = \zeta_j$ and $u_j(z) = -\frac{I_j}{c(y,z)} + \zeta_j$, for some $\zeta_j \in \mathbb{R}$.

We consider the Problem 3.0.2 with data pair $(\boldsymbol{u}, \boldsymbol{s})$ and the edge set of the complete graph in $V$, $E(K_V) = \{e_{xy}, e_{xz}, e_{yz}\}$. Then, a DC electrical network $\Gamma' = (V, c')$ with Laplacian $\mathcal{L}'$ is a solution of the problem if and only if we have that $c' \in \mathscr{C}^+(E)$ is a solution of

$$\begin{cases} c'(x,y)\big(u_j(x) - u_j(y)\big) + c'(x,z)\big(u_j(x) - u_j(z)\big) = I_j \\ c'(x,z)\big(u_j(z) - u_j(x)\big) + c'(y,z)\big(u_j(z) - u_j(y)\big) = -I_j \\ c'(x,y)\big(u_j(y) - u_j(x)\big) + c'(y,z)\big(u_j(y) - u_j(z)\big) = 0, \end{cases}$$

for all $j = 1, ..., m$. For each $j = 1, ..., m$, the third equation in that system depends linearly on the rest. If $I_j = 0$, then $u_j$ is constant on $V$, so any value of the conductance $c'$ satisfies

that $s_j = u_j \mathcal{L}'(u_j)$. If, on the contrary, $I_j \neq 0$, then the previous system is equivalent to the following system, which is independent of $I_j$ and $\zeta_j$:

$$\begin{cases} \dfrac{c'(x,y)}{c(x,y)} + \left(\dfrac{1}{c(x,y)} + \dfrac{1}{c(x,z)}\right) c'(x,z) = 1 \\ \left(\dfrac{1}{c(x,y)} + \dfrac{1}{c(x,z)}\right) c'(x,z) + \dfrac{c'(y,z)}{c(x,z)} = 1. \end{cases} \tag{3.1}$$

The function $\alpha \in \mathscr{C}(E)$; which is determined by the values $\alpha(x,y) = -1 - \frac{c(x,y)}{c(y,z)}$, $\alpha(x,z) = 1$ and $\alpha(y,z) = -1 - \frac{c(y,z)}{c(x,y)}$; is a solution to the homogeneous system associated to (3.1). Therefore, any network $\Gamma' = (V, c')$ whose conductance is of the form $c' = c + \beta\alpha$, with $\beta \in \left[0, \frac{c(x,y)c(y,z)}{c(x,y)+c(y,z)}\right]$, is a solution to Problem 3.0.2.

Among the solutions with conductance of this form $c' = c + \beta\alpha$, the one with $\beta = 0$ is the real network $\Gamma$. The solution $\Gamma' = (V, c')$ with $\beta = \frac{c(x,y)c(y,z)}{c(x,y)+c(y,z)}$ satisfies $c'(x,y) = c'(y,z) = 0$, so it has only one edge, $E(\Gamma') = \{e_{xz}\}$. Moreover, its conductance satisfies

$$\frac{1}{c'(x,z)} = \frac{1}{c(x,y)} + \frac{1}{c(y,z)}, \tag{3.2}$$

so $\Gamma'$ is the union of the isolated vertex $\{y\}$ and the Kron reduction of $\Gamma$ with respect to $\{y\}$; and $c'(x,z)$ is equal to the effective conductance in $\Gamma$ between $x$ and $z$, $c^e(x,z)$. The fact that this network is a solution of the problem is because its Laplacian is the Dirichlet-to-Neumann map of $\Gamma$ and $\{y\}$, which gives us the relationship between potential and injected current at $V \setminus \{y\} = \{x, z\}$ when the potential is harmonic on $y$. Additionally, the rest of solutions with conductance of form $c' = c + \beta\alpha$, are the infinite solutions with $\beta \in \left(0, \frac{c(x,y)c(y,z)}{c(x,y)+c(y,z)}\right)$, which have the topology of $(V, E(K_V))$, the complete graph in $V$. Note that Problem 3.0.2 can be ill-posed even in cases in which the set of edges $E$ considered is the set of edges of a solution, as happens in this example.

In a numerical context, we usually have errors in the data pair $(\boldsymbol{u}, \boldsymbol{s})$, and as a consequence often there is no exact solution to Problem 3.0.2. We reformulate the problem in Problem 3.1.2, in order to have a solution for any data pair. We seek a network for which the power flow equations are the closest possible to be satisfied in the least squares sense. If $\Gamma = (V, c)$ is a DC network, we define the *error of the network* $\Gamma$ *in the data pair* $(\boldsymbol{u}, \boldsymbol{s})$, $\mathsf{rms}(\Gamma, \boldsymbol{u}, \boldsymbol{s})$, as the root mean square of the set of evaluations at all vertices of the residuals $u_j \mathcal{L}(u_j) - s_j$ of all the power flow equations corresponding with all the pairs $(u_j, s_j)$, $j = 1, \ldots, m$. That is,

$$\mathsf{rms}(\Gamma, \boldsymbol{u}, \boldsymbol{s}) = \frac{||\mathscr{P}_c(\boldsymbol{u}, \boldsymbol{u}) - \boldsymbol{s}||}{\sqrt{m|V|}} = \sqrt{\frac{1}{m|V|} \sum_{j=1}^{m} \int_V \left(u_j \mathcal{L}(u_j) - s_j\right)^2 dx}.$$

If $\Gamma = (V, a)$ is an AC network, we define the *error of the network* $\Gamma$ *in the data pair* $(\boldsymbol{u}, \boldsymbol{s})$, $\mathsf{rms}(\Gamma, \boldsymbol{u}, \boldsymbol{s})$, as the root mean square of the set of evaluations at all vertices of the real and

imaginary parts of the residuals $u_j\overline{\mathcal{L}(u_j)} - s_j$ of all the power flow equations corresponding with all the pairs $(u_j, s_j)$, $j = 1, \ldots, m$. That is,

$$\mathsf{rms}(\Gamma, \boldsymbol{u}, \boldsymbol{s}) = \frac{||\mathscr{P}_a(\boldsymbol{u}, \boldsymbol{u}) - \boldsymbol{s}||}{\sqrt{2m|V|}} = \sqrt{\frac{1}{2m|V|}\sum_{j=1}^{m}\int_V \left|u_j\overline{\mathcal{L}(u_j)} - s_j\right|^2 dx}.$$

**Problem 3.1.2.** *Let $V$ be a finite set of vertices, let $E$ be a set of edges, let $0 < |u|_{\min} \leq |u|_{\max}$ be positive values, let $m \in \mathbb{N}^*$ and let $\boldsymbol{u}, \boldsymbol{s} \in \mathscr{C}(V, \mathbb{C}^m)$, respectively $\boldsymbol{u}, \boldsymbol{s} \in \mathscr{C}(V, \mathbb{R}^m)$, such that $|u|_{\min} \leq |u_j| \leq |u|_{\max}$ for all $j = 1, \ldots, m$. Determine an AC, respectively a DC, electrical network $\Gamma = (V, a)$ with set of edges $E(\Gamma) \subseteq E$ and such that the error $\mathsf{rms}(\Gamma, \boldsymbol{u}, \boldsymbol{s})$ is minimum.*

Finding a solution to Problem 3.1.2 is equivalent to solving a Nonnegative Least Squares (NNLS) problem, that is, a least squares problem with the restriction that the coefficients must be nonnegative, (see [92]). In order to see that, given $\boldsymbol{u} \in \mathscr{C}(V, \mathbb{R}^m)$ and a set of edges $E$, we define the linear operator $\mathcal{M}_{E,\boldsymbol{u}} \colon \mathscr{C}(E) \longrightarrow \mathscr{C}(V, \mathbb{R}^m)$ as

$$\mathcal{M}_{E,\boldsymbol{u}}(c) = \big(u_1\mathcal{L}_c(u_1), \ldots, u_m\mathcal{L}_c(u_m)\big) = \mathscr{P}_c(\boldsymbol{u}, \boldsymbol{u}).$$

Then, for any DC network $\Gamma = (V, c)$ with set of edges $E(\Gamma) \subseteq E$, and any data pair $(\boldsymbol{u}, \boldsymbol{s}) \in \mathscr{C}(V, \mathbb{R}^m) \times \mathbb{C}(V, \mathbb{R}^m)$, we have that

$$\mathsf{rms}(\Gamma, \boldsymbol{u}, \boldsymbol{s}) = \frac{||\mathcal{M}_{E,\boldsymbol{u}}(c) - \boldsymbol{s}||}{\sqrt{m|V|}}. \tag{3.3}$$

Similarly, given $\boldsymbol{u} \in \mathscr{C}(V, \mathbb{C}^m)$ and a set of edges $E$, we define the linear operator $\mathcal{M}_{E,\boldsymbol{u}} \colon \mathscr{C}(E) \times \mathscr{C}(E) \longrightarrow \mathscr{C}(V, \mathbb{R}^{2m})$ as

$$\mathcal{M}_{E,\boldsymbol{u}}(c, b) = \Big(\Re\big(u_1\overline{\mathcal{L}_a(u_1)}\big), \Im\big(u_1\overline{\mathcal{L}_a(u_1)}\big), \ldots, \Re\big(u_m\overline{\mathcal{L}_a(u_m)}\big), \Im\big(u_m\overline{\mathcal{L}_a(u_m)}\big)\Big),$$

where $a = c - ib$.

We also consider the operator $\mathcal{S} \colon \mathscr{C}(V, \mathbb{C}^m) \longrightarrow \mathscr{C}(V, \mathbb{R}^{2m})$ defined as

$$\mathcal{S}(\boldsymbol{s}) = \Big(\Re(s_1), \Im(s_1), \ldots, \Re(s_m), \Im(s_m)\Big).$$

Then, for any AC network $\Gamma = (V, a)$ with set of edges $E(\Gamma) \subseteq E$, where $a = c - ib$, and any data pair $(\boldsymbol{u}, \boldsymbol{s}) \in \mathscr{C}(V, \mathbb{C}^m) \times \mathbb{C}(V, \mathbb{C}^m)$, we have that

$$\mathsf{rms}(\Gamma, \boldsymbol{u}, \boldsymbol{s}) = \frac{||\mathcal{M}_{E,\boldsymbol{u}}(c, b) - \mathcal{S}(\boldsymbol{s})||}{\sqrt{2m|V|}}. \tag{3.4}$$

Both for DC and AC networks, Problem 3.1.2 consists in seeking for a nonnegative function $c \in \mathscr{C}^+(E)$ in the case of DC networks, or two nonnegative functions $c, b \in \mathscr{C}^+(E)$ in the case of AC networks, such that the norm of the difference between its image under the real linear operator $\mathcal{M}_{E,\boldsymbol{u}}$ and the vector function $\boldsymbol{s}$, or $\mathcal{S}(\boldsymbol{s})$, is minimum, so Problem 3.1.2 is equivalent to a NNLS problem.

Any NNLS problem is a convex quadratic optimization problem, (see [92]), so every local minimum of it is a global minimum. We can obtain a solution $\Gamma$ to Problem 3.1.2 calculating a minimum of its associated NNLS problem with an interior point method. The interior point methods are among the main numerical algorithms used to solve NNLS problems, (see [43]). We denote the numerical solution $\Gamma$ with error $\mathsf{rms} \equiv \mathsf{rms}(\Gamma, \boldsymbol{u}, \boldsymbol{s})$ obtained from $E$ and $(\boldsymbol{u}, \boldsymbol{s})$ as $[\Gamma, \mathsf{rms}] = \mathsf{network\_recovery}(E, \boldsymbol{u}, \boldsymbol{s})$.

A sufficient condition that implies that Problem 3.1.2 has a unique solution is that $m \geq \frac{|E|}{|V|}$ and $\kappa(\mathcal{M}_{E,\boldsymbol{u}}) < \infty$, *i.e.*, the *condition number of* $\mathcal{M}_{E,\boldsymbol{u}}$ is finite, (see [92]). We will require in Section 3.6 that the data sets used to test the sparse network recovery algorithm satisfy $m \geq \frac{|E|}{|V|}$. Nevertheless, often the condition $\kappa(\mathcal{M}_{E,\boldsymbol{u}}) < \infty$ is not satisfied, and thus there are multiple solutions to Problem 3.1.2; as seen in Example 3.1.1, in which there are multiple solutions with zero error.

As we will see in Section 3.6, in cases in which the pair $(\boldsymbol{u}, \boldsymbol{s})$ contains voltage and power data corresponding to an electrical network with some error, the value of the condition number $\kappa(\mathcal{M}_{E,\boldsymbol{u}})$ is finite but it is very high, so Problem 3.1.2 has a unique solution but it is severely ill-posed.

## 3.2 Reformulation of the problem: Recovery of a sparse electrical network

This section is a review of the beginning of [88, Section 4]. As we have discussed in the previous section, given a data data pair $(\boldsymbol{u}, \boldsymbol{s})$ and a set of edges $E$, the Problem 3.1.2 of recovering a network $\Gamma$ with minimum error such that $E(\Gamma) \subseteq E$ is ill-posed. Because of that, even if there is a solution $\Gamma^*$ to the exact Problem 3.0.2 whose topology is much more sparse than $(V, E)$, *i.e.*, $|E(\Gamma^*)| \ll |E|$, solving Problem 3.1.2 we usually get a solution whose topology is $(V, E)$. If the number of edges in $E$ is high, a solution with that topology is not efficient for applications. We are interested in recovering a sparse network such that the fitting error to the data is below a fixed tolerance. Such a network would allow the efficient and accurate resolution of usual problems in electrical networks which require the admittance and topology. Those applications include failure identification, power flow optimization or generation scheduling [57].

We formulate the following problem of recovering a sparse network. Given a fixed tolerance, we seek to recover a network such that its $\mathsf{rms}$ is below this tolerance and none of the networks with the same set of vertices as our network and a subset of its edges has a $\mathsf{rms}$ below the tolerance.

**Problem 3.2.1** ([88])**.** *Let $V$ be a finite set of vertices, let $E$ be a set of edges, let $0 < |u|_{\min} \leq |u|_{\max}$ be positive values, let $m \in \mathbb{N}^*$, let $\boldsymbol{u}, \boldsymbol{s} \in \mathscr{C}(V, \mathbb{C}^m)$, respectively $\boldsymbol{u}, \boldsymbol{s} \in \mathscr{C}(V, \mathbb{R}^m)$, such that $|u|_{\min} \leq |u_j| \leq |u|_{\max}$ for all $j = 1, \ldots, m$ and let $\mathsf{tol} > 0$ be a tolerance. Determine an AC network $\Gamma = (V, a)$, respectively a DC network $\Gamma = (V, c)$, with set of edges $E(\Gamma) \subseteq E$ such that $\mathsf{rms}(\Gamma, \boldsymbol{u}, \boldsymbol{s}) \leq \mathsf{tol}$ and $\Gamma$ is "minimal" in the following sense: Given any electrical network $\Gamma' = (V, a')$, respectively $\Gamma' = (V, c')$, with edge set $E(\Gamma')$, we have that*

1. *If $E(\Gamma') = E(\Gamma)$, then $\mathsf{rms}(\Gamma', \boldsymbol{u}, \boldsymbol{s}) \geq \mathsf{rms}(\Gamma, \boldsymbol{u}, \boldsymbol{s})$.*

2. *If* $E(\Gamma') \subsetneq E(\Gamma)$, *then* $\mathsf{rms}(\Gamma', \boldsymbol{u}, \boldsymbol{s}) > \mathsf{tol}$.

**Remark 3.2.2.** In particular, we have $\mathsf{rms}(\Gamma', \boldsymbol{u}, \boldsymbol{s}) > \mathsf{tol} \geq \mathsf{rms}(\Gamma, \boldsymbol{u}, \boldsymbol{s})$ if $E(\Gamma') \subsetneq E(\Gamma)$. However, notice that there could be an electrical network $E(\Gamma') = (V, a')$ such that $\mathsf{rms}(\Gamma', \boldsymbol{u}, \boldsymbol{s}) < \mathsf{rms}(\Gamma, \boldsymbol{u}, \boldsymbol{s})$ and $E(\Gamma') \not\subset E(\Gamma)$.

A first naive idea to solve Problem 3.2.1 could be to recover a network $\Gamma$ solving Problem 3.1.2 with the set of edges $E$, *i.e.*, $[\Gamma, \mathsf{rms}] = \mathsf{network\_recovery}(E, \boldsymbol{u}, \boldsymbol{s})$, and then to remove from $E(\Gamma)$ the edges whose admittance values are close to zero. However, this approach presents some problematic issues.

First, let $\Gamma^*$ be a solution to Problem 3.2.1, with set of edges $E(\Gamma^*)$. As we will see in Section 3.6, if $E(\Gamma^*)$ is much smaller than $E$, then usually the condition number of the operator associated with the network recovery Problem 3.1.2 using set $E$, $\kappa(\mathcal{M}_{E,\boldsymbol{u}})$, is much bigger than the condition number of the operator associated with the network recovery Problem 3.1.2 using set $E(\Gamma^*)$, $\kappa(\mathcal{M}_{E(\Gamma^*),\boldsymbol{u}})$. Then, the values of the admittance of $\Gamma$ at the edges of $E \setminus E(\Gamma^*)$ are usually far from zero. For instance, in Example 3.3.4, solving the Problem 3.1.2 with the edge set $E(K_V) = \{e_{xy}, e_{xz}, e_{yz}\}$, we can get solutions with zero error such that the values of the admittance at all edges of $E(K_V)$ are far from zero, despite the fact that there are solutions with zero error and less than three edges.

Second, in $\Gamma$ could exist edges with admittance close to zero whose removal would lead to a network which would not correctly fit the data (see Example 3.6.1). In order to avoid those problems, the algorithm that we propose in Section 3.5 algorithm uses techniques of spectral sparsification of networks in order to remove edges from networks.

## 3.3 Spectral network sparsification

This section is a review of [88, Subsection 4.1]. Spielman and Teng introduced the notion of spectral sparsification of a real weighted graph, (that is, a DC network), in [95], (see also the subsequent papers [16, 93, 94] on this topic).

**Definition 3.3.1** ([93])**.** For $\varepsilon > 0$, we say that a DC network $\Gamma' = (V, c')$ with energy $\mathcal{E}'$ is an $\varepsilon$-approximation of a DC network $\Gamma = (V, c)$ with energy $\mathcal{E}$ if for all $u \in \mathscr{C}(V)$:

$$\frac{1}{1+\varepsilon}\mathcal{E}(u,u) \leq \mathcal{E}'(u,u) \leq (1+\varepsilon)\mathcal{E}(u,u). \tag{3.5}$$

The energy of an AC network $\Gamma = (V, a)$, with $a = c - ib$ and $c, b \in \mathscr{C}^+(E(\Gamma))$, is a complex bilinear form, so we can not apply Definition 3.3.1 to it. Nevertheless, we can apply this definition separately to its conductance and susceptance networks, $\Gamma_c = (V, c)$ and $\Gamma_b = (V, b)$. We introduce the following definition.

**Definition 3.3.2.** For $\varepsilon > 0$, we say that an AC network $\Gamma'$ is an $\varepsilon$-approximation of an AC network $\Gamma$ if the conductance and susceptance networks of $\Gamma'$ are $\varepsilon$-approximations of the conductance and susceptance networks of $\Gamma$, respectively.

**Algorithm 1** $\Gamma' = \mathsf{Sparsify}(\Gamma, \varepsilon)$.

Set $t = 8|V| \cdot log(|V|)/\varepsilon^2$, $c' = 0$, and $E(\Gamma') = \emptyset$.
**for** each edge $e_{xy} \in E(\Gamma)$ **do**
Assign to edge $e_{xy}$ a probability $p_{xy}$ proportional to $c(x,y)r^e(x,y)$.
**end for**
Take $t$ samples independently with replacement from $E(\Gamma)$, and each time the edge $e_{xy}$ is sampled, increase the value of $c'(x,y)$ and $c'(y,x)$ by $c(x,y)/tp_{xy}$, (and as a consequence, add the edge $e_{xy}$ to $E(\Gamma')$ if it is the first time that $e_{xy}$ is sampled).

In [16] there is a procedure (Algorithm 1) that can be used to construct a sparse approximation $\Gamma' = (V, c')$ of a DC network $\Gamma = (V, c)$ such that $E(\Gamma') \subseteq E(\Gamma)$.

Algorithm 1 is not guaranteed to produce an $\varepsilon$-approximation of $\Gamma$, but in [16] there is a proof of the following theorem:

**Theorem 3.3.3** (Batson, Spielman, Srivastava, Teng)**.** *Let $\Gamma$ be a DC network, let $\varepsilon \in \mathbb{R}$, $0 < \varepsilon \leq 1$ and let $\Gamma' = \mathsf{Sparsify}(\Gamma, \varepsilon)$. Then $\Gamma'$ is an $\varepsilon$-approximation of $\Gamma$ with probability at least $1/2$.*

Note that the edges that are removed in Algorithm 1 are the ones that are never sampled. The choice of the sampling probabilities in the algorithm has an interesting physical interpretation. By (1.13), for each edge $e_{xy} \in E$, the probability of sampling it, $p_{xy}$, is proportional to the dimensionless ratio

$$c(x,y)r^e(x,y) = \frac{c(x,y)}{c^e(x,y)} = \frac{c(x,y)}{c(x,y) + c^e_{\setminus e_{xy}}(x,y)} \in (0,1],$$

where $c^e_{\setminus e_{xy}}(x,y) \geq 0$ is the effective conductance between $x$ and $y$ in the network $\Gamma \setminus e_{xy}$ obtained from $\Gamma$ by removing the edge $e_{xy}$, which is equal to the contribution to the effective conductance $c^e(x,y)$ of the paths between $x$ and $y$ through the rest of vertices of the network $\Gamma$.

The probability of choosing edge $e_{xy}$ in each sample is high if the contribution of the value $c(x,y)$ to the effective conductance between $x$ and $y$ in $\Gamma$, $c^e(x,y)$, is very important, that is, if $c(x,y)$ is big compared to $c^e_{\setminus e_{xy}}(x,y)$. The limit case is that in which the removal of $e_{xy}$ isolates $x$ and $y$, in which $c^e_{\setminus e_{xy}}(x,y) = 0$, so $c(x,y)r^e(x,y) = 1$; and thus the probability of keeping $e_{xy}$ in $\Gamma'$ is the highest possible.

The probability $p_{xy}$ is low in the opposite case, that is, when $c(x,y) \ll c^e_{\setminus e_{xy}}(x,y)$. In that case removal of edge $e_{xy}$ does not significantly affect the effective conductance between $x$ and $y$, because $c^e_{\setminus e_{xy}}(x,y) \approx c^e(x,y)$. In that case, the probability of keeping $e_{xy}$ in $\Gamma'$ is low.

**Example 3.3.4.** We consider the DC network in Figure 3.2, with conductance $c$ whose values at each edge are given in Table 3.1. In the same table we indicate the sampling probabilities calculated for each edge in Algorithm 1.

The values of the conductance at edges $\{x_1, x_2\}$ and $\{x_3, x_4\}$ are two orders of magnitude smaller than at the rest of edges, nevertheless, edge $\{x_3, x_4\}$ is crucial because it is the only

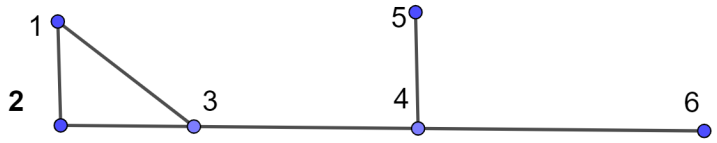


Figure 3.2: Topology of the network in Example 3.3.4.

Table 3.1: Conductances and sampling probabilities of the edges in the network.

| | Edges | | | | | |
|---|---|---|---|---|---|---|
| | $\{x_1, x_2\}$ | $\{x_1, x_3\}$ | $\{x_2, x_3\}$ | $\{x_3, x_4\}$ | $\{x_4, x_5\}$ | $\{x_4, x_6\}$ |
| Conductance | 0.5797 | 75.980 | 75.980 | 0.4698 | 94.599 | 79.909 |
| Conductance times effective resistance | 0.0150 | 0.9925 | 0.9925 | 1 | 1 | 1 |
| Sampling probability | 0.0030 | 0.1985 | 0.1985 | 0.2 | 0.2 | 0.2 |

connection between vertices $x_3$ and $x_4$, so it has a great probability of being sampled to form any sparse approximation of the network, while edge $\{x_1, x_2\}$ is expendable, because its conductance $c(x_1, x_2)$ is equal to only 1.5% of the effective conductance between nodes $x_1$ and $x_2$. The current can flow from node $x_1$ to node $x_2$ with much greater ease by edges $\{x_1, x_3\}$ and $\{x_2, x_3\}$, so the sampling probability of $\{x_1, x_2\}$ is close to zero.

In the case of an AC network $\Gamma = (V, a)$, we will denote by $\Gamma' = \mathsf{Sparsify}(\Gamma, \varepsilon)$ an AC network constructed following the next procedure. First, we apply Algorithm 1 separately to the conductance and susceptance networks, $\Gamma_c$ and $\Gamma_b$, of $\Gamma$; getting $\Gamma'_c = (V, c')$ and $\Gamma'_b = (V, b')$, respectively. Then, $\Gamma' = (V, a') = (V, c' - ib')$. Note that $E(\Gamma') = E(\Gamma'_c) \cup E(\Gamma'_b)$, so in the sparsification process of an AC network we remove the edges erased in the sparsification of both $\Gamma_c$ and $\Gamma_b$.

By definition, $\Gamma'$ will be an $\varepsilon$-approximation of $\Gamma$ iff $\Gamma'_c$ is an $\varepsilon$-approximation of $\Gamma_c$ and $\Gamma'_b$ is an $\varepsilon$-approximation of $\Gamma_b$. By Theorem 3.3.3, if $0 < \varepsilon \leq 1$, then $\Gamma'$ is an $\varepsilon$-approximation of $\Gamma$ with probability at least $\frac{1}{4}$.

## 3.4 Sparsification of recovered electrical networks

This section is a review of [88, Subsection 4.2]. Once we have a procedure to sparsify any network, the key observation to develop our algorithm of sparse network recovery is that spectral sparsification is guaranteed to preserve the fitting properties of a network to some extent.

We introduce some notation for the main result of the chapter in the case of DC networks. Let $\Gamma = (V, c)$ be a DC network with Laplacian $\mathcal{L}$ and let $\boldsymbol{u}, \boldsymbol{s} \in \mathscr{C}(V, \mathbb{R}^m)$, such that $0 < |u|_{\min} \leq |u_j| \leq |u|_{\max}$ for all $j = 1, \ldots, m$. For each $j = 1, ..., m$, we denote as $\mathscr{Q}_{\Gamma, u_j}$ the linear operator on $\mathscr{C}(V)$ defined for each $v \in \mathscr{C}(V)$ as $\mathscr{Q}_{\Gamma, u_j}(v) = u_j \mathcal{L}(u_j v)$. Clearly, $\mathscr{Q}_{\Gamma, u_j}$ is a self-adjoint and positive semidefinite operator. Now, we denote as $\mathscr{Q}_{\Gamma, \boldsymbol{u}}$ the linear operator on $\mathscr{C}(V, \mathbb{R}^m)$ defined for each $(v_1, ..., v_m) \in \mathscr{C}(V, \mathbb{R}^m)$ as $\mathscr{Q}_{\Gamma, \boldsymbol{u}}(v_1, ..., v_m) =$

$(\mathscr{Q}_{\Gamma,u_1}(v_1),...,\mathscr{Q}_{\Gamma,u_m}(v_m))$. For any $\boldsymbol{v}=(v_1,...,v_m),\boldsymbol{w}=(w_1,...,w_m)\in\mathscr{C}(V,\mathbb{R}^m)$, we have that

$$\begin{aligned}\langle\mathscr{Q}_{\Gamma,\boldsymbol{u}}(\boldsymbol{v}),\boldsymbol{w}\rangle &= \sum_{j=1}^m\int_V\mathcal{L}(u_jv_j)u_jw_jdx=\sum_{j=1}^m\int_V u_jv_j\mathcal{L}(u_jw_j)dx\\ &= \langle\boldsymbol{v},\mathscr{Q}_{\Gamma,\boldsymbol{u}}(\boldsymbol{w})\rangle,\end{aligned}$$

so the operator $\mathscr{Q}_{\Gamma,\boldsymbol{u}}$ is self-adjoint. From the same expression, when $\boldsymbol{v}=\boldsymbol{w}$, we can see that $\mathscr{Q}_{\Gamma,\boldsymbol{u}}$ is also positive semidefinite. We denote by $\mathbf{1}_m=(\chi_V,...,\chi_V)\in\mathscr{C}(V,\mathbb{R}^m)$ the vector function whose value is equal to 1 at all vertices. Note that $\mathscr{Q}_{\Gamma,\boldsymbol{u}}(\mathbf{1}_m)=\mathcal{M}_{E(\Gamma),\boldsymbol{u}}(c)$.

For each $j=1,...,m$, we denote as $u_j^{-1}\in\mathscr{C}(V)$ the function defined for each $x\in V$ as $u_j^{-1}(x)=1/u_j(x)$. We also define the vector function

$$\phi_{\boldsymbol{u}}=\left(\frac{\int_V u_1^{-1}dx}{||u_1^{-1}||^2}u_1^{-1},...,\frac{\int_V u_m^{-1}dx}{||u_m^{-1}||^2}u_m^{-1}\right)\in\mathscr{C}(V,\mathbb{R}^m).$$

Our main original result consists in the following upper bound for the $\mathsf{rms}$ of any sparse approximation in a fixed data set.

**Theorem 3.4.1** (Main theorem)**.** *Given a DC network $\Gamma=(V,c)$, positive values $0<|u|_{\min}\leq|u|_{\max}$, $m\in\mathbb{N}^*$ and $\boldsymbol{u},\boldsymbol{s}\in\mathscr{C}(V,\mathbb{R}^m)$ such that $|u|_{\min}\leq|u_j|\leq|u|_{\max}$ for all $j=1,\dots,m$; if $\Gamma'$ is an $\varepsilon$-approximation of $\Gamma$, then:*

$$\mathsf{rms}(\Gamma',\boldsymbol{u},\boldsymbol{s})\leq\mathsf{rms}(\Gamma,\boldsymbol{u},\boldsymbol{s})+\varepsilon\frac{\|\mathscr{Q}_{\Gamma,\boldsymbol{u}}\|_2\cdot\|\mathbf{1}_m-\phi_{\boldsymbol{u}}\|}{\sqrt{m|V|}}.$$

*Proof.* Let $\Gamma'=(V,c')$ be an $\varepsilon$-approximation of $\Gamma$, with Laplacian $\mathcal{L}'$. As $\mathscr{Q}_{\Gamma',\boldsymbol{u}}(\mathbf{1}_m)=\mathcal{M}_{E(\Gamma'),\boldsymbol{u}}(c')$, by (3.3) we get that

$$\begin{aligned}\mathsf{rms}(\Gamma',\boldsymbol{u},\boldsymbol{s}) &= \frac{1}{\sqrt{m|V|}}\|\mathscr{Q}_{\Gamma',\boldsymbol{u}}(\mathbf{1}_m)-\boldsymbol{s}\|\\ &\leq \frac{1}{\sqrt{m|V|}}\|\mathscr{Q}_{\Gamma,\boldsymbol{u}}(\mathbf{1}_m)-\boldsymbol{s}\|+\frac{1}{\sqrt{m|V|}}\|\mathscr{Q}_{\Gamma',\boldsymbol{u}}(\mathbf{1}_m)-\mathscr{Q}_{\Gamma,\boldsymbol{u}}(\mathbf{1}_m)\|\\ &= \mathsf{rms}(\Gamma,\boldsymbol{u},\boldsymbol{s})+\frac{1}{\sqrt{m|V|}}\|\left(\mathscr{Q}_{\Gamma',\boldsymbol{u}}-\mathscr{Q}_{\Gamma,\boldsymbol{u}}\right)(\mathbf{1}_m)\|.\end{aligned}$$

The constant functions belong to the null space of any Laplacian, therefore $\phi_{\boldsymbol{u}}$ belongs to the null space of $\mathscr{Q}_{\Gamma',\boldsymbol{u}}-\mathscr{Q}_{\Gamma,\boldsymbol{u}}$, and thus

$$\begin{aligned}\|\left(\mathscr{Q}_{\Gamma',\boldsymbol{u}}-\mathscr{Q}_{\Gamma,\boldsymbol{u}}\right)(\mathbf{1}_m)\| &= \|\left(\mathscr{Q}_{\Gamma',\boldsymbol{u}}-\mathscr{Q}_{\Gamma,\boldsymbol{u}}\right)(\mathbf{1}_m-\phi_{\boldsymbol{u}})\|\\ &\leq \|\mathscr{Q}_{\Gamma',\boldsymbol{u}}-\mathscr{Q}_{\Gamma,\boldsymbol{u}}\|_2\cdot\|\mathbf{1}_m-\phi_{\boldsymbol{u}}\|.\end{aligned}\tag{3.6}$$

In order to complete the proof, it is enough to show that $\|\mathscr{Q}_{\Gamma',\boldsymbol{u}}-\mathscr{Q}_{\Gamma,\boldsymbol{u}}\|_2\leq\varepsilon\|\mathscr{Q}_{\Gamma,\boldsymbol{u}}\|_2$. Now, $\mathscr{Q}_{\Gamma',\boldsymbol{u}}-\mathscr{Q}_{\Gamma,\boldsymbol{u}}$ is a self-adjoint operator, so its spectral norm is equal to the maximum of the absolute value of its eigenvalues. It is straightforward to prove that its eigenvalues are those of the operators $\mathscr{Q}_{\Gamma',u_j}-\mathscr{Q}_{\Gamma,u_j}$ for all $1\leq j\leq m$. In particular, there is at least one index $k$ such that

$$\|\mathscr{Q}_{\Gamma',\boldsymbol{u}}-\mathscr{Q}_{\Gamma,\boldsymbol{u}}\|_2=\|\mathscr{Q}_{\Gamma',u_k}-\mathscr{Q}_{\Gamma,u_k}\|_2.$$

Let $u_0 \in \mathscr{C}(V)$ be an eigenvector of $\mathscr{Q}_{\Gamma',u_k} - \mathscr{Q}_{\Gamma,u_k}$ corresponding with its eigenvalue that has the largest absolute value such that $\|u_0\| = 1$. Then

$$\|\mathscr{Q}_{\Gamma',\boldsymbol{u}} - \mathscr{Q}_{\Gamma,\boldsymbol{u}}\|_2 = |\langle u_0, (\mathscr{Q}_{\Gamma',u_k} - \mathscr{Q}_{\Gamma,u_k})(u_0)\rangle|.$$

Now, denoting as $\mathcal{E}$ and $\mathcal{E}'$ the energy of $\Gamma$ and $\Gamma'$, respectively, we have that

$$\begin{aligned}\langle u_0, (\mathscr{Q}_{\Gamma',u_k} - \mathscr{Q}_{\Gamma,u_k})(u_0)\rangle &= \langle u_0, u_k(\mathcal{L}' - \mathcal{L})(u_k u_0)\rangle \\ &= \int_V u_0 u_k (\mathcal{L}' - \mathcal{L})(u_0 u_k) dx \\ &= \mathcal{E}'(u_0u_k, u_0u_k) - \mathcal{E}(u_0u_k, u_0u_k).\end{aligned}$$

Evaluating (3.5) at $u = u_0u_k \in \mathscr{C}(V)$ we get

$$\frac{1}{1+\varepsilon}\mathcal{E}(u_0u_k, u_0u_k) \leq \mathcal{E}'(u_0u_k, u_0u_k) \leq (1+\varepsilon)\mathcal{E}(u_0u_k, u_0u_k). \tag{3.7}$$

From the right inequality of (3.7), we have:

$$\mathcal{E}'(u_0u_k, u_0u_k) - \mathcal{E}(u_0u_k, u_0u_k) \leq \varepsilon\mathcal{E}(u_0u_k, u_0u_k),$$

and from the left inequality in (3.7):

$$-(\mathcal{E}'(u_0u_k, u_0u_k) - \mathcal{E}(u_0u_k, u_0u_k)) \leq \frac{\varepsilon}{1+\varepsilon}\mathcal{E}(u_0u_k, u_0u_k) < \varepsilon\mathcal{E}(u_0u_k, u_0u_k).$$

Joining the last two inequalities, we get

$$\|\mathscr{Q}_{\Gamma',\boldsymbol{u}} - \mathscr{Q}_{\Gamma,\boldsymbol{u}}\|_2 \leq \varepsilon\mathcal{E}(u_0u_k, u_0u_k).$$

Moreover,

$$\begin{aligned}\mathcal{E}(u_0u_k, u_0u_k) &= \int_V u_0u_k\mathcal{L}(u_0u_k)dx \\ &= \langle u_0, u_k\mathcal{L}(u_ku_0)\rangle \\ &= \langle u_0, \mathscr{Q}_{\Gamma,u_k}(u_0)\rangle.\end{aligned}$$

By the Courant-Fisher theorem [94], the evaluation of the quadratic form associated with the operator $\mathscr{Q}_{\Gamma,u_k}$ at any unit vector is less or equal than its maximum eigenvalue, which is equal to the norm of this operator because it is positive semidefinite, so:

$$\|\mathscr{Q}_{\Gamma',\boldsymbol{u}} - \mathscr{Q}_{\Gamma,\boldsymbol{u}}\|_2 \leq \varepsilon\|\mathscr{Q}_{\Gamma,u_k}\|_2 \leq \varepsilon\|\mathscr{Q}_{\Gamma,\boldsymbol{u}}\|_2, \tag{3.8}$$

where the last inequality holds because the eigenvalues of $\mathscr{Q}_{\Gamma,\boldsymbol{u}}$ are those of the operators $\mathscr{Q}_{\Gamma,u_j}$ for all $1 \leq j \leq m$. □

**Remark 3.4.2.** In (3.6), it is possible to introduce any vector function equal to $\left(\lambda_1 u_1^{-1}, ..., \lambda_m u_m^{-1}\right) \in \mathscr{C}(V, \mathbb{R}^m)$, for any choice of $\lambda_1, ..., \lambda_m \in \mathbb{R}$, because all of them belong to the null space of $\mathscr{Q}_{\Gamma',\boldsymbol{u}} - \mathscr{Q}_{\Gamma,\boldsymbol{u}}$. Among them, we choose to introduce the term $\phi_{\boldsymbol{u}}$ because it is the choice that minimizes $\rho(\lambda_1, .., \lambda_m) \equiv \left\|\mathbf{1}_m - \left(\lambda_1 u_1^{-1}, ..., \lambda_m u_m^{-1}\right)\right\|^2 =$

$\sum_{j=1}^{m}\int_V \left(\chi_V - \lambda_j u_j^{-1}\right)^2 dx$. Effectively, if we look for a minimum of $\rho$, its partial derivatives must be zero:

$$\frac{\partial\rho(\lambda_1,..,\lambda_m)}{\partial\lambda_k} = 2\int_V \left(-u_k^{-1} + \lambda_k\left(u_k^{-1}\right)^2\right)dx = 0,$$

so the only possible choice for the $\lambda_k$ is:

$$\lambda_k = \frac{\int_V u_k^{-1}dx}{||u_k^{-1}||^2},$$

which is indeed the global minimum of $\rho$ because its Hessian is positive definite: if $j \neq k$, then $\frac{\partial^2\rho(\lambda_1,..,\lambda_m)}{\partial\lambda_k\partial\lambda_j} = 0$, and for each $k = 1, ..., m$,

$$\frac{\partial^2\rho(\lambda_1,..,\lambda_m)}{\partial\lambda_k^2} = 2\int_V \left(u_k^{-1}\right)^2 dx > 0.$$

**Remark 3.4.3.** The term $\frac{\|\mathscr{Q}_{\Gamma,\boldsymbol{u}}\|_2\cdot\|\mathbf{1}_m-\phi_{\boldsymbol{u}}\|}{\sqrt{m|V|}}$ that appears in the upper bound given by the last theorem depends only on the electrical network $\Gamma$ and the first element of the data pair $(\boldsymbol{u},\boldsymbol{s})$, so if we want a sparse approximation of $\Gamma$ such that the $\mathsf{rms}$ of the approximation does not increase (with respect to $\mathsf{rms}(\Gamma,\boldsymbol{u},\boldsymbol{s})$) in the sparsification procedure above a fixed value, there is an $\varepsilon > 0$ such that any $\varepsilon$-approximation of $\Gamma$ is guaranteed to meet this requirement.

In the case of an AC electrical network $\Gamma$, we denote by $\Gamma_c = (V,c)$ and $\Gamma_b = (V,b)$ the conductance and susceptance networks of $\Gamma$, whose respective Laplacians are $\mathcal{L}_c$ and $\mathcal{L}_b$. Additionally, we define the function

$$\Delta(\Gamma,\boldsymbol{u}) = \Bigg(\Big(\sqrt{m|V|}(\|\mathscr{Q}_{\Gamma_c,\Re(\boldsymbol{u})}\|_2 + \|\mathscr{Q}_{\Gamma_c,\Im(\boldsymbol{u})}\|_2) + \|\mathcal{L}_b\|_2\left(\|\Re(\boldsymbol{u})\|_\infty\|\Im(\boldsymbol{u})\|_2 + \|\Im(\boldsymbol{u})\|_\infty\|\Re(\boldsymbol{u})\|_2\right)\Big)^2 +$$
$$+\Big(\sqrt{m|V|}(\|\mathscr{Q}_{\Gamma_b,\Re(\boldsymbol{u})}\|_2 + \|\mathscr{Q}_{\Gamma_b,\Im(\boldsymbol{u})}\|_2) + \|\mathcal{L}_c\|_2(\|\Im(\boldsymbol{u})\|_\infty\|\Re(\boldsymbol{u})\|_2 + \|\Re(\boldsymbol{u})\|_\infty\|\Im(\boldsymbol{u})\|_2)\Big)^2\Bigg)^{1/2},$$

and we have the following result, which is the AC analogous to Theorem 3.4.1:

**Theorem 3.4.4.** *Given an AC network $\Gamma = (V,a)$, $m \in \mathbb{N}^*$ and $\boldsymbol{u},\boldsymbol{s} \in \mathscr{C}(V,\mathbb{C}^m)$, if $\Gamma'$ is an $\varepsilon$-approximation of $\Gamma$, then:*

$$\mathsf{rms}(\Gamma',\boldsymbol{u},\boldsymbol{s}) \leq \mathsf{rms}(\Gamma,\boldsymbol{u},\boldsymbol{s}) + \varepsilon\frac{\Delta(\Gamma,\boldsymbol{u})}{\sqrt{2m|V|}},$$

*where $\Delta(\Gamma,\boldsymbol{u})$ is a function which depends only on $\Gamma$ and $\boldsymbol{u}$.*

*Proof.* First, for every $u \in \mathscr{C}(V,\mathbb{C})$, we have that

$$u\overline{\mathcal{L}(u)} = u\mathcal{L}^*(\overline{u}) = (\Re(u) + i\Im(u))(\mathcal{L}_c + i\mathcal{L}_b)((\Re(u) - i\Im(u))),$$

and therefore

$$\Re(u\overline{\mathcal{L}(u)}) = \Re(u)\mathcal{L}_c(\Re(u)) + \Re(u)\mathcal{L}_b(\Im(u)) + \Im(u)\mathcal{L}_b(\Re(u)) + \Im(u)\mathcal{L}_c(\Im(u)), \qquad (3.9)$$

and also

$$\Im(u\overline{\mathcal{L}(u)}) = \Im(u)\mathcal{L}_c(\Re(u)) + \Im(u)\mathcal{L}_b(\Im(u)) + \Re(u)\mathcal{L}_b(\Re(u)) + \Re(u)\mathcal{L}_c(\Im(u)). \quad (3.10)$$

Now, let $\Gamma' = (V, a')$ be an $\varepsilon$-approximation of $\Gamma$, with Laplacian $\mathcal{L}'$. Let $\Gamma'_c = (V, c')$ and $\Gamma'_b = (V, b')$ be the conductance and susceptance networks of $\Gamma'$, whose respective Laplacians are $\mathcal{L}'_c$ and $\mathcal{L}'_b$. By (3.3) we get that

$$\begin{aligned}\mathsf{rms}(\Gamma', \boldsymbol{u}, \boldsymbol{s}) &= \frac{1}{\sqrt{m|V|}}\|\mathcal{M}_{E(\Gamma'),\boldsymbol{u}}(c', b') - \mathcal{S}(\boldsymbol{s})\| \\ &\leq \frac{1}{\sqrt{m|V|}}\|\mathcal{M}_{E(\Gamma),\boldsymbol{u}}(c, b) - \mathcal{S}(\boldsymbol{s})\| + \frac{1}{\sqrt{m|V|}}\|\mathcal{M}_{E(\Gamma'),\boldsymbol{u}}(c', b') - \mathcal{M}_{E(\Gamma),\boldsymbol{u}}(c, b)\| \\ &= \mathsf{rms}(\Gamma, \boldsymbol{u}, \boldsymbol{s}) + \frac{1}{\sqrt{m|V|}}\|\mathcal{M}_{E(\Gamma'),\boldsymbol{u}}(c', b') - \mathcal{M}_{E(\Gamma),\boldsymbol{u}}(c, b)\|.\end{aligned}$$

The square of the norm in the last equation is equal to

$$\begin{aligned}\|\mathcal{M}_{E(\Gamma'),\boldsymbol{u}}(c', b') - \mathcal{M}_{E(\Gamma),\boldsymbol{u}}(c, b)\|^2 &= \|\big(\Re(u_1\overline{(\mathcal{L}' - \mathcal{L})(u_1)}), ..., \Re(u_m\overline{(\mathcal{L}' - \mathcal{L})(u_m)})\big)\|^2 \\ &+ \|\big(\Im(u_1\overline{(\mathcal{L}' - \mathcal{L})(u_1)}), ..., \Im(u_m\overline{(\mathcal{L}' - \mathcal{L})(u_m)})\big)\|^2.\end{aligned} \quad (3.11)$$

By equations (3.9), (3.10) and (3.11), we can write

$$\begin{aligned}\|\mathcal{M}_{E(\Gamma'),\boldsymbol{u}}(c', b') - \mathcal{M}_{E(\Gamma),\boldsymbol{u}}(c, b)\|^2 &= \|\beta_1 + \beta_2 - \beta_3 + \beta_4\|^2 + \|\beta_5 + \beta_6 + \beta_7 - \beta_8\|^2 \\ &\leq (\|\beta_1\| + \|\beta_2\| + \|\beta_3\| + \|\beta_4\|)^2 \\ &+ (\|\beta_5\| + \|\beta_6\| + \|\beta_7\| + \|\beta_8\|)^2,\end{aligned} \quad (3.12)$$

where:

$$\begin{aligned}\beta_1 &= (\mathscr{P}_{c'} - \mathscr{P}_c)(\Re(\boldsymbol{u}), \Re(\boldsymbol{u})), & \beta_2 &= (\mathscr{P}_{b'} - \mathscr{P}_b)(\Re(\boldsymbol{u}), \Im(\boldsymbol{u})), \\ \beta_3 &= (\mathscr{P}_{b'} - \mathscr{P}_b)(\Im(\boldsymbol{u}), \Re(\boldsymbol{u})), & \beta_4 &= (\mathscr{P}_{c'} - \mathscr{P}_c)(\Im(\boldsymbol{u}), \Im(\boldsymbol{u})), \\ \beta_5 &= (\mathscr{P}_{c'} - \mathscr{P}_c)(\Im(\boldsymbol{u}), \Re(\boldsymbol{u})), & \beta_6 &= (\mathscr{P}_{b'} - \mathscr{P}_b)(\Im(\boldsymbol{u}), \Im(\boldsymbol{u})), \\ \beta_7 &= (\mathscr{P}_{b'} - \mathscr{P}_b)(\Re(\boldsymbol{u}), \Re(\boldsymbol{u})), & \beta_8 &= (\mathscr{P}_{c'} - \mathscr{P}_c)(\Re(\boldsymbol{u}), \Im(\boldsymbol{u})).\end{aligned}$$

Then, on one hand, $\mathscr{P}_c(\Re(\boldsymbol{u}), \Re(\boldsymbol{u})) = \mathscr{Q}_{\Gamma_c,\Re(\boldsymbol{u})}(\mathbf{1}_m)$ and $\mathscr{P}_{c'}(\Re(\boldsymbol{u}), \Re(\boldsymbol{u})) = \mathscr{Q}_{\Gamma'_c,\Re(\boldsymbol{u})}(\mathbf{1}_m)$, so by (3.8), we get

$$\begin{aligned}\|\beta_1\| &\leq \|\mathscr{Q}_{\Gamma'_c,\Re(\boldsymbol{u})} - \mathscr{Q}_{\Gamma_c,\Re(\boldsymbol{u})}\|_2 \cdot \|\mathbf{1}_m\| = \sqrt{m|V|}\|\mathscr{Q}_{\Gamma'_c,\Re(\boldsymbol{u})} - \mathscr{Q}_{\Gamma_c,\Re(\boldsymbol{u})}\|_2 \\ &\leq \varepsilon\sqrt{m|V|}\|\mathscr{Q}_{\Gamma_c,\Re(\boldsymbol{u})}\|_2.\end{aligned}$$

Reasoning analogously, we also obtain that $\|\beta_4\| \leq \varepsilon\sqrt{m|V|}\|\mathscr{Q}_{\Gamma_c,\Im(\boldsymbol{u})}\|_2$, $\|\beta_6\| \leq \varepsilon\sqrt{m|V|}\|\mathscr{Q}_{\Gamma_b,\Im(\boldsymbol{u})}\|_2$ and $\|\beta_7\| \leq \varepsilon\sqrt{m|V|}\|\mathscr{Q}_{\Gamma_b,\Re(\boldsymbol{u})}\|_2$.

On the other hand, $\mathcal{L}_c = \mathscr{Q}_{\Gamma_c,\chi_V}$, $\mathcal{L}'_c = \mathscr{Q}_{\Gamma'_c,\chi_V}$, $\mathcal{L}_b = \mathscr{Q}_{\Gamma_b,\chi_V}$ and $\mathcal{L}'_b = \mathscr{Q}_{\Gamma'_b,\chi_V}$, so, by the proof of Theorem 3.4.1, we have that $\|\mathcal{L}'_c - \mathcal{L}_c\|_2 \leq \varepsilon\|\mathcal{L}_c\|_2$ and $\|\mathcal{L}'_b - \mathcal{L}_b\|_2 \leq \varepsilon\|\mathcal{L}_b\|_2$.

As a consequence, for any $(\boldsymbol{v},\boldsymbol{w}) = ((v_1,...,v_m),(w_1,...,w_m)) \in \mathscr{C}(V,\mathbb{R}^m)\times\mathscr{C}(V,\mathbb{R}^m)$ it is satisfied that

$$\begin{aligned}\|(\mathscr{P}_{c'}-\mathscr{P}_c)(\boldsymbol{v},\boldsymbol{w})\|^2 &= \sum_{j=1}^m \int_V v_j^2(\mathcal{L}_c'-\mathcal{L}_c)(w_j)^2dx\\ &\leq \|\boldsymbol{v}\|_\infty^2 \sum_{j=1}^m \int_V (\mathcal{L}_c'-\mathcal{L}_c)(w_j)^2dx = \|\boldsymbol{v}\|_\infty^2 \sum_{j=1}^m \|(\mathcal{L}_c'-\mathcal{L}_c)(w_j)\|_2^2\\ &\leq \|\boldsymbol{v}\|_\infty^2 \sum_{j=1}^m \|(\mathcal{L}_c'-\mathcal{L}_c)\|_2^2\cdot\|w_j\|_2^2 = \|\boldsymbol{v}\|_\infty^2\cdot\|(\mathcal{L}_c'-\mathcal{L}_c)\|_2^2\cdot\|\boldsymbol{w}\|_2^2\\ &\leq \varepsilon^2\|\mathcal{L}_c\|_2^2\cdot\|\boldsymbol{v}\|_\infty^2\cdot\|\boldsymbol{w}\|_2^2.\end{aligned}$$

And, analogously, it is satisfied that $\|(\mathscr{P}_{b'}-\mathscr{P}_b)(\boldsymbol{v},\boldsymbol{w})\| \leq \varepsilon\|\mathcal{L}_b\|_2\cdot\|\boldsymbol{v}\|_\infty\cdot\|\boldsymbol{w}\|_2$. Applying this result, we get the following bounds: $\|\beta_2\| \leq \|\mathcal{L}_b\|_2\cdot\|\Re(\boldsymbol{u})\|_\infty\cdot\|\Im(\boldsymbol{u})\|_2$, $\|\beta_3\| \leq \|\mathcal{L}_b\|_2\cdot\|\Im(\boldsymbol{u})\|_\infty\cdot\|\Re(\boldsymbol{u})\|_2$, $\|\beta_5\| \leq \|\mathcal{L}_c\|_2\cdot\|\Im(\boldsymbol{u})\|_\infty\cdot\|\Re(\boldsymbol{u})\|_2$ and $\|\beta_8\| \leq \|\mathcal{L}_c\|_2\cdot\|\Re(\boldsymbol{u})\|_\infty\cdot\|\Im(\boldsymbol{u})\|_2$.

Considering in (3.12) all the upper bounds obtained for $\|\beta_1\|,...,\|\beta_8\|$, we conclude the proof. □

## 3.5 Algorithm for sparse network recovery

This section is a review of [88, Subsection 4.3]. In this section we propose an algorithm to solve the Problem 3.2.1 of recovering simultaneously the topology and admittance of a sparse electrical network.

If we have an electrical network $\Gamma = (V,a)$, a data pair $(\boldsymbol{u},\boldsymbol{s})$ and we choose an $\varepsilon$ such that the $\mathsf{rms}$ of any $\varepsilon$-approximation of $\Gamma$ in the data pair $(\boldsymbol{u},\boldsymbol{s})$ does not surpass a fixed tolerance $\mathsf{tol} > 0$ (by Theorems 3.4.1 and 3.4.4 such a $\varepsilon$ exists if $\mathsf{rms}(\Gamma,\boldsymbol{u},\boldsymbol{s}) < \mathsf{tol}$), the only guarantee about the number of edges that any $\varepsilon$-approximation obtained by executing $\mathsf{Sparsify}(\Gamma,\varepsilon)$ will have is that this number of edges will be less or equal than the number of edges sampled in Algorithm 1, $t = 8|V|\cdot\log(|V|)/\varepsilon^2$. If $\mathsf{tol}$ is small, the number of edges sampled will be large, so most $\varepsilon$-approximations of $\Gamma$ will have the same number of edges as the original network, thus they will not be useful for our purposes.

In the experimentation we have found that, if we choose an $\varepsilon$ such that $\Gamma' = \mathsf{Sparsify}(\Gamma,\varepsilon)$ satisfies that $|E(\Gamma')| < |E(\Gamma)|$, and then we solve Problem 3.1.2 with the set $E(\Gamma')$; (that is, we execute $[\Gamma'',\mathsf{rms}''] = \mathsf{network\_recovery}(E(\Gamma'),\boldsymbol{u},\boldsymbol{s})$, determining a network $\Gamma'' = (V,a'')$ with set of edges $E(\Gamma'') \subseteq E(\Gamma')$ such that the error $\mathsf{rms}'' = \mathsf{rms}(\Gamma'',\boldsymbol{u},\boldsymbol{s})$ is minimum), then we have $\mathsf{rms}'' \leq \mathsf{tol}$ in many cases, even in cases in which $\mathsf{rms}(\Gamma',\boldsymbol{u},\boldsymbol{s}) > \mathsf{tol}$.

Our approach to solve Problem 3.2.1 consists in the application of Algorithm 2. The algorithm starts by fitting a network $\Gamma = \mathsf{network\_recovery}(E,\boldsymbol{u},\boldsymbol{s})$ solving Problem 3.1.2 with the data pair $(\boldsymbol{u},\boldsymbol{s})$ and the set of edges $E$. Then, our goal is to perform a sparsification of $\Gamma$, $\Gamma' = \mathsf{Sparsify}(\Gamma,\varepsilon)$, followed by a recovery of another network $\Gamma''$ solving Problem 3.1.2

with the set of edges of the sparse approximation, $E(\Gamma')$, as in the paragraph above, looking for a network with less edges than the current one, and with a rms below the input tolerance tol.

We do not know which choices of $\varepsilon$ can lead us to a network with these characteristics, so we use a procedure of exploration to let Algorithm 2 find suitable values of $\varepsilon$. We start the algorithm with an initial input value of $\varepsilon$, and we do an iterative procedure. Each iteration begins by checking if $\Gamma' = \mathsf{Sparsify}(\Gamma, \varepsilon)$ has less edges than the current network $\Gamma$. If this is not the case, there is a high probability, from Theorem 3.3.3, of $\Gamma'$ being a sparse approximation so close to $\Gamma$ that it has the same set of edges, so we increase the value of $\varepsilon$ multiplying it by the input parameter $\psi > 1$, and we finish the iteration. In this way, in the next iteration the number of edges sampled in Sparsify will be lower than in the previous one, increasing the probability of getting sparse approximations with less edges than $\Gamma$.

If, on the contrary, $|E(\Gamma')| < |E(\Gamma)|$, we recover the network $\Gamma''$ solving Problem 3.1.2 with set of edges $E(\Gamma')$, that is, we compute $[\Gamma'', \mathsf{rms}''] = \mathsf{network\_recovery}(E(\Gamma'), \boldsymbol{u}, \boldsymbol{s})$.

Then, we check if $\mathsf{rms}'' \leq \mathsf{tol}$. If this is the case, we replace the current network $\Gamma$ by this new $\Gamma''$ and we finish the iteration, using the new network as input for Sparsify in the next iteration, repeating the process, in order to look for networks with less edges than it. If, on the opposite case, $\mathsf{rms}'' > \mathsf{tol}$, this means we have removed edges that are necessary for the network to correctly fit the data in the sparsification process, because there are no networks with set of edges contained in $E(\Gamma')$ whose rms is lower or equal than tol. We reject the network $\Gamma''$, we decrease the value of $\varepsilon$ dividing it by $\psi$ and we finish the iteration because, from theorems 3.4.1 and 3.4.4, we know that decreasing the value of $\varepsilon$ assures that the rms on any subsequent $\varepsilon$-approximation of $\Gamma$ will have a smaller upper bound.

It is possible to define different stopping criteria for Algorithm 2, such as the total running time if we are interested on the best network that the algorithm can find in that period, or a maximum number of consecutive iterations in which the network has not changed. In the case of distribution networks, it is usual that the position of the switches is set so that the network topology is a tree, so in this case, reaching a tree topology can be another stopping criterion. A detailed discussion about the stopping criteria is left for future work.

## 3.6 Experimental results and discussion

Lastly, we present some results of the application of Algorithm 2 to solve examples of Problem 3.2.1. This section is a review of [88, Section 5]. The algorithm has been written in MATLAB using Casadi [101], an open-source software tool that provides a symbolic framework suited for numerical optimization, and the interior-point solver IPOPT [102], an open-source software package for large-scale nonlinear optimization, for the network_recovery process. The tolerance used in IPOPT is equal to $10^{-8}$. In all the examples, we use $\psi = 1.5$ as input of Algorithm 2.

In each example, we have chosen a network $\Gamma$ and we have sampled a data pair $(\boldsymbol{u}, \boldsymbol{s})$ consisting in $m = 1000$ pairs of voltage and power injected at $\Gamma$. Each pair $(u_j, s_j)$ has been computed numerically solving the power flow equations of $\Gamma$, $s_j = u_j\overline{\mathcal{L}(u_j)}$, along with

**Algorithm 2** Sparse network recovery.

Inputs: $(\boldsymbol{u}, \boldsymbol{s})$, $E$, $\varepsilon$, $\psi > 1$, $\mathsf{tol}$, *total_time*.
$[\Gamma, \mathsf{rms}] := \mathsf{network\_recovery}(E, \boldsymbol{u}, \boldsymbol{s})$.
**while** *running_time* $<$ *total_time* **do** // (Stopping criteria)
  Set $\Gamma' := \mathsf{Sparsify}(\Gamma, \varepsilon)$.
  **if** $|E(\Gamma')| < |E(\Gamma)|$ **then**
    $[\Gamma'', \mathsf{rms}''] = \mathsf{network\_recovery}(E(\Gamma'), \boldsymbol{u}, \boldsymbol{s})$.
    **if** $\mathsf{rms}'' \leq \mathsf{tol}$ **then**
      $\Gamma := \Gamma''$.
    **else**
      $\varepsilon := \varepsilon/\psi$.
    **end if**
  **else**
    $\varepsilon = \varepsilon \cdot \psi$.
  **end if**
**end while**
Return $\Gamma$.

different additional restrictions. Restrictions that are common for all the pairs $(u_j, s_j)$, such as for instance having $s_j(x) = 0$ for a vertex $x \in V$ for all $i = 1, ...m$, will be highlighted only if they are relevant for the analysis of the results.

In all the examples, we solve Problem 3.2.1 using $E = E(K_V)$ as set of edges, that is, we solve the problem without any *a priori* information about the topology of the network. We fix a labeling $\{x_1, ..., x_n\}$ on the set of vertices of each network and in the figures we denote each vertex $x_j$ as $j$ for the sake of clarity.

**Example 3.6.1.** We start with the DC network in Example 3.3.4, (whose conductance is shown in Table 3.1). In the data pair $(\boldsymbol{u}, \boldsymbol{s})$, for each $j = 1, ..., m$ we have different loads, (that is, negative power injected $s_j$) at all nodes, except at node $x_1$, where the power feeding the entire network is generated ($s_j(x_1) \geq 0$). We apply Algorithm 2 with $\mathsf{tol} = 10^{-5}$ and an initial value for $\varepsilon$ equal to 0.1 and we obtain the results of Table 3.2 (we only write the results of iterations in which the number of edges has decreased, and we consider the first network recovery with the set of edges $E(K_V)$ of the complete graph previous to the iterative process as the iteration number 1).

Table 3.2: Example 3.6.1 network fitting results with tolerance $10^{-5}$.

| Iteration number | $\lvert E(\Gamma)\rvert$ | $\mathsf{rms}(\Gamma, \boldsymbol{u}, \boldsymbol{s})$ | $\kappa(\mathcal{M}_{E(\Gamma),\boldsymbol{u}})$ | $\varepsilon$ |
|---|---|---|---|---|
| 1 | 15 | $1.011 \cdot 10^{-6}$ | $1.040 \cdot 10^{4}$ | 0.1000 |
| 2 | 9 | $9.415 \cdot 10^{-7}$ | $4.316 \cdot 10^{3}$ | 0.1000 |
| 3 | 7 | $4.632 \cdot 10^{-7}$ | $3.021 \cdot 10^{3}$ | 0.1000 |
| 4 | 6 | $1.491 \cdot 10^{-8}$ | $2.100 \cdot 10^{3}$ | 0.1000 |

The last row in Table 3.2 corresponds to the final network found by the algorithm, that has the real topology of the network (Figure 3.2). The difference between the values at each edge of the conductance obtained and of the real conductance is of the order of magnitude of $10^{-4}$. We obtain almost the real network in just 4 iterations.

If we repeat the experiment with a looser tolerance $\mathsf{tol} = 10^{-3}$, we obtain the results in Table 3.3. The final network is a sparse approximation of the original, with the same edges than it except for edge $\{x_1, x_2\}$, that is removed. This removal barely distorts the structure of the network, as we discussed in Example 3.3.4. It is important to remark that the algorithm never removes the low conductance edge $\{x_3, x_4\}$. That removal would make impossible satisfying the demand of power at nodes $x_4$, $x_5$ and $x_6$, because node $x_1$ is the only node with generated power, so the $\mathsf{rms}$ of the resulting network would be higher than $\mathsf{tol}$.

Table 3.3: Example 3.6.1 network fitting results with tolerance $10^{-3}$.

| Iteration number | $\lvert E(\Gamma)\rvert$ | $\mathsf{rms}(\Gamma, \boldsymbol{u}, \boldsymbol{s})$ | $\kappa(\mathcal{M}_{E(\Gamma),\boldsymbol{u}})$ | $\varepsilon$ |
|---|---|---|---|---|
| 1 | 15 | $1.011 \cdot 10^{-6}$ | $1.040 \cdot 10^{4}$ | 0.1000 |
| 2 | 11 | $8.418 \cdot 10^{-7}$ | $6.354 \cdot 10^{3}$ | 0.1000 |
| 3 | 6 | $3.580 \cdot 10^{-5}$ | $1.320 \cdot 10^{3}$ | 0.1000 |
| 5 | 5 | $3.579 \cdot 10^{-5}$ | $7.028 \cdot 10^{2}$ | 0.1500 |

From now on, we will use $\mathsf{tol} = 10^{-5}$ for all experiments.

**Example 3.6.2.** The next experiment uses the CIGRE test AC network named "Medium voltage distribution network with PV and Wind DER" [63].

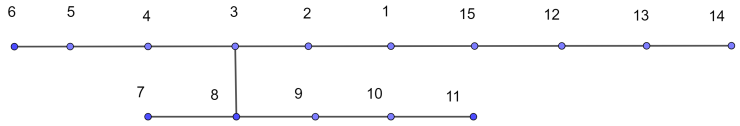


Figure 3.3: Topology of the CIGRE Network. (Example 3.6.2).

An application of Algorithm 2 gives the results in Table 3.4.

Table 3.4: Example 3.6.2 network fitting results.

| Iteration number | $\lvert E(\Gamma)\rvert$ | $\mathsf{rms}(\Gamma, \boldsymbol{u}, \boldsymbol{s})$ | $\kappa(\mathcal{M}_{E(\Gamma),\boldsymbol{u}})$ | $\varepsilon$ |
|---|---|---|---|---|
| 1 | 105 | $2.905 \cdot 10^{-5}$ | $4.200 \cdot 10^{15}$ | 0.3000 |
| 2 | 24 | $8.772 \cdot 10^{-6}$ | $1.492 \cdot 10^{15}$ | 0.3000 |
| 3 | 18 | $6.405 \cdot 10^{-6}$ | $1.526 \cdot 10^{15}$ | 0.3000 |
| 4 | 17 | $6.397 \cdot 10^{-6}$ | $1.497 \cdot 10^{15}$ | 0.3000 |
| 6 | 16 | $4.343 \cdot 10^{-6}$ | $1.482 \cdot 10^{15}$ | 0.4500 |
| 8 | 15 | $1.668 \cdot 10^{-8}$ | $1.476 \cdot 10^{15}$ | 0.6750 |
| 15 | 14 | $1.668 \cdot 10^{-8}$ | $7.965 \cdot 10^{2}$ | 3.417 |

As we can see in Figure 3.4, in this example, the sparsification parameter starts with a value of $\varepsilon = 0.3$, and succeeds at eliminating most edges in the first few iterations. After getting a network with 15 edges, there are some iterations in which Algorithm 1 does not remove any edge. Therefore, Algorithm 2 looks for looser sparse approximations of the network increasing the value of $\varepsilon$, but decreasing its value when a sparse approximation does not fit the data up to the desired tolerance; until at iteration number 15. In this iteration

the algorithm arrives to the real topology, with almost the real values of the admittance. After this iteration, the algorithm never removes any more edges, and the value of $\varepsilon$ tends to oscillate, taking values between 2.28 and 7.69. In Figure 3.4, the iterations in which edges were removed are marked with a circle.

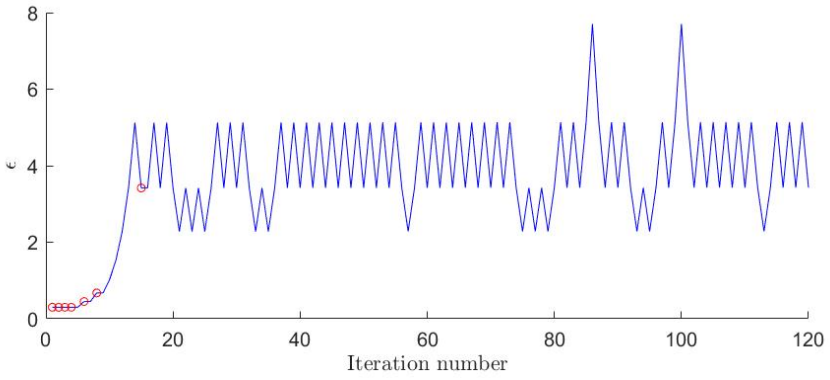


Figure 3.4: Evolution of $\varepsilon$ with the iteration number. Example 3.6.2.

**Example 3.6.3.** In the next experiment, we use a DC network with the topology of the Heawood graph. The results of the application of Algorithm 2 with an initial value of $\varepsilon$ equal to 0.1 are shown in Table 3.5. The algorithm is able to find the topology of the real network in just 5 iterations in this case.

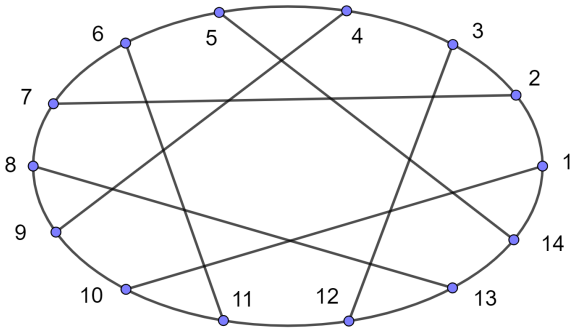


Figure 3.5: Iteration number: 5, $|E(\Gamma)| = 21$. (Heawood graph network).

Table 3.5: Heawood graph network fitting results.

| Iteration number | $\lvert E(\Gamma)\rvert$ | $\mathsf{rms}(\Gamma, \boldsymbol{u}, \boldsymbol{s})$ | $\kappa(\mathcal{M}_{E(\Gamma),\boldsymbol{u}})$ | $\varepsilon$ |
|---|---|---|---|---|
| 1 | 91 | $3.705 \cdot 10^{-6}$ | $2.119 \cdot 10^{4}$ | 0.1000 |
| 2 | 35 | $9.267 \cdot 10^{-7}$ | $2.472 \cdot 10^{3}$ | 0.1000 |
| 3 | 24 | $6.378 \cdot 10^{-7}$ | $5.365 \cdot 10^{2}$ | 0.1000 |
| 4 | 21 | $9.164 \cdot 10^{-10}$ | $2.586 \cdot 10^{2}$ | 0.1000 |

In Table 3.6 we compare the rms of the sparse approximation in each iteration that removes any edge with the upper bound on this rms given by Theorem 3.4.1.

The rms of the sparse approximations are an order of magnitude smaller than the upper bound guaranteed by Theorem 3.4.1. The network recovery step that follows any sparsification step decreases the rms of the network various orders of magnitude. It helps at keeping

Table 3.6: Heawood graph rms on the sparse approximations.

| Iteration number | Upper bound on the rms given by Theorem 3.4.1 | rms of the sparse approximation |
|---|---|---|
| 2 | 0.4429 | 0.0369 |
| 3 | 0.4432 | 0.0308 |
| 4 | 0.4432 | 0.0388 |
| 5 | 0.4432 | 0.0318 |

the rms of the network below tol and lets us avoid the possibility of accumulation of error on successive sparsification steps, which could lead to a network that does not correctly fit the data.

**Example 3.6.4.** Finally, we present an example of sparse network recovery on the AC low voltage network called "Landnetz Freileitung 1 network" (Figure 3.6), that belongs to the Kerber test networks [64].

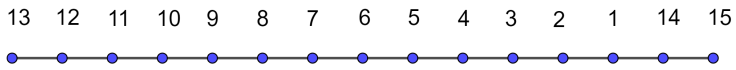


Figure 3.6: Landnetz Freileitung 1 network.

In the data pair $(\boldsymbol{u}, \boldsymbol{s})$ there is no injected power at node $x_{14}$ for any component of $\boldsymbol{s}$, that is, $s_j(x_{14}) = 0$ and thus the potential $u_j$ is harmonic on $x_{14}$, for all $j = 1, ..., m$. We apply Algorithm 2 with an initial value of $\varepsilon$ equal to 0.3; which gives the results in Table 3.7.

Table 3.7: Kerber network fitting results.

| Iteration number | $\lvert E(\Gamma)\rvert$ | $\mathsf{rms}(\Gamma, \boldsymbol{u}, \boldsymbol{s})$ | $\kappa(\mathcal{M}_{E(\Gamma),\boldsymbol{u}})$ | $\varepsilon$ |
|---|---|---|---|---|
| 1 | 105 | $2.069 \cdot 10^{-7}$ | $1.488 \cdot 10^{15}$ | 0.3 |
| 2 | 16 | $2.757 \cdot 10^{-7}$ | $3.829 \cdot 10^{14}$ | 0.3 |
| 3 | 15 | $2.485 \cdot 10^{-12}$ | $3.825 \cdot 10^{14}$ | 0.3 |
| 10 | 14 | $3.885 \cdot 10^{-7}$ | $1.044 \cdot 10^{2}$ | 3.417 |
| 34 | 13 | $2.288 \cdot 10^{-12}$ | $1.029 \cdot 10^{2}$ | 5.126 |

The final network $\Gamma' = (V, a')$ has one edge less than the real one $\Gamma = (V, a)$, and has the following topology, which is shown in Figure 3.7: the edges $\{x_1, x_{14}\}$ and $\{x_{14}, x_{15}\}$ of the real network are substituted in the recovered network by edge $\{x_1, x_{15}\}$. The values of admittance on these edges in the real network $\Gamma$ are $a(x_1, x_{14}) = 16.7913 - 2.6154i$ and $a(x_{14}, x_{15}) = 1.1999 - 3.8157i$, and the value of the admittance of $\Gamma'$ at edge $\{x_1, x_{15}\}$ is $a'(x_1, x_{15}) = 1.6852 - 3.1333i$. The values of $a$ and $a'$ at the edges that are common to both networks, $\Gamma$ and $\Gamma'$, are practically equal.

The difference between $\Gamma$ and $\Gamma'$ is analogous to the difference in Example 3.6.2 between the real network of that example whose set of edges is $\{e_{xy}, e_{yz}\}$ and the recovered network

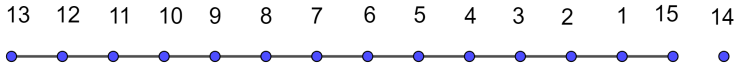


Figure 3.7: Iteration number: 34, $|E(\Gamma)| = 13$. (Kerber network).

of that example whose set of edges is $\{e_{xz}\}$. That is, it is satisfied that

$$\frac{1}{a'(x_1, x_{15})} = \frac{1}{a(x_1, x_{14})} + \frac{1}{a(x_{14}, x_{15})}, \tag{3.13}$$

which is the AC analogue to (3.2). As a consequence, $\Gamma'$ is the union of the isolated vertex $\{x_{14}\}$ and the Kron reduction of $\Gamma$ with respect to $\{x_{14}\}$. Also, $a'(x_1, x_{15})$ is equal to the effective admittance in $\Gamma$ between $x_1$ and $x_{15}$, $a^e(x_1, x_{15})$. Analogously to Example 3.6.2, the Laplacian of $\Gamma'$ is the Dirichlet-to-Neumann map of $\Gamma$ and $\{x_{14}\}$, which gives us the relationship between potential and injected current at $V \setminus \{x_{14}\} = \{x, z\}$ when the potential is harmonic on $x_{14}$.

In all the examples, the condition number of the operators $\mathcal{M}_{E(\Gamma),\boldsymbol{u}}$ decreases dramatically in the algorithm, being much lower in the last electrical network fitted than in the first one. This is especially pronounced in Examples 3.6.2 and 3.6.4, in which the condition number in the first iteration is of the order of magnitude of $10^{15}$, and it is 13 orders of magnitude lower in the last network topology obtained.

In some cases, the rms of a network decreases after removing some edges and recovering a network solving Problem 3.1.2 with the new set of edges. We conjecture that this phenomenon might be due to the finite precision of the interior-point solver.

As a conclusion, the application of Algorithm 2 to different problems of sparse recovery of an electrical network has yielded promising results. In all cases the algorithm recovers a sparse network after few iterations. In this sparse network topology, the Problem 3.1.2 of network recovery becomes well-posed.

# Conclusions

In this thesis we have studied inverse problems on electrical networks from the perspective of discrete vector calculus on finite networks. A version of discrete vector calculus has been introduced in detail in Chapter 1. Our version has extended the discrete vector calculus for DC networks developed in [18, 20, 35, 36] to include the case of AC networks in which all lines are inductive and short.

In the case of AC networks, the tangent space at each vertex of the network has been defined as a complex vector space. With this definition, we have been able to extend to the AC case the definitions of difference operators such as the derivative, gradient, divergence, Laplacian, normal derivative and Dirichlet-to-Neumann map and to study their properties. We have shown that the relation between potential, current and power injected at a network can be expressed using those difference operators both in the DC and AC cases. Therefore, the discrete vector calculus has provided an adequate framework to formulate the inverse problems on DC and AC networks that we have studied throughout the thesis.

Moreover, unlike in [35], we studied Dirichlet and Poisson problems on a subset $F \subseteq V$ of the vertices of a network $\Gamma = (V, a)$ in the case in which $F$ is not connected. This has made possible to extend the definition of the Dirichlet-to-Neumann map of $\Gamma$ and $F$ to the case in which $F$ is not necessarily connected and in which there may exist edges between vertices of $F^c$. This has allowed us to introduce the effective admittance between two vertices of a network from a Dirichlet-to-Neumann map and to relate it to a Kron reduction of the network.

As a consequence, we have given a novel physical interpretation to the sampling probabilities in Algorithm 1, which was proposed in 1 to construct a sparse approximation of a network. These probabilities are proportional to the product of the conductance of an edge by its effective resistance. Also, as a consequence, the fact that the effective conductance between every pair of vertices of a Kron reduction of a network is the same as in the original network has been obtained as a straightforward consequence of Proposition 1.6.8 (see Corollary 1.7.3).

We have seen that some results on electrical networks which had been previously proved in the literature using techniques from other fields, such as the composition property of the Kron reduction (see Proposition 1.6.8), can alternatively be proved using discrete vector calculus tools. We think that the further development of the discrete vector calculus could lead to the discovery of new mathematical properties of electrical networks. Also, we believe that the future study of additional problems on networks within the framework of the discrete vector calculus proposed in this thesis could yield new insights and advances in those problems.

Chapter 2 was dedicated to studying of the inverse conductance problem on a DC network. This problem consists in recovering the conductance of a network from its Dirichlet-to-Neumann map, and it is ill-posed. In particular, we have reviewed and extended the results from [38] and [37]. In [38] the authors proposed Problem 2.3.1 as a reformulation of the inverse conductance problem. We have seen that Problem 2.3.1 is a polynomial optimization problem with a regularization term. This term penalizes deviations with respect to the conductance being piecewise constant on a partition of the edge set known *a priori*.

We have presented numerous experimental examples that suggest that when the conductance is truly piecewise constant on the considered partition, the Lipschitz stability constant of the problem grows exponentially with the number of subsets in the partition. In particular, when the number of subsets is small relative to the total number of edges, we have been able to solve the inverse conductance problem with stability, for different partitions and sizes of the network.

We have also discussed an example from [37] of resolution of the inverse conductance problem using the formulation of Problem 2.3.1 with a partition such that the actual conductance is not piecewise constant on it. In this example, the resolution of Problem 2.3.1 with a certain positive value of the penalty parameter yields better results than enforcing the recovered conductance to be piecewise constant on the partition or solving the problem without any regularization. This supports our penalty formulation of Problem 2.3.1 and the applicability of this approach to solve real-world problems, in which it is expected that the actual conductance is not exactly piecewise constant on the known partition. We have also explained how we can look for a guarantee that a minimum of this optimization problem obtained with a numerical method is a global minimum using techniques of Sum of Squares (SOS) decompositions of polynomials, (see [37]).

We think that our approach of reformulation to solve the inverse conductance problem is promising, considering the results presented in this thesis. In particular, it would be interesting to solve the inverse conductance problem with this approach as part of a process to get a numerical solution of Calderón's problem. Currently, the use of spider networks in applications of Calderón's problem to noninvasive medical imaging is typically restricted to networks with fewer than 16 nodes on the boundary. As we have seen that our method remains stable when the size of the network increases, our method would enable the use of larger networks, thus improving the numerical results.

We believe that it would also be interesting to solve Problem 2.3.1 for other network topologies for which we know that the inverse conductance problem has a unique solution, such as for critical planar graphs different from the spider graphs. Also, it would be interesting to carry out experiments with a supercomputer applying the mentioned SOS techniques for larger networks. If, in an experiment, a numerical method provides a minimum of Problem 2.3.1, but SOS techniques do not guarantee it is a global minimum, then we could look for another minimum of Problem 2.3.1 by using the numerical method with another initial guess, or by using a different numerical method.

Chapter 3 has been devoted to extend and review the results from [88]. The aim of the chapter was to study the inverse problem of simultaneously recovering the admittance and topology of an AC or DC network from a set of measurements of voltage and its corresponding power injected at all vertices. Nevertheless, as we have discussed, this problem is

ill-posed, and thus we usually get a solution with a large set of edges, which is not efficient for applications. Therefore, Problem 3.2.1 was proposed as a reformulation. The goal of this reformulated inverse problem is to recover a sparse network such that the fitting error to the data is below a fixed tolerance. A solution to this problem would be desirable from an applied point of view because it would allow the efficient and accurate resolution of usual problems in electrical networks.

Motivated by our mentioned novel physical insights on Algorithm 1, we have studied its application to solve Problem 3.2.1. We have seen that given $\varepsilon > 0$ and a network $\Gamma = (V, c)$, this algorithm generates a network $\Gamma' = (V, c')$ by removing edges from $\Gamma$, and there is a certain probability that $\Gamma'$ is an $\varepsilon$-approximation of $\Gamma$, (see Definition 3.3.1). Then, we have proved original theoretical results (see Theorems 3.4.1 and 3.4.4) that give an upper bound on the fitting error of any $\varepsilon$-approximation a network.

Later, we have proposed Algorithm 2 to obtain a solution to Problem 3.2.1, which is based on Theorems 3.4.1 and 3.4.4. This algorithm consists in an iterative procedure of solving a convex problem and applying Algorithm 1. We presented diverse experimental results, which suggest that Algorithm 2 is promising for efficiently solving the problem. In all experiments, after just a few iterations, we recovered a network that was either the real one, electrically equivalent to the real one under the conditions satisfied by the data set, or a sparse approximation of the real network.

Therefore, we believe it would be interesting to further study Algorithm 2 in the future. One line of research currently in progress is the study of stopping criteria for it. Another promising direction for future research is exploring the application of alternative graph sparsification procedures to remove edges in the algorithm.

To conclude, the discrete vector calculus on networks developed in this thesis has provided us the tools and definitions necessary to formulate and achieve significant advances in inverse problems on networks. In particular, we have proposed a stable reformulation of the inverse conductance problem and we have introduced an algorithm to solve Problem 3.2.1, based on original theoretical results.

# Bibliography


[1] Abdulla, U.G., Bukshtynov, V., Seif, S., 2021. Cancer detection through electrical impedance tomography and optimal control theory: theoretical and computational analysis. Math. Biosci. Eng. 18, 4834–4859.

[2] Abur, A., Gómez, A., 2004. Power System State Estimation: Theory and Implementation. Marcel Dekker, Inc.

[3] Adams, R.A., Fournier, J., 2003. Sobolev spaces. volume 140 of *Pure and Applied Mathematics (Amsterdam)*. Second ed., Elsevier/Academic Press, Amsterdam.

[4] Adler, A., Holder, D., 2022. Electrical Impedance Tomography: Methods, History and Applications. Second ed., CRC Press.

[5] Alessandrini, G., 1988. Stable determination of conductivity by boundary measurements. Appl. Anal. 27, 153–172.

[6] Alessandrini, G., Vessella, S., 2005. Lipschitz stability for the inverse conductivity problem. Adv. Appl. Math. 35, 207–241.

[7] Araúz, C., 2014. The inverse problem on finite networks. PhD Thesis, UPC.

[8] Araúz, C., Carmona, Á., Encinas, A.M., 2015a. Dirichlet-to-Robin maps on finite networks. Appl. Anal. Discrete Math. 9, 85–102.

[9] Araúz, C., Carmona, Á., Encinas, A.M., 2015b. Discrete Serrin's problem. Linear Algebra Appl. 468, 107–121.

[10] Araúz, C., Carmona, Á., Encinas, A.M., 2015c. Overdetermined partial boundary value problems on finite networks. J. Math. Anal. Appl. 423, 191–207.

[11] Araúz, C., Carmona, Á., Encinas, A.M., Mitjana, M., 2016. Recovering the conductances on grids: a theoretical justification, in: A panorama of mathematics: pure and applied. Amer. Math. Soc., Providence, RI. volume 658 of *Contemp. Math.*, pp. 149–166.

[12] Astala, K., Päivärinta, L., 2006a. A boundary integral equation for Calderón's inverse conductivity problem. Collect. Math. (2006) 57, 127–139.

[13] Astala, K., Päivärinta, L., 2006b. Calderón's inverse conductivity problem in the plane. Ann. Math. 163, 265–299.

[14] Barceló, J.A., Barceló, T., Ruiz, A., 2001a. Stability of the inverse conductivity problem in the plane for less regular conductivities. J.Differential Equations 173, 231–270.

[15] Barceló, J.A., Barceló, T., Ruiz, A., 2001b. Unicidad y estabilidad para el problema de conductividad inverso, in: Margarita Matemática en Memoria de José Javier Guadalupe Henández, Servicio de Publicaciones de la Universidad de La Rioja, Logroño, Spain. pp. 401–413.

[16] Batson, J., Spielman, D., Srivastava, N., Teng, S., 2013. Spectral Sparsification of Graphs: Theory and Algorithms. Commun. ACM 56, 87–94.

[17] Bendito, E., Carmona, Á., Encinas, A.M., 2000. Solving boundary value problems on networks using equilibrium measures. J. Funct. Anal. 171, 155–176.

[18] Bendito, E., Carmona, Á., Encinas, A.M., 2004. Difference schemes on uniform grids performed by general discrete operators. Appl. Num. Math. 50, 343–370.

[19] Bendito, E., Carmona, Á., Encinas, A.M., 2005. Potential theory for Schrödinger operators on finite networks. Rev. Mat. Iberoamericana 21, 771–818.

[20] Bendito, E., Carmona, Á., Encinas, A.M., 2008. Boundary value problems on weighted networks. Discrete Appl. Math. 156, 3443–3463.

[21] Benning, M., Burger, M., 2018. Modern regularization methods for inverse problems. Acta Numer. 27, 1–111.

[22] Bensoussan, A., Menaldi, J., 2005. Difference equations on weighted graphs,. J. Convex Anal. 12, 13–44.

[23] Borcea, L., Druskin, V., Guevara, F., 2008. Electrical Impedance Tomography with resistor networks. Inverse Problems 24, 035013.

[24] Borcea, L., Druskin, V., Guevara, F., Mamonov, A., 2011. Resistor network approaches to electrical impedance tomography, in: Inverse problems and applications: inside out. II (G. Uhlmann ed.). Cambridge Univ. Press, Cambridge. volume 60 of *Math. Sci. Res. Inst. Publ.*, pp. 55–118.

[25] Borcea, L., Druskin, V., Knizhnerman, L., 2005. On the continuum limit of a discrete inverse spectral problem on optimal finite difference grids. Comm. Pure Appl. Math. 58, 1231–1279.

[26] Borcea, L., Druskin, V., Mamonov, A.V., 2010. Circular resistor networks for electrical impedance tomography with partial boundary measurements. Inverse Problems 26, 045010.

[27] Borcea, L., Guevara, F., Mamonov, A.V., 2013. Study of noise effects in electrical impedance tomography with resistor networks. Inverse Probl. Imaging 7, 417–443.

[28] Borcea, L., Guevara, F., Mamonov, A.V., 2017. A discrete Liouville identity for numerical reconstruction of Schrödinger potentials. Inverse Probl. Imaging 11, 623–641.

[29] Bottura, R., Babazadeh, D., Zhu, K., Borghetti, A., Nordström, L., Nucci, C.A., 2013. Sitl and hla co-simulation platforms: Tools for analysis of the integrated ict and electric power system, in: Eurocon 2013, IEEE. pp. 918–925.

[30] Boyer, J., Garzella, J.J., Guevara-Vasquez, F., 2016. On the solvability of the discrete conductivity and Schrödinger inverse problems. SIAM J. Appl. Math. 76, 1053–1075.

[31] Brezis, H., 2011. Functional analysis, Sobolev spaces and partial differential equations. Universitext, Springer, New York.

[32] Brown, R.M., Uhlmann, G.A., 1997. Uniqueness in the inverse conductivity problem for nonsmooth conductivities in two dimensions. Comm. Partial Differential Equations 22, 1009–1027.

[33] Bunge, A., Botsch, M., 2023. A Survey on Discrete Laplacians for General Polygonal Meshes. Comput. Graph. Forum 42, 521–544.

[34] Calderón, A.P., 2006. On an inverse boundary value problem. Comput. Appl. Math. 25, 133–138. (Reprint of the original work in Seminar on Numerical Analysis and its Applications to Continuum Physics, Soc. Brasil. Mat. Rio de Janeiro 65-73, 1980.).

[35] Carmona, Á., 2018. Boundary value problems on finite networks, in: Combinatorial Matrix Theory (Encinas A.M. and Mitjana, M. eds.). Birkhäuser/Springer, Cham. Advanced Courses in Mathematics. CRM Barcelona, pp. 173–217.

[36] Carmona, Á., Encinas, A.M., 2024. Discrete operators on graphs and networks, in: Inverse Problems, Regularization Methods and Related Topics. A Volume in Honour of Thamban Nair (Pereverzyev, S.V. and Radha, R. and S. Sampath, S. eds.). Springer. Industrial and Applied Mathematics, to appear.

[37] Carmona, Á., Encinas, A.M., Jiménez, M.J., Samperio, Á., 2024a. Stable and optimal conductance recovery on networks. Submitted .

[38] Carmona, Á., Encinas, A.M., Jiménez, M.J., Samperio, Á., 2024b. Stable recovery of piecewise constant conductance on spider networks. Int. J. Comput. Math. , 1–18.

[39] Caro, P., García-Ferrero, M.Á., Rogers, K.M., 2024. Reconstruction for the Calderón problem with Lipschitz conductivities. ArXiv preprint: 2401.06120v1 .

[40] Caro, P., Rogers, K.M., 2016. Global uniqueness for the Calderón problem with Lipschitz conductivities. Forum Math., Pi 4, 20 pages.

[41] Chan, M., Tae, J., Jeongchan, N., Hyeuknam, K., Kiwan, J., Kyounghun, L., 2023. Machine learning-based signal quality assessment for cardiac volume monitoring in electrical impedance tomography. Mach. Learn.: Sci. Technol. 4, 015034.

[42] Cheney, M., Isaacson, D., Newell, J.C., 1999. Electrical impedance tomography. SIAM Rev. 41, 85–101.

[43] Chou, H., Maly, J., Verdun, C., 2022. Non-negative Least Squares via Over-parametrization. arXiv preprint: 2207.08437 .

[44] Chung, F., 1997. Spectral Graph Theory. volume 92 of *CBMS Regional Conf. Ser. in Math.* American Mathematical Society, Providence, RI,.

[45] Chung, F., Gilbert, A., Hoskins, J., Schotland, J., 2017. Optical tomography on graphs. Inverse Problems 33, 055016, 21.

[46] Chung, F., Yau, S.T., 2000. Discrete Green's Functions. J. Combin. Theory Ser. A 91, 191–214.

[47] Chung, S., Berenstein, C., 2005. $\omega$-harmonic functions and inverse conductivity problems on networks. SIAM J. Appl. Math. 65, 1200–1226.

[48] Colin de Verdière, Y., 1994. Réseaux électrique planaires i. Commentarii Mathematici Helvetici 69, 351–374.

[49] Conway, J.B., 2007. A Course in Functional Analysis. volume 96 of *Graduate Texts in Mathematics*. Springer New York, NY.

[50] Crabtree, D.E., Haynsworth, E.V., 1969. An identity for the Schur complement of a matrix. Proc. Am. Math. Soc. 22, 364–366.

[51] Curtis, E.B., Ingerman, D., Morrow, J.A., 1998. Circular planar graphs and resistor networks. Linear Algebra Appl. 283, 115–150.

[52] Curtis, E.B., Morrow, J.A., 1990. Determining the resistors in a network. SIAM J. Appl. Math. 50, 918–930.

[53] Curtis, E.B., Morrow, J.A., 1991. The Dirichlet to Neumann map for a resistor network. SIAM J. Appl. Math. 51, 1011–1029.

[54] Curtis, E.B., Morrow, J.A., 2000. Inverse problems for electrical networks. volume 13. World Scientific.

[55] Curtis, E.B., Morrow, J.A., Mooers, E., 1994. Finding the conductors in circular networks from boundary measurements, rairo model. RAIRO Modél. Math. Anal. Numér. 28, 781–814.

[56] D., C., Parrilo, P., 2017. Sampling algebraic varieties for sum of squares programs. SIAM J. Optimiz. 27, 2381–2404.

[57] Deka, D., Backhaus, S., Chertkov, M., 2015. Structure Learning in Power Distribution Networks. IEEE Trans. Control Netw. Syst. 5, 1061–1074.

[58] Devriendt, K., 2022. Effective resistance is more than distance: Laplacians, Simplices and the Schur complement. Linear Algebra Appl. 639, 24–49.

[59] Dodziuk, J., 1986. Laplacian on manifolds and analogous difference operator for graphs, in: Complex differential geometry and nonlinear differential equations (Brunswick, Maine, 1984). Amer. Math. Soc., Providence, RI. volume 49 of *Contemp. Math.*, pp. 45–49.

[60] Dorfler, F., Bullo, F., 2013. Kron reduction of graphs with applications to electrical networks. IEEE Trans. Circuits Syst. I. Regul. Pap. 60, 150–163.

[61] Engl, H., Hanke, M., Neubauer, A., 1996. Regularization of inverse problems. volume 375 of *Mathematics and it Applications*. Kluwer Academic Publishers Group, Dordrecht.

[62] Ervedoza, S., de Gournay, F., 2011. Uniform stability estimates for the discrete Calderón problems. Inverse problems 27, 125012.

[63] Fraunhofer IEE and University of Kassel, a. Pandapower documentation. CIGRE networks. `https://pandapower.readthedocs.io/en/v2.6.0/networks/cigre.html`. Accessed: 22/07/2024.

[64] Fraunhofer IEE and University of Kassel, b. Pandapower documentation. Kerber Networks. `https://pandapower.readthedocs.io/en/v2.6.0/networks/kerber.html`. Accessed: 22/07/2024.

[65] George, T., 2024. The twist for electrical networks and the inverse problem. Int. Math. Res. Notices 8, 1073–7928.

[66] Gernandt, H., Rohleder, J., 2022. A Calderón type inverse problem for tree graphs. Linear Algebra Appl. 646, 29–42.

[67] Grigoryán, A., 2018. Introduction to analysis on graphs. volume 71 of *University Lecture Series*. American Mathematical Society, Providence, RI.

[68] Hyman, J., Shashkov, M., 1997. Adjoint operators for the natural discretizations of the divergence, gradient and curl on logically rectangular grids. Appl. Numer. Math. 25, 413–442.

[69] Hyman, J., Shashkov, M., Steinberg, S., 2001. The effect of inner products for discrete vector fields on the accuracy of mimetic finite difference methods. Comput. Math. Appl. 42, 1527–1547.

[70] Kayano, T., Yamasaki, M., 1988/89. Discrete Dirichlet integral formula. Discrete Appl. Math. 22, 53–68.

[71] Kenyon, R., Wilson, D., 2017. The space of circular planar electrical networks. SIAM J. Discrete Math. 31, 1–28.

[72] Khan, A., Chakrabarti, S., Sharma, A., Alam, M., 2019. Parameter and Topology Estimation for Electrical Power Distribution System, in: 2019 8th International Conference on Power Systems (ICPS), pp. 1–5.

[73] Lasserre, J., 2010. Moments, positive polynomials and their applications. volume 1 of *Imperial College Press Optimization Series*. Imperial College Press, London.

[74] Lim, L.H., 2020. Hodge Laplacians on graphs. SIAM Rev. 62, 685–715.

[75] Liu, L., 1997. Stability estimates for the two-dimensional inverse conductivity problem. PhD Thesis, University of Rochester, New York.

[76] Lukaschewitsch, M., Maass, P., Pidcock, M., 2003. Tikhonov regularization for electrical impedance tomography on unbounded domains. Inverse Problems 19, 585–610.

[77] Mandache, N., 2001. Exponential instability in an inverse problem for the Schrödinger equation. Inverse Problems 17, 1435–1444.

[78] Milton, G.W., Seppecher, P., 2008. Realizable response matrices of multi-terminal electrical, acoustic and elastodynamic networks at a given frequency. Proc. R. Soc. A. 464, 967–986.

[79] Montes, A., Castro, J., 1995. Solving the load flow problem using Gröbner basis. ACM SIGSAM Bulletin 29, 1–13.

[80] Papachristodoulou, A., Anderson, J., Valmorbida, G., Prajna, S., Seiler, P., Parrilo, P., Peet, M., Jagt, D., 2021. SOSTOOLS Version 4.00 Sum of Squares Optimization Toolbox for MATLAB. ArXiv preprint: 1310.4716 .

[81] Parrilo, P., 2005. Exploiting Algebraic Structure in Sum of Squares Programs. Springer, Berlin, Heidelberg. pp. 181–194.

[82] Putensen, C., Hentze, B., Muenster, S., Muders, T., 2019. Electrical impedance tomography for cardio-pulmonary monitoring. J. Clin. Med. 8, 1176.

[83] Ramon, S., Putinar, M., 2007. Complex symmetric operators and applications II. Trans. Amer. Math. Soc. 359, 3913–3931.

[84] Ribando-Gros, E., Wang, R., Chen, J., Tong, Y., Wei, G.W., 2024. Combinatorial and Hodge Laplacians: Similarities and differences. SIAM Rev. 66, 575–601.

[85] Rondi, L., 2006. A remark on a paper by Alessandrini and Vessella. Adv. Appl. Math. 36, 67–69.

[86] Rondi, L., 2016. Discrete approximation and regularisation for the inverse conductivity problem. Rend. Istit. Mat. Univ. Trieste 48, 315–352.

[87] Rote, G., 2020. Characterization of the response maps of alternating-current networks. Electron. J. Linear Algebra 36, 698–703.

[88] Samperio, Á., 2023. Sparse recovery of an electrical network. ArXiv preprint: 2304.06676 .

[89] Sarode, V., Patkar, S., Cheeran, A.N., 2013. Comparison of 2-d algorithms in eit based image reconstruction. Int. J. Comput. Appl. 69, 6–11.

[90] Shashkov, M., 1996. Conservative finite-difference methods on general grids. Symbolic and Numeric Computation Series, CRC Press, Boca Raton, FL.

[91] Shi, Y., Yang, Z., Xie, F., Ren, S., Xu, S., 2021. The research progress of electrical impedance tomography for lung monitoring. Front. Bioeng. Biotechnol. 9, 726652.

[92] Slawski, M., Hein, M., 2013. Non-negative least squares for high-dimensional linear models: Consistency and sparse recovery without regularization. Electron. J. Statist. 7, 3004–3056.

[93] Spielman, D., 2017. Graphs, Vectors and Matrices. Bull. Amer. Math. Soc. (N.S.) 54, 45–61.

[94] Spielman, D., Srivastava, N., 2011. Graph Sparsification by Effective Resistances. SIAM J. Comput. 40, 1913–1926.

[95] Spielman, D., Teng, S.H., 2011. Spectral Sparsification of Graphs. SIAM J. Comput. 40, 981–1025.

[96] Stagg, G., El-Abiad, A., 1968. Computer Methods in Power System Analysis. McGraw-Hill series in electronic systems, McGraw-Hill.

[97] Sylvester, J., Uhlmann, G., 1987. A global uniqueness theorem for an inverse boundary value problem. Ann. Math. , 153–169.

[98] Uhlmann, G., 1998. Inverse boundary value problems for partial differential equations, in: Proceedings of the International Congress of Mathematicians, Vol. III (Berlin, 1998), pp. 77–86.

[99] Wadhwa, C.L., 2012. Electrical Power Systems. New Academic Science Limited.

[100] Webpage, 2019. Calculus on finite weighted graphs. URL: `https://en.wikipedia.org/wiki/Calculus_on_finite_weighted_graphs`.

[101] Webpage, 2024a. Casadi. URL: `https://web.casadi.org/`.

[102] Webpage, 2024b. Ipopt documentation. URL: `https://coin-or.github.io/Ipopt/`.

[103] Webpage, 2024c. Sedumi. URL: `https://sedumi.ie.lehigh.edu/`.

[104] Zhang, T., Jang, G.Y., Oh, T.I., Jeung, K.W., Wi, H., Woo, E.J., 2020. Source consistency electrical impedance tomography. SIAM J. Appl. Math. 80, 499–520.